ANALYSIS OF THE MINOR STRUCTURAL FEATURES IN THE NORTH-CENTRAL PORTION OF THE PELHAM DOME

BY CHARLES M. ONASCH

CONTRIBUTION NO. 12
GEOLOGY DEPARTMENT
UNIVERSITY OF MASSACHUSETTS
AMHERST, MASSACHUSETTS

ANALYSIS OF THE MINOR STRUCTURAL FEATURES IN THE NORTH-CENTRAL PORTION OF THE PELHAM DOME

by

Charles M. Onasch

Contribution No. 12

Department of Geology

University of Massachusetts

Amherst, Massachusetts

September, 1973

TABLE OF CONTENTS

ILLUSTRATIONS

Figure Page

ABSTRACT

The Jerusalem Hill area lies in the north-central portion of the Millers Falls quadrangle in west-central Massachusetts. It is in the northern portion of the Pelham dome, one of the gneiss domes composing the Bronson Hill anticlinorium. The stratigraphy of the Jerusalem Hill area consists of various granitic gneisses, related quartzites and amphibolites of Cambrian or Precambrian age. The regional structural pattern is complex and reflects several Devonian (Acadian) deformations which include episodes of nappe and recumbent fold formation and two phases of gneiss dome formation. A period of folding and faulting associated with retrograde metamorphism may be Alleghenian, and a period of brittle deformation is Triassic.

By studying the minor structural features, evidence for six phases of deformation was found in the Jerusalem Hill area. The first phase was the formation of isoclinal folds with a strong axial plane foliation which forms the regional foliation. These folds are apparently associated with larger recumbent folds in the Pelham dome. The second phase consists of generally tight folds in bedding and foliation with a strong mineral lineation that pervades the entire dome, and weakly developed axial plane foliation. This phase is believed to belong to the main phase of gneiss dome formation.

The third phase is the dominant phase in the area and the most intensely studied. Folds of this phase have diverse axial directions and a wide variety of shapes. They are generally flattened flexural slip folds in quartzite-rich beds and passive slip folds in the

gneissic and schistose beds. The folds are found in discrete tabular zones with orientations close to that of the slip planes determined by separation angle measurements. The movement line associated with these folds is constant over the whole area and is oriented at N0°E, 15°N. The folds formed in response to a gross shear couple with top moved south with respect to the bottom and with σ_1 oriented approximately S7°W, 14°S. Correlation to the regional structural features is unknown.

The fourth phase is represented by a set of low angle shear planes that cut third phase folds and display a shear sense opposite to that of the third phase and are also of unknown regional correlation. The fifth phase is a generation of boudinaging in two directions at approximately 90° from each other. This phase may be correlated with one of the generations of boudinaging outside the Pelham dome. The sixth phase consists of high angle jointing and faulting and rare low angle gravity faults that relate to the formation of the Triassic border fault to the west.

INTRODUCTION

Location

The area studied lies within the northern portion of the Pelham dome in the central portion of the Millers Falls 7.5 minute quadrangle in west-central Massachusetts (Figure 1). The Jerusalem Hill area was mapped in detail and lies within the towns of Wendell and Montague and includes about 9 square miles (Figure 2). In addition to the Jerusalem Hill area, data from Ashenden (1973) to the north is included on Plate 2 for completeness.

Topography and Drainage

The area lies in the western margin of the Central Upland of Massachusetts (Davis, 1895; Alden, 1924) and consists of upland terrain. The hills are rounded and the valleys are deeply incised with a maximum relief of about 900 feet. The correlation between topography and bedrock is unclear. The present topography is a result mainly of preglacial erosion with some minor modifications due to glacial action and subsequent erosion. Most of the north-facing slopes are covered with till and have poor exposures, while slopes facing in other directions commonly have bluffs and abundant outcrop.

The area is drained by two major streams, Davis Brook and Morman Hollow Brook, and several minor streams. All of these drain into the Millers River which forms the northern boundry of the area and flows into the Connecticut River a short distance to the west.

Geological Setting

The study area is located in the northern portion of the Pelham dome (Figure 3.). This dome is part of a complex of mantled gneiss domes

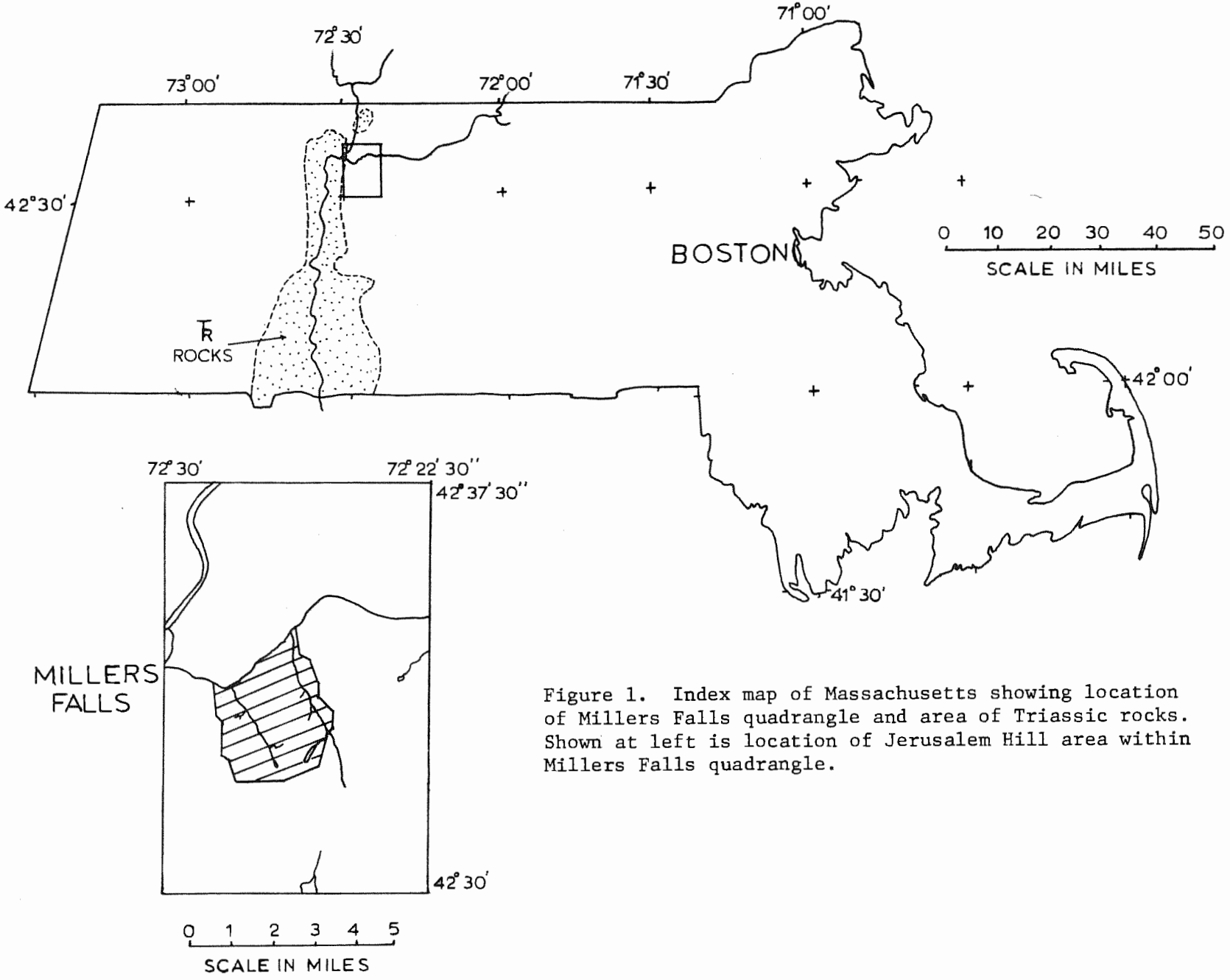

Figure 1. Index map of Massachusetts showing location of Millers Falls quadrangle and area of Triassic rocks. Shown at left is location of Jerusalem Hill area within Millers Falls quadrangle.

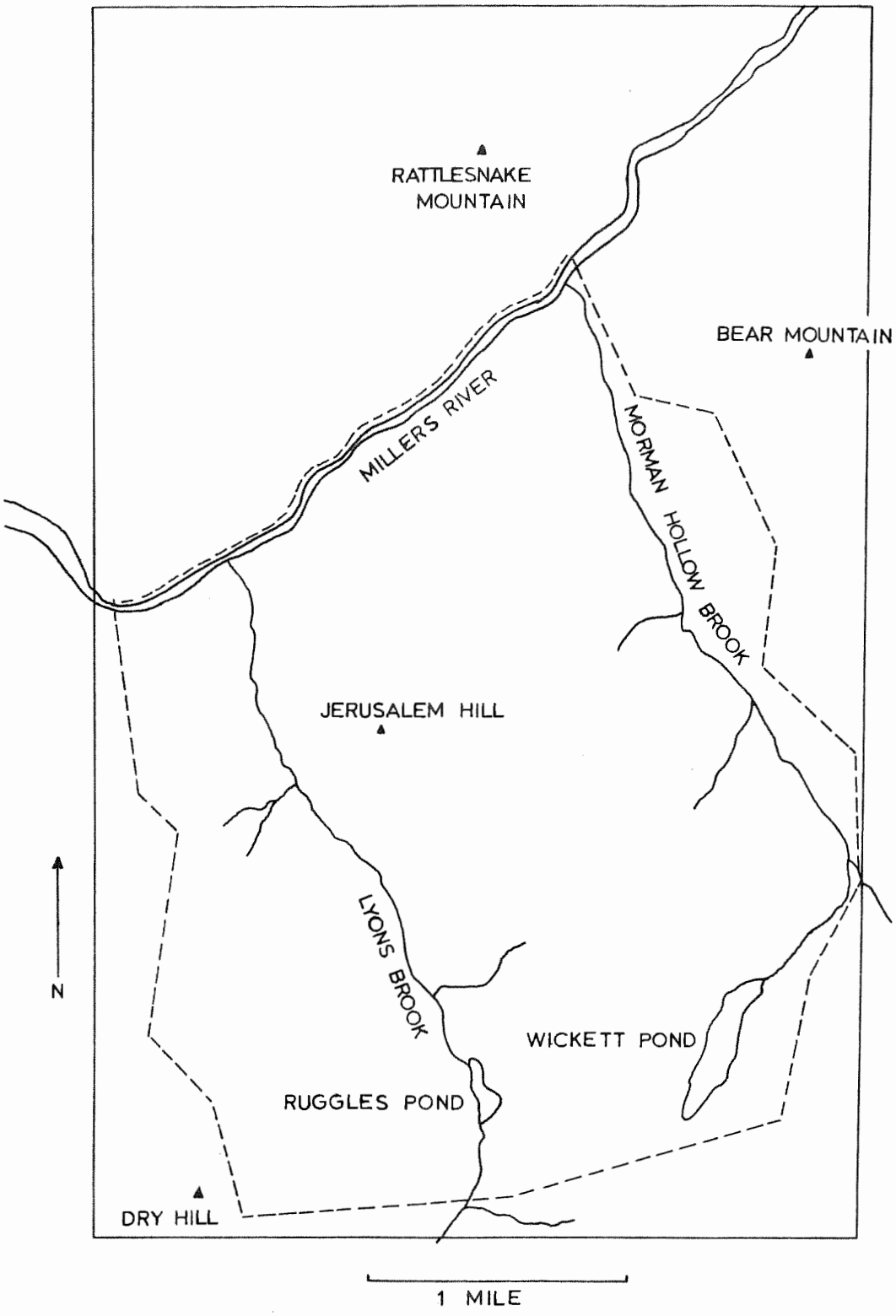

Figure 2. Sketch map of region showing area included in Plate 2. Area bounded by dashed lines is the Jerusalem Hill area.

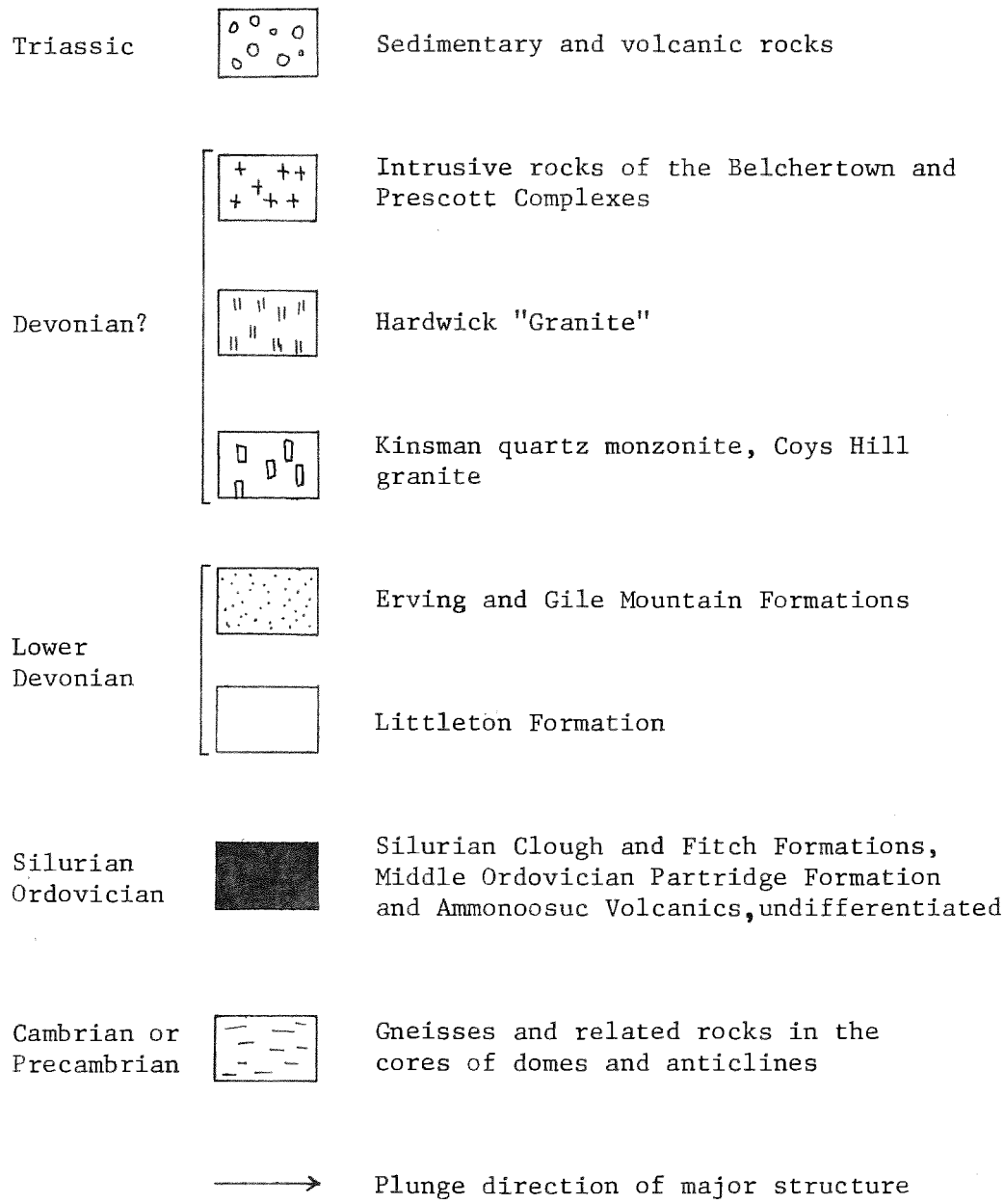

Figure 3. Regional geologic sketch map showing location of Pelham dome on the Bronson Hill anticlinorium (Robinson, 1972).

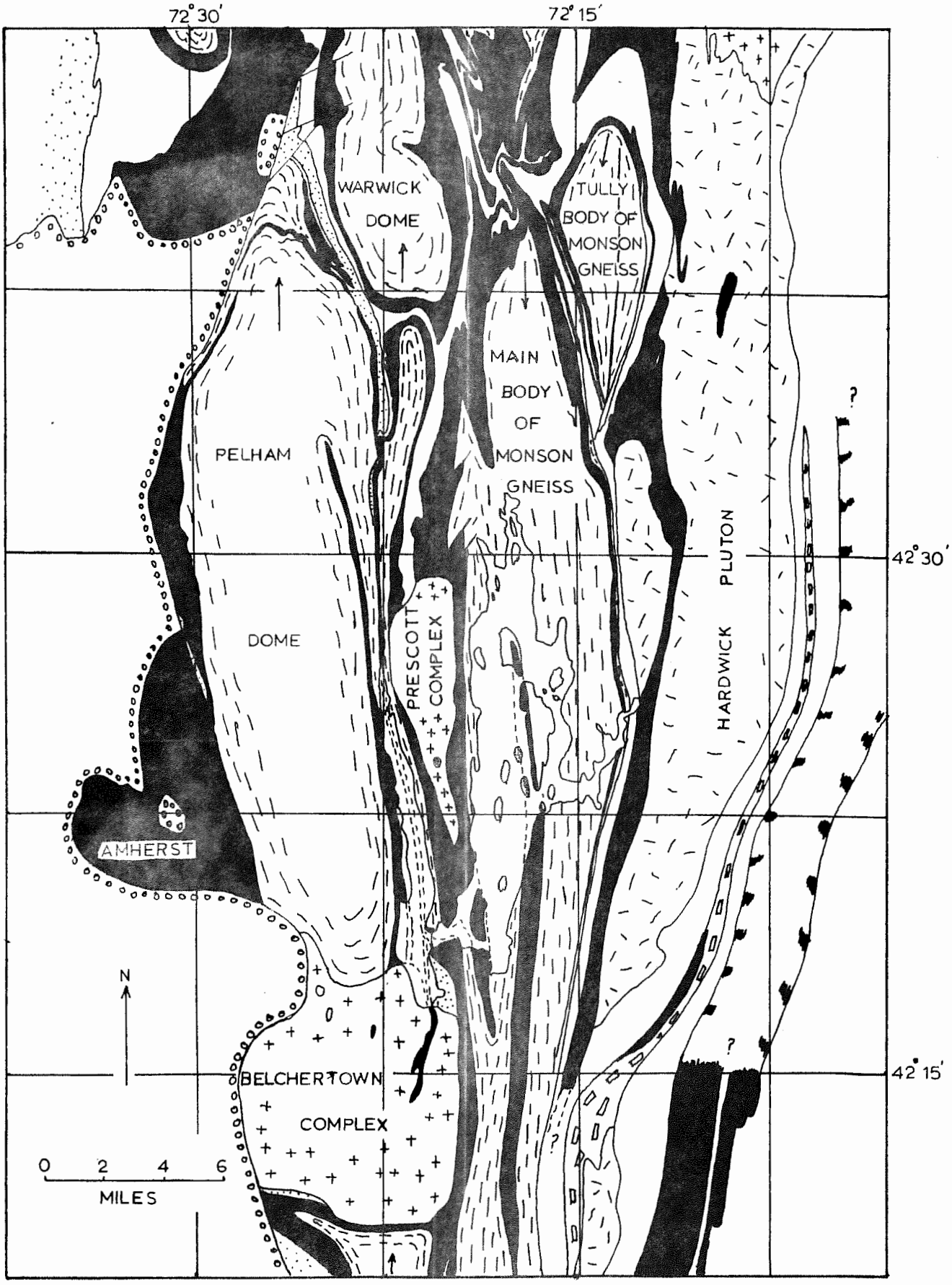
72° 30'
72° 15'
WARWICK DOME
TULLY BODY OF MONSON GNEISS
MAIN BODY OF MONSON GNEISS
PELHAM DOME
PRESCOTT COMPLEX
HARDWICK PLUTON
AMHERST
BELCHERTOWN COMPLEX
42° 30'
42° 15'
N
0 2 4 6
MILES

that compose the Bronson Hill anticlinorium, a major structural feature of the northern Appalachians that is recognized from Long Island Sound in Connecticut to the Maine-New Hampshire border (Thompson et al., 1968). It is flanked on the east by the Merrimack synclinorium and to the west by the Triassic basin and the Connecticut Valley-Gaspé synclinorium. The Triassic rocks of New England cover the eastern portion of the Connecticut Valley-Gaspé synclinorium unconformably and are in fault contact with the rocks of the Bronson Hill anticlinorium in Massachusetts.

The Pelham dome can be considered a typical example of a mantled gneiss dome in the Bronson Hill anticlinorium, in that it consists of various Cambrian or Precambrian gneisses and related rocks overlain apparently unconformably by mantling Middle Ordovician metamorphosed sedimentary and volcanic rocks (Plate 1). The Pelham dome can also be considered to be a unique gneiss dome in the Bronson Hill anticlinorium in that it has a well defined stratigraphy which is invaluable if a thorough knowledge of the complex structure is to be gained.

Previous Work

The area was first mentioned by Emerson (1898, 1917) as part of a reconnaisance mapping while doing detailed work in adjacent quadrangles. Balk (1956) was the first to study the Jerusalem Hill area in detail as part of his mapping of the Millers Falls quadrangle. Robinson (1963, 1967a,b) studied the rocks to the east and did

reconnaissance work in the Pelham dome. Ashenden (1971, 1973) studied the area to the north, including subsurface mapping during the construction of the Northfield Mountain Pumped Storage Hydroelectric Project and conventional surface mapping. His work provided the revised stratigraphy followed in this study (Ashenden, 1971).

Purpose

The purpose of this study is to produce a detailed map and cross sections of an area of critical exposures and an analysis of the minor structural features and their relationship to the regional structural pattern. Particular emphasis is devoted to the origin and relationship of the third phase-late asymmetric folds to the other structural features. It is also hoped that this work will help clarify the complex regional structural pattern.

Method of Study

The geology of the Jerusalem Hill area was mapped in detail on a topographic base map enlarged from a scale of 1:24,000 to 1:12,000. Locations were determined with the assistance of a Brunton compass and a pocket aneroid altimeter. Planar and linear features were measured with a Brunton compass at recorded stations. Where outcrop permitted, a concentrated number of measurements were taken and plotted on an equal area net. Also where exposure permitted, fold dimensions such as height, width, depth, and limb thickness were measured with a tape measure and the interlimb angle with a protractor. Sketches were made from photographs and polished slabs to illustrate certain features.

Ten thin sections from R. Balk's collection were examined for mineralogy and structural details. Several areas outside the Jerusalem Hill area were examined for comparison purposes. The field work was carried out during the summer and early fall months of 1972, with some field checks during the winter and spring of 1973.

Acknowledgments

The author would like to extend his sincere thanks to Peter Robinson who suggested the field area and provided the stimulus needed to complete the project. Donald U. Wise, by frequently playing the devil's advocate, helped the author see many problems in a different light. Discussions between the author and Leo M. Hall on many of the problems proved fruitful. Field assistance was given by Don Curran. Discussions with other workers in the area, Scott Laird and Dave Ashenden, are greatly appreciated. Field work, field assistant, and manuscript preparation were supported by National Science Foundation Grant GA-33857 to Peter Robinson.

STRATIGRAPHY

The study area lies entirely within the core of the Pelham dome and is underlain by various granitoid gneisses and related quartzites and amphibolites (Figure 4). These rocks are tentatively dated as Early Cambrian or Late Precambrian on the basis of a Pb_{207}/Pb_{206} age of 575 ± 30 million years on zircon separated from a sample of the Dry Hill Gneiss, hornblende member from Northfield Mountain. (Naylor, Boone, Boudette, Ashenden, and Robinson, 1973). This date is consistent with ages of lithically similar gneisses in a similar stratigraphic position in Connecticut, New York, and Massachusetts, some of which are known to be Precambrian (Ashenden, 1973; P. Robinson, pers. comm., 1973).

The complex of gneisses and related rocks in the Pelham dome was collectively called the Pelham granite by Emerson (1917). Balk (1956) subdivided these gneisses into two units, the Poplar Mountain Gneiss, with gneiss and quartzite members, and the Dry Hill Gneiss. Ashenden (1972) further subdivided the gneisses to include the Four Mile Gneiss, and in addition, he subdivided the Dry Hill Gneiss into hornblende and biotite members.

The two major stratigraphic units in the Jerusalem Hill area are the Dry Hill Gneiss and the Poplar Mountain Gneiss. In the Dry Hill Gneiss only the biotite member was found. In the Poplar Mountain Gneiss the gneiss member and the quartzite member are present. Several lithologies within the quartzite and gneiss members were mapped separately (Figure 4).

The relative ages of these rocks cannot be deduced from relations within the study area. On the basis of structural considerations and

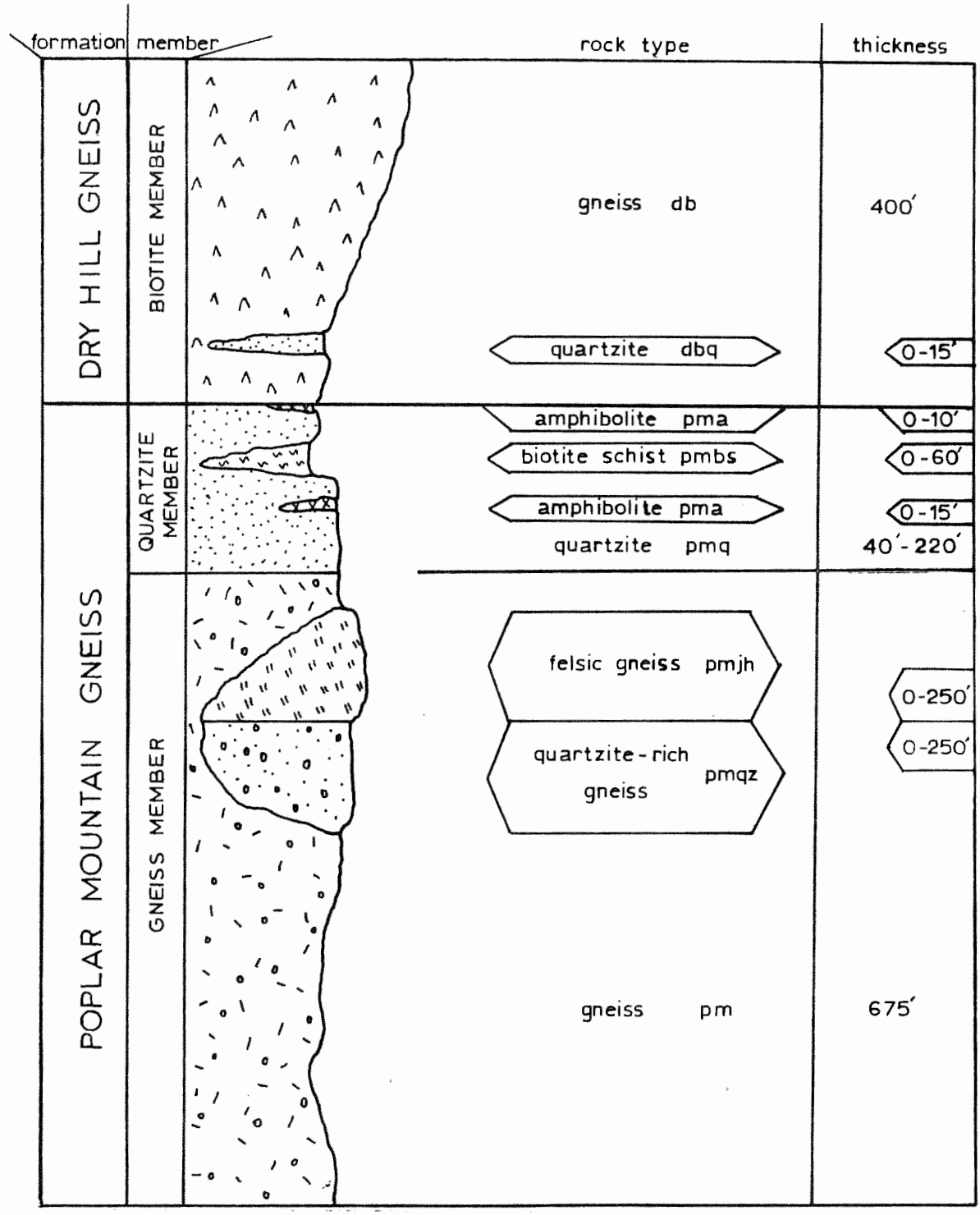

Figure 4. Physical sequence of rock types found in the Jerusalem Hill area. All rocks shown are of probable Late Precambrian or Early Cambrian age (Naylor et. al., 1973) and may be an inverted sequence as a result of early recumbent folding (Ashenden, 1971, 1973). The thicknesses shown for the Dry Hill Gneiss, biotite member and the Poplar Mountain Gneiss, gneiss member are only partial thicknesses since upper and lower contacts are not exposed in the Jerusalem Hill area.

subsurface mapping in the Northfield Mountain area (Ashenden, 1971, 1973), the relative ages are believed to be, from oldest to youngest: Dry Hill Gneiss, hornblende member; Dry Hill Gneiss, biotite member; Poplar Mountain Gneiss, quartzite member; Poplar Mountain Gneiss, gneiss member. According to this hypothesis, the entire Jerusalem Hill area lies on the inverted limb of a major recumbent anticline and hence has a completely inverted stratigraphy.

Dry Hill Gneiss

The Dry Hill Gneiss was originally named by Balk (1956) for the exposure on Dry Hill (Plate 2). It is subdivided into hornblende and biotite members on the basis of the abundance of these two minerals (Ashenden, 1971, 1973). The hornblende member was not found in the Jerusalem Hill area but is common in adjacent areas. The biotite member can be seen on the bluffs in the area east of Jerusalem Hill and on the west side of Bear Mountain.

Hornblende Member. The hornblende member differs from the biotite member (see below) in that it contains abundant knots of hornblende (Table 1.). The hornblende is dark bluish-green in thin section and is optically negative with a 2V close to 0^{o}.

Biotite Member. The biotite member is a medium-grained, well foliated, pink to light gray quartz-microcline-oligoclase-biotite gneiss, with megacrysts of hornblende and microcline or plagioclase (some of which exhibit a schiller effect) up to 1 to 2 inches in diamenter. The rock is commonly well bedded, but massive varieties are also common.

Estimated modes of this member from Ashenden (1973) show the following ranges (Table 1): quartz 25-32%; microcline 40-57%;

Table 1. Estimated modes and ranges of modes of the Dry Hill Gneiss.

	1.	2.	3.	4.
Quartz	40	40	25-32	20-39
Plagioclase *	5 An_{18}	20 An_{18}	8-24 An_{16-18}	2-15 An_{17-18}
Microcline	50	30	40-57	43-60
Muscovite**	tr	tr	0-1	0-1
Biotite	5	5	3-25	3-18
Garnet	tr		0-2	0-5
Hornblende	tr	tr	0-tr	0-10
Epidote		tr	0-tr	0-tr
Allanite			0-tr	0-tr
Calcite**	tr	5	0-tr	0-tr
Sphene	tr	tr	0-tr	0-tr
Apatite			0-tr	0-tr
Magnetite			0-2	0-tr
Zircon	tr	tr	0-tr	0-tr
Chlorite**			0-tr	0-tr

1. M-105 collected by R. Balk. Buff, well foliated quartz-microcline-plagioclase-biotite gneiss with megacrysts of feldspar. S end of Dirth Rd., 1 mi. SE of S end of Ruggles Rd. (Dry Hill Gneiss, Biotite member)

2. M-123, collected by R. Balk. Light gray, well foliated quartz-microcline-plagioclase-biotite gneiss with megacrysts of microcline. S side of power line, 1.5 mi. NW of Wendell on E side of swamp. (Dry Hill Gneiss, Biotite member)

3. Range of 9 modes of biotite member (Ashenden, 1971, 1973).

4. Range of 21 modes of hornblende member (Ashenden, 1971, 1973).

* An determinations were made by the Michel-Levy method.

** Secondary.

tr Mineral present in trace amounts

oligoclase (An_{16-18}) 8-24%; and green biotite 3-25%. Common accessory minerals include apatite, sphene, allanite, calcite, hornblende, magnetite, pyrite, and secondary muscovite. These modes are in general agreement with the two thin sections examined during this study (Table 1, nos. 1&2).

Variations in lithology were noted at several locations. A quartzite-rich zone east of Jerusalem Hill in the biotite member near the contact with the Poplar Mountain Gneiss quartzite member was mapped separately. It is a lens-like body several hundred feet long and up to 15 feet thick. This zone consists of quartzites interbedded with gneissic beds more leucocratic than the biotite member. This zone, along with minor gneissic beds of different compositions, constitutes the main lithologic variation within the biotite member.

Derivation. The Dry Hill gneiss has been thought to be of igneous intrusive origin (Balk, 1942, 1956). The well-bedded nature and the presence of interbeds of quartzites and gneisses of various compositions dispute this interpretation (Ashenden, 1971, 1973). Both members were more likely deposited as a sedimentary or volcaniclastic sequence that has subsequently undergone kyanite grade regional metamorphism.

Thickness. The maximum thickness of the biotite member found by Ashenden (1971, 1973) is 800 feet. Based on the thickness determined from cross sections, the maximum thickness exposed in the Jerusalem Hill area is 400 feet. The contact with the hornblende member is not exposed so this figure does not represent the total thickness of this member in the northern portion of the Pelham dome.

Poplar Mountain Gneiss

The Poplar Mountain Gneiss was originally named and described by Balk (1956) from exposures on Poplar Mountain, north of the Millers River (Plate 2). Two members of this unit are exposed in the Jerusalem Hill area, the gneiss and quartzite members. Together, these two members comprise a large portion of the area mapped.

Quartzite member. The quartzite member is found at the contact of the Poplar Mountain Gneiss with the Dry Hill Gneiss and is well exposed east of Jerusalem Hill at this contact. It consists largely of interbedded quartzites, gneissic layers similar to the Dry Hill Gneiss in appearance and composition, and biotite-rich schists and gray gneisses. Less common are beds of amphibolite and calc-silicate rocks.

The quartzite beds are the most common and consist largely of well bedded, vitreous, buff-colored quartzite. The purity of the quartzite varies. It commonly contains brown biotite, feldspar, or actinolite in various amounts. Estimated modes of these rocks show the following ranges: quartz, 60-92%; microcline, 0-20%; fine brown biotite, tr.-15%; plagioclase of variable composition, 0-10%; muscovite, 0-8%; and actinolite, 0-7% (Ashenden, 1971, 1973). Common accessory minerals include garnet, sphene, calcite, epidote, zircon, and apatite (Table 2).

Table 2. Estimated modes and ranges of modes of quartzite member, quartzite calc-silicate granulite, biotite schist, and amphibolite.

	1.	2.	3.	4.	5.	6.
Quartz	60-92	0-55	30	30	20	
Plagioclase*	0-10 An_{18-28}	0-35 An_{18-25}	10 An_{20}	10 An_{22}	30 An_{18}	21-35 An_{18-30}
Microcline	0-20	0-20				
Muscovite	0-8	0-tr	tr	tr	tr	0-tr
Biotite	tr-15	0-20	30	25	40	15-50
Hornblende		0-40	tr		tr	21-47
Epidote	0-2	0-2	20	tr	6	
Calcite	tr	0-tr				0-2
Sphene	0-5	0-3	5	5	tr	2-4
Apatite	0-tr	0-1	tr	tr	2	tr-2
Magnetite	0-tr					
Zircon	0-tr	0-tr				0-tr
Actinolite	0-7	0-45	5	25	tr	
Chlorite**	0-tr	0-tr	tr	tr	2	0-1
Diopside		0-60	tr	5	tr	

1. Range of 20 modes of quartzite member, quartzite (Ashenden, 1971, 1973).

2. Range of 6 modes of calc-silicate rocks in quartzite member (Ashenden, 1971, 1973).

3. M-39 collected by R. Balk. Dark gray, strongly foliated biotite-quartz-plagioclase schist. E flank of Whales Head, 1010' W of Mormon Hollow Brook. (Biotite schist from quartzite member.)

4. M-57 collected by R. Balk. Gray, fine-grained, well foliated biotite-quartz-actinolite-plagioclase schist with porphroblasts of feldspar and actinolite. .75 mi. due E of Jerusalem Hill 1 mi. N of S end of Ruggles Rd. (Calc-silicate rich rock in biotite schist in quartzite member.)

5. M-151 collected by R. Balk. Dark gray, weakly foliated, biotite-quartz-plagioclase schist. W of Jerusalem Rd. 1.3 mi. N of Ruggles Pond. (Biotite schist in quartzite member.)

6. Range of 5 modes of amphibolite in quartzite member (Ashenden, 1971, 1973).

* An content determined by Michel-Levy method.

** Secondary.

The gneissic beds are composed of quartz, microcline, oligoclase, and biotite. They are commonly segregated into light and dark layers by biotite concentration. These beds generally constitute only 20% of the total thickness of the quartzite member.

Thin beds of calc-silicate rocks up to 3-4 inches in thickness are fairly common throughout the quartzite member. They commonly have a greenish tinge imparted by numerous fine actinolite needles.

The biotite schist portion of this member is present in sufficient extent to warrant separate mapping. It is well exposed east of Jerusalem Hill in the center of the quartzite member, but is not present everywhere the quartzite is found (Plate 2). It is believed that the schist forms a lens in the quartzite member. This rock is a well foliated, dark gray, biotite-quartz-plagioclase schist commonly containing significant amounts of diopside, sphene, tremolite and epidote. Accessory minerals include apatite, magnetite, and secondary chlorite (Table 2). Commonly interbedded with this schist are beds of gray, fine-grained, quartz-microcline-plagioclase-biotite gneiss which is usually strongly segregated into light and dark layers.

The amphibolites found in the quartzite member were also separately mapped. They occur as thin lenses, both at the Dry Hill Gneiss contact and in the center of the quartzite. This rock is generally composed of hornblende, biotite, and oligoclase. Epidote-rich layers are common and minor minerals include sphene, actinolite, diopside, apatite, and chlorite (Table 2). Blocks of exotic rocks are commonly contained in the amphibolites. One such block is composed almost entirely of fine-grained garnet with minor quartz and plagioclase; another is composed of coarse-grained hornblende, diopside, and plagioclase.

Gneiss member. The gneiss member is the most abundant member in the Jerusalem Hill area. It is dark gray, well foliated, microcline-quartz-plagioclase-biotite gneiss with conspicuous round megacrysts of feldspar up to 4 inches in diameter. Estimated modes from Ashenden (1973) range as follows: quartz, 25-56%; brown biotite, 5-27%; and oligoclase (An_{12-19}), 20-49% (Table 3). Accessory minerals are muscovite, allanite, calcite, apatite, zircon, and secondary chlorite. Other lithologies found in this member are quartzite beds 1-3 inches thick, and calc-silicate beds 1-2 inches thick.

Two distinctive lithologies, quartzite-rich gneiss and felsic gneiss, were found within the gneiss member and were mapped separately as lenses. The most abundant of these two is a felsic gneiss exposed in the bluffs on the west and northwest sides of Jerusalem Hill and on the north slope of Country Hill, 1 mile southwest of the Jerusalem Hill area (Scott Laird, pers. comm., 1973). It is a quartz-microcline-oligoclase gneiss, similar to the gneiss member with the exception that it contains less biotite and in many ways resembles the Dry Hill

Table 3. Estimated modes and ranges of modes of Poplar Mountain Gneiss, gneiss member and felsic gneiss on Jerusalem Hill.

	1.	2.	3.	4.
Quartz	50	40	25-56	50
Plagioclase*	10 An_{19}	30 An_{20}	20-49 An_{12-19}	13 An_{18}
Microcline	30	10	5-27	20
Muscovite	tr	tr	0-15	tr
Biotite (brown)	10	15	5-27	10
Hornblende				2
Epidote	tr		0-tr	2
Allanite	tr		0-tr	2
Calcite**	tr	tr	0-tr	tr
Sphene			0-tr	tr
Apatite	tr	5	0-tr	1
Magnetite			0-tr	tr
Zircon	tr		0-tr	
Chlorite**	tr		0-tr	tr

1. M-37 collected by R. Balk. Gray, well foliated biotite-quartz-feldspar-muscovite gneiss with feldspar megacrysts. W flank of hill 1274' E of Mormon Hollow Brook, .75 mi. S of Farley. (Poplar Mountain Gneiss, gneiss member)

2. M-48 collected by R. Balk. Gray, foliated quartz-biotite-feldspar-muscovite gneiss with megacrysts of feldspar. .50 mi. NNE of Jerusalem Hill on Jerusalem Rd. (Poplar Mountain Gneiss, gneiss member)

3. Range of 12 modes of gneiss member (Ashenden, 1971, 1973).

4. M-147 collected by R. Balk. Light gray, fine-grained quartz-feldspar-biotite gneiss. SW flank of Jerusalem Hill, 1 mi. NNW of S end of Ruggles Rd.. (Poplar Mountain Gneiss, felsic gneiss of Jerusalem Hill)

* An content determined by the Michel-Levy method.

** Secondary.

Gneiss biotite member in appearance (Table 3). It differs from the biotite member in that it contains brown biotite instead of green biotite (Tables 1 and 3). The smaller amount of biotite along with its characteristic and distinctive rotten weathering makes it readily distinguishable from the gneiss member. The rock commonly displays large (1-2 inch) megacrysts of feldspar and has apatite, zircon, muscovite, epidote, hornblende, magnetite, and secondary chlorite as accessory minerals (Table 3). It is more massive than the gneiss member and contains no quartzite beds.

A quartzite-rich zone separating the felsic gneiss from the gneiss member was also mapped separately. This zone contains numerous 1-5 inch thick quartzite beds and some calc-silicate beds. Like the felsic gneiss, this zone appears to be a lens.

Derivation. The quartzite member is undoubtedly of sedimentary origin with the possible exception of the amphibolite lenses. The pure quartzite was probably clean quartz sand. The gneissic layers and biotite schist were probably feldspar-rich sediment or pelite. The calc-silicate beds represent dolomitic impure quartz sand. The amphibolites could have been either mafic ash deposits or lava flows. The exotic blocks in the amphibolites could be volcanic bombs or breccia fragments of some type, and deserve to be studied in greater detail.

The gneiss member of the Poplar Mountain Gneiss with its interbedded gneisses, quartzites, and calc-silicates probably has a sedimentary origin. This original sediment could have been primarily immature volcanic material with interbedded quartz sand and dolomitic-quartz sand. The brown biotite suggests that the sediment was deposited and

metamorphosed in a reducing environment. The exact origin of the felsic gneiss on Jerusalem Hill is not known. The more massive portions could be a felsic intrusive sill while the well-bedded zones could be felsic ash beds. The contacts with the gneiss member and especially the quartzite-rich zone are gradational suggesting a depositional origin rather than an intrusive one.

Thickness. The thickness of the quartzite member ranges from a maximum of 220 feet to a minimum of 40 feet where no biotite schist or amphibolite are present. Of the maximum thickness of 220 feet, the biotite schist is 60 feet thick and the amphibolite is 25 feet thick.

The maximum thickness of the gneiss member in the study area is 1175 feet with up to 250 feet of that being the quartzite-rich zone and up to 250 feet the felsic gneiss on Jerusalem Hill. The contact with the Four Mile Gneiss is not exposed in the area, hence the total thickness of the gneiss member cannot be observed. Further north, both the contacts with the Dry Hill Gneiss and Four Mile Gneiss are exposed and the unit is 200 feet thick (Ashenden, 1971, 1973). This thickness was measured on the right-side-up limb of the proposed major recumbent anticline (Ashenden, 1973) where it is much thinner than on the inverted limb where more than 1200 feet are exposed (Ashenden, 1971, 1973).

STRUCTURAL GEOLOGY

The structural geology of the Bronson Hill Anticlinorium is very complex and has been the focus of much interest and work (Billings, 1937; Thompson, 1956; Robinson, 1963; Thompson et al., 1968; Ashenden, 1971, 1973). Simply stated, the Bronson Hill Anticlinorium in central Massachusetts and southwestern New Hampshire is a zone of intense deformation consisting of up to 3 levels of nappes which have been refolded and domed up by a series of en echelon gneiss domes.

Generalized Structural History of the Pelham Dome

The Pelham dome is attractive for a study of structural geology because its stratigraphy is reasonably well defined and it exposes a deeper structural level than is found in any other dome in west-central Massachusetts (Robinson, 1972). A summary of the Paleozoic structural history of the Pelham dome and surrounding area as presently understood is as follows (Robinson, 1967a, 1972):

1. Formation of regional nappes with east towards west overfolding and amplitudes of up to 15 miles. The Pelham dome has been covered at a higher structural level by at least two separate nappes, the Skitchewaug nappe and the Fall Mountain nappe. These are believed to be rooted on the east limb of the Bronson Hill Anticlinorium. In the frontal regions of these nappes, the metamorphic isograds are approximately parallel to the axial surfaces indicating that this phase of deformation was synchronous with part of the regional metamorphism, which reaches kyanite grade in the Pelham dome. The

regional nappes affect rocks as young as Lower Devonian and are believed to have formed during the Acadian orogeny.

2. Formation of recumbent folds on the margins of the Keene and Pelham domes with a northwest towards southeast overfolding with amplitudes up to 6 miles. These folds cause the repetition of the stratigraphy in the northern portion of the Pelham dome (Ashenden, 1971, 1973) (Plate 1). The age of this recumbent folding relative to the regional nappes is uncertain.

3. An early phase of gneiss dome formation accompanied by folding of the nappe axial surfaces back towards the east and north. This was accompanied by a period of cataclasis seen at outcrop scale in the Quabbin Reservoir area 16 miles southeast of the Jerusalem Hill area (Robinson, 1967b) and farther to the east.

4. The main phase of gneiss dome formation and formation of upright isoclinal folds that resulted in the foliation arch that defines the Pelham and other domes. This doming was in part a result of gravitational upward movement of core gneisses relative to higher density mantling strata, probably within the context of an east-west compression. Associated with the formation of the gneiss domes is the formation of intense isoclinal folds and a prominent N-S mineral lineation seen in the Pelham dome and adjacent synclines.

5. Formation of asymmetric folds in the core of the Pelham dome and rare occurrences outside the dome (Ashenden, 1973). These fold the prominent N-S mineral lineation. The movement line has been determined from rotated lineations (Ramsay, 1961) and separation angle measurements (Hansen, 1971) and is N-S, which is about 90^{o} from the

inferred movement line of the earlier structural features, and is parallel to the prominent mineral lineation which it folds.

6. Late phase of folding and faulting associated with retrograde metamorphism in areas near the Prescott and Belchertown complexes.

7. Late period of brittle faulting and hydrothermal alteration associated with the development of the Triassic border fault.

In the study of the minor structural features within the Jerusalem Hill area concrete evidence was found only for early recumbent folding (2 and possibly 1 of above); the main phase of gneiss dome formation (4 above); formation of late asymmetric folds (5 above); and post-metamorphic faulting (7 above). In addition, two minor phases between regional phases 5 and 7 were identified. Table 4 correlates the regional features of Robinson (1967a, 1972) with those found in the Jerusalem Hill area.

The absolute and relative age of these features is not well known. The youngest rocks that are deformed and metamorphosed are Devonian, while the Triassic rocks are practically unmetamorphosed and relatively undeformed. The Prescott intrusive complex which cuts the axial surface of the first generation of nappes and is deformed by the main phase of gneiss dome formation has been dated at 385 million years (Naylor, 1970; Thompson et al., 1968). This date means that the first five phases are probably Acadian. The sixth phase could possibly be Alleghanian while the last phase is Triassic.

The possibility of an earlier deformation in the basement gneisses exists, but has not been recognized. The Avalonian age of these gneisses dates a period of felsic vulcanism from which portions of these

Table 4. Correlation chart of recognized regional phases of deformation to phases defined by minor structural features in the Jerusalem Hill area

	Robinson 1967a	Robinson 1972, pages 23, 24, and 25 this paper	Jerusalem Hill area
Formation of regional nappes with east towards west overfolding and amplitudes of up to 15 miles	1A	1	1
			↑
			?
Formation of recumbent folds on the margins of the Keene and Pelham domes with northwest toward southeast overfolding of amplitudes up to 6 miles	1B	2	↓ 1
Early phase of gneiss dome formation accompanied by folding of the nappe axial surfaces back towards the east and north	2A	3	
Main phase of gneiss dome formation and formation of upright, isoclinal folds and strong N-S regional mineral lineation	2B	4	2
Formation of asymmetric folds in the core of the Pelham dome		5	3
Formation of late shears of reversed sense			4
Episode of late flattening and extension			5
Late phase of folding and faulting associated with retrograde metamorphism in areas near the Prescott and Belchertown Complexes	3	6	
Late period of brittle faulting and hydrothermal alteration	4	7	6

gneisses were derived. This vulcanism could be related to the event in which granites of similar ages in eastern Massachusetts and Newfoundland were intruded (Lyons and Faul, 1968).

Structural Geology of the Jerusalem Hill Area

The geology of the Jerusalem Hill area was studied in detail to produce a geologic map and cross sections and to analyze the several phases of minor structural features. Data from Ashenden (1973) to the north is included in Plate 2 for completeness. The structural geology of the Jerusalem Hill area will be discussed in the probable chronological order of the different phases. The term phase is used because most of the different generations of structural features probably are not related to discrete events, but may well be pulses of a continuous deformation.

Six phases of deformation of varying degrees of importance are recorded in the area (Figures 5, 6). The first five phases probably occurred during the Acadian orogeny and are Middle to Late Devonian, while the last phase is Triassic.

First Phase-Early Recumbent Folding

The earliest deformation observed in the area is a generation of isoclinal folds in bedding with a prominent axial plane foliation subparallel to bedding in most areas. The folds are identifiable because they are the only ones that do not deform foliation; therefore, they are one of the oldest structural features in the area. These folds were found mainly in the quartzite member of the Poplar Mountain Gneiss, but are present in all rock types.

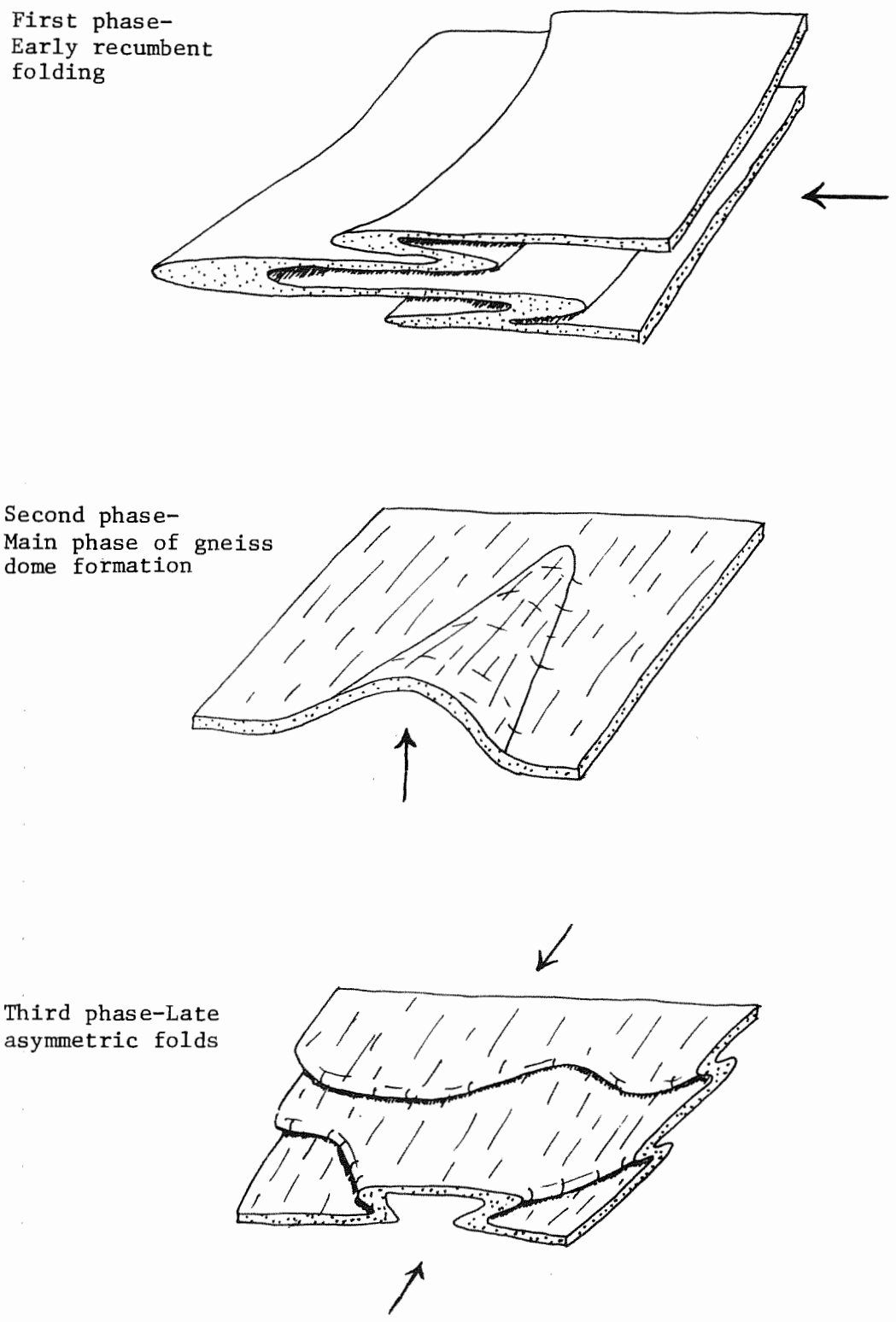

Figure 5. Structural relief diagrams illustrating first three phases of deformation. Arrows in first and second phase diagrams show major transport direction. Arrows in third phase diagram are direction of shear couple acting on area during this phase. In all diagrams north is to the back of the diagram.

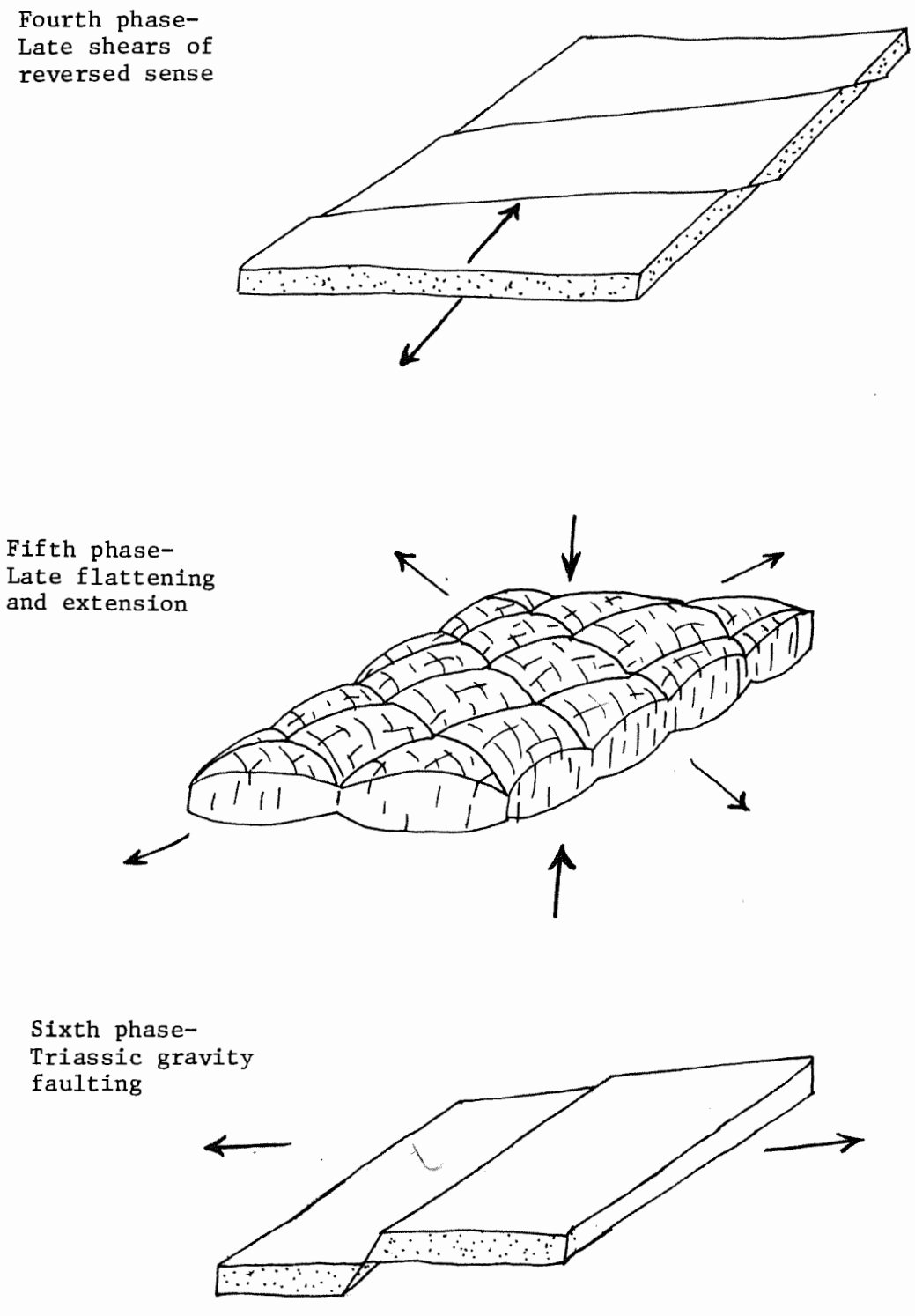

Figure 6. Structural relief diagrams illustrating fourth, fifth, and sixth phases of deformation. Arrows in fourth phase diagram are direction of shear couple acting on area at that time. Arrows in fifth and sixth phase diagrams are directions of relative movement. In all diagrams north is to the back of the diagram.

Folds. Only a small number of folds of this phase were identified and the majority of these are refolded by later folds (Figure 7). They are generally tight to isoclinal in profile and appear to have a similar fold style. They are found on both outcrop and map scale. The map pattern formed by the contact between the Dry Hill Gneiss and the quartzite member of the Poplar Mountain Gneiss east of Jerusalem Hill, north of Dry Hill, and on Rattlesnake Mountain, probably is a result of large folds of this phase (Plates 2 and 3). These folds are considered first phase strctures because of bedding foliation relationships noted near the hinge of the fold in the Dry Hill Gneiss east of Jerusalem Hill. An outcrop was found where the foliation intersects the bedding at a high angle as one would expect in the hinge area if the fold is in bedding and has the regional foliation as an axial surface. If this is a fold then there should be a separation of asymmetry of the minor folds on the opposite limbs. Figure 8 is an equal area plot of the minor fold axes of this phase on the two limbs of the fold in the Dry Hill Gneiss east of Jerusalem Hill that were measured in the surrounding quartzite member. While the separation of asymmetry of the minor folds between the two limbs is not perfect, it supports the hypothesis that this structure is a fold rather than a stratigraphic pinch-out. The double hook map pattern of the biotite schist in the quartzite member could be interpreted as a refolded fold pattern, but is actually a result of the lens-shaped body of schist being folded by this fold system (Plates 2 and 3, sections B and C).

Figure 8b is an equal area plot of all first phase minor fold axes. The diverse trends of the axes are a result of later folding and the curved nature of the major hinges. The original orientation of

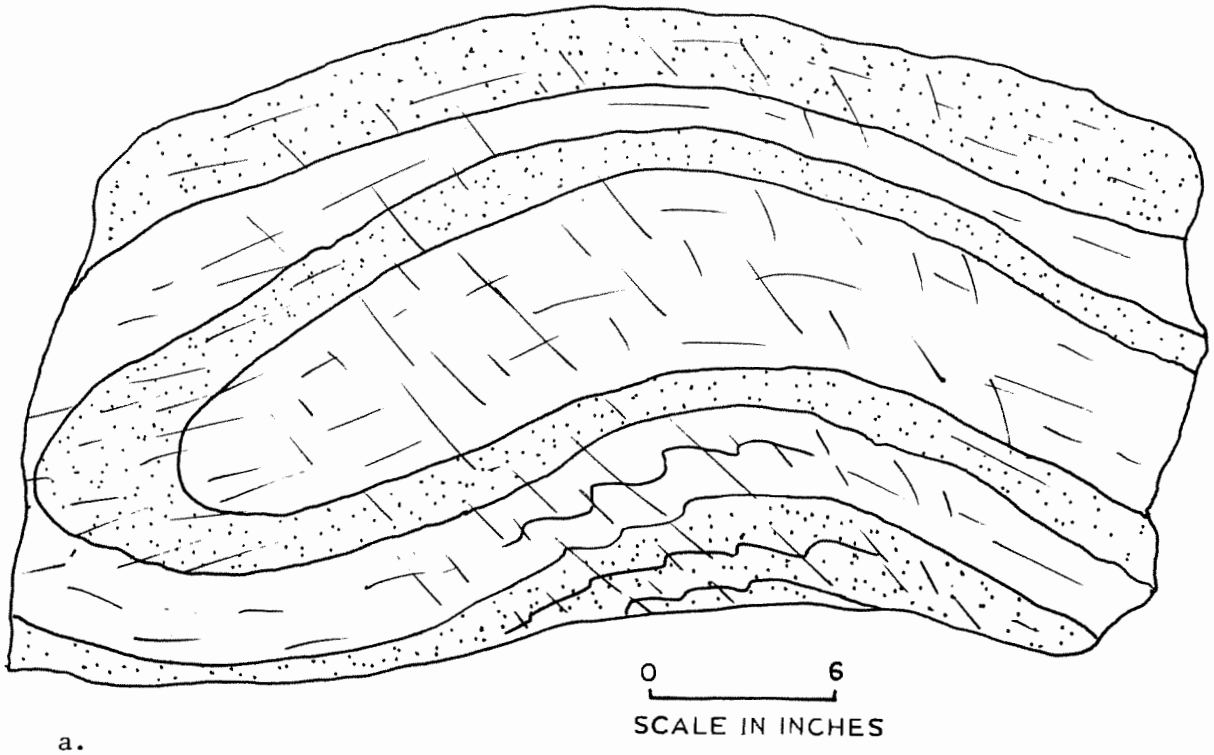

a.

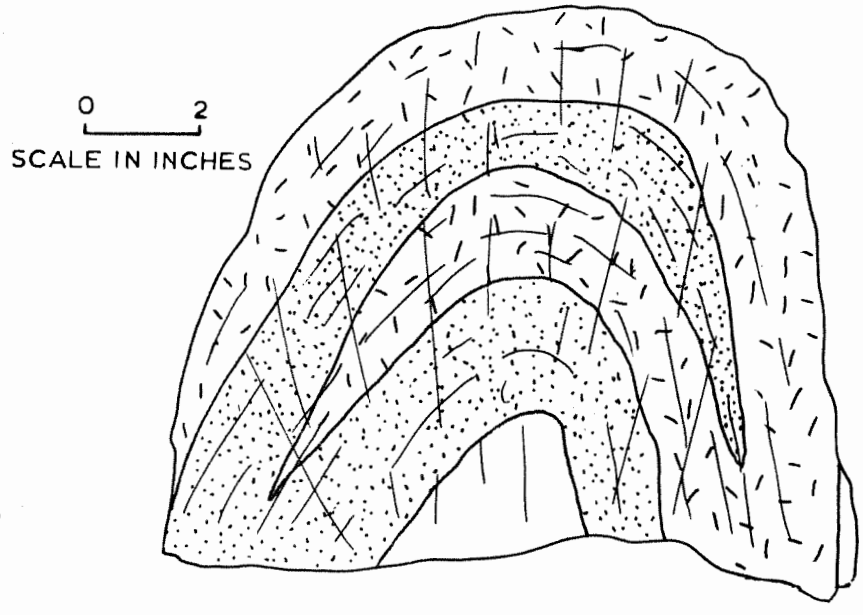

b.

Figure 7. First phase folds refolded by third phase folds in the quartzite member. a. Sketch of photograph of refolded fold on Bear Mountain. First phase fold is isoclinal and third phase fold is asymmetric. Note the development of incipient third phase axial plane foliation. Both axes plunge into the diagram and trend NW. b. Sketch of loose block of quartzite illustrating first phase fold refolded by third phase fold.

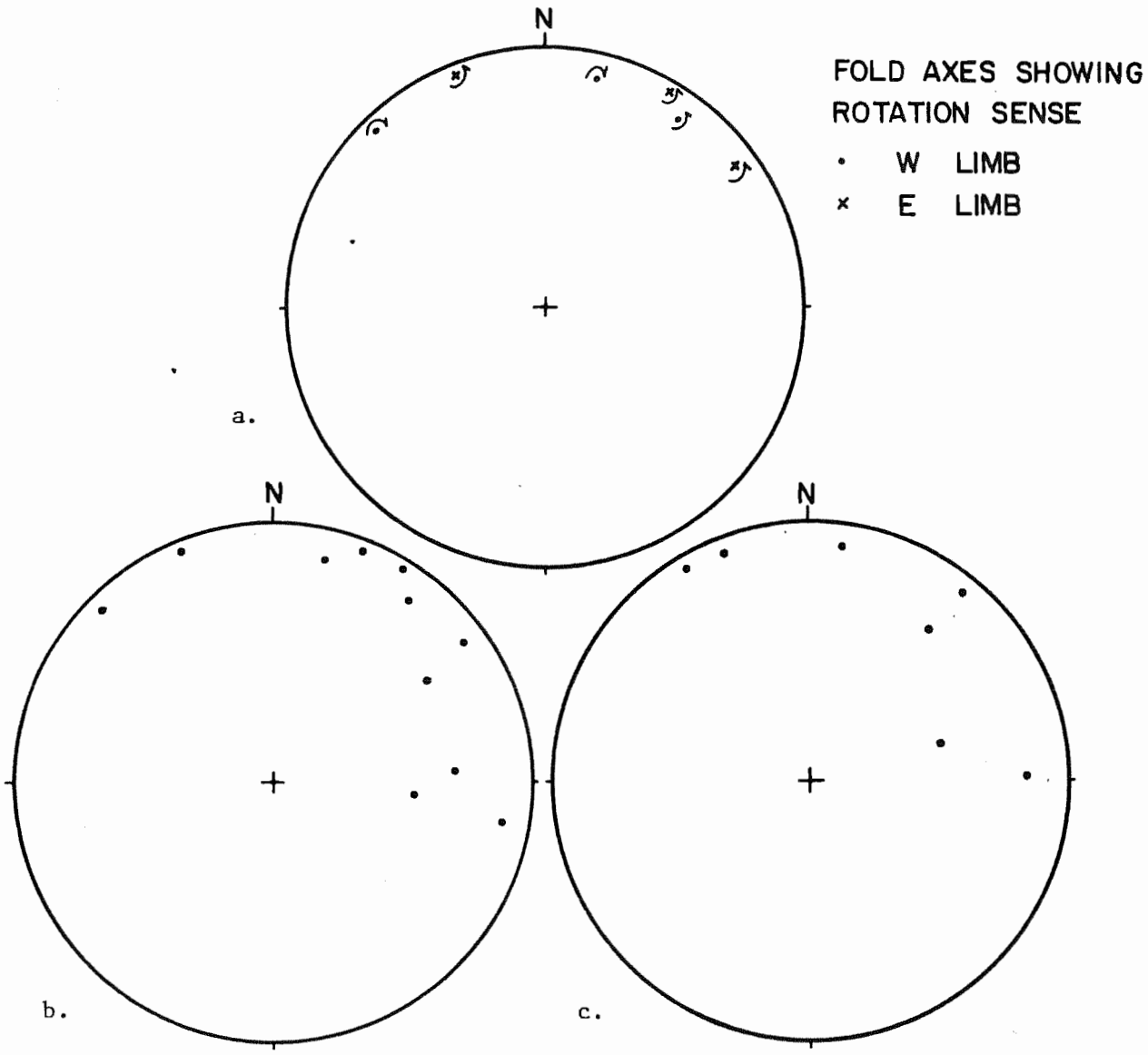

Figure 8. Equal area plots of first phase features. a. Minor fold axes measured in the quartzite member on the two limbs of the fold in the biotite member, east of Jerusalem Hill, showing separation of asymmetry. b. All fold axes measured in the study area. c. Lineations formed by the intersection of bedding and foliation measured in the study area.

these axes can only be guessed from the map pattern where they seem to be trending in diverse directions based on connecting hinges (Plate 2). Lineations formed by the intersection of bedding and foliation in the hinge areas (Figure 8c) do, however, mostly trend between north and east. Whether this is an original orientation or a modified one is not certain. If the fold interpretation of the map pattern is correct, then the hinge lines would be curved over a distance of several miles. Based on elevations of the hinges on the geologic map (Plate 2) the hinge goes through a depression between the area east of Jerusalem Hill and Dry Hill. The cause of this depression is not known. A structural relief diagram of this fold system is shown in Figure 9.

Planar features. The major planar feature associated with this phase is the regional foliation which has an axial plane orientation with respect to the folds of this phase. It is very close to parallel to bedding except at the fold hinges where it intersects bedding at high angles.

Lineations. No mineral lineations of this phase were found, but several lineations formed by the intersection of bedding and foliation were measured. These trend N or NE (Figure 8c) in essentially the same direction as the minor fold axes (Figure 8b).

Kinematics. The similar fold style and strong foliation indicate folding occurred by passive slip or passive flow in planes parallel to foliation. Folding must have been accompanied by regional metamorphism as shown by the strong foliation. The local transport direction must have been parallel to foliation with a strong E-W component based on the curvature of the axes (Figure 9) limiting the direction of movement.

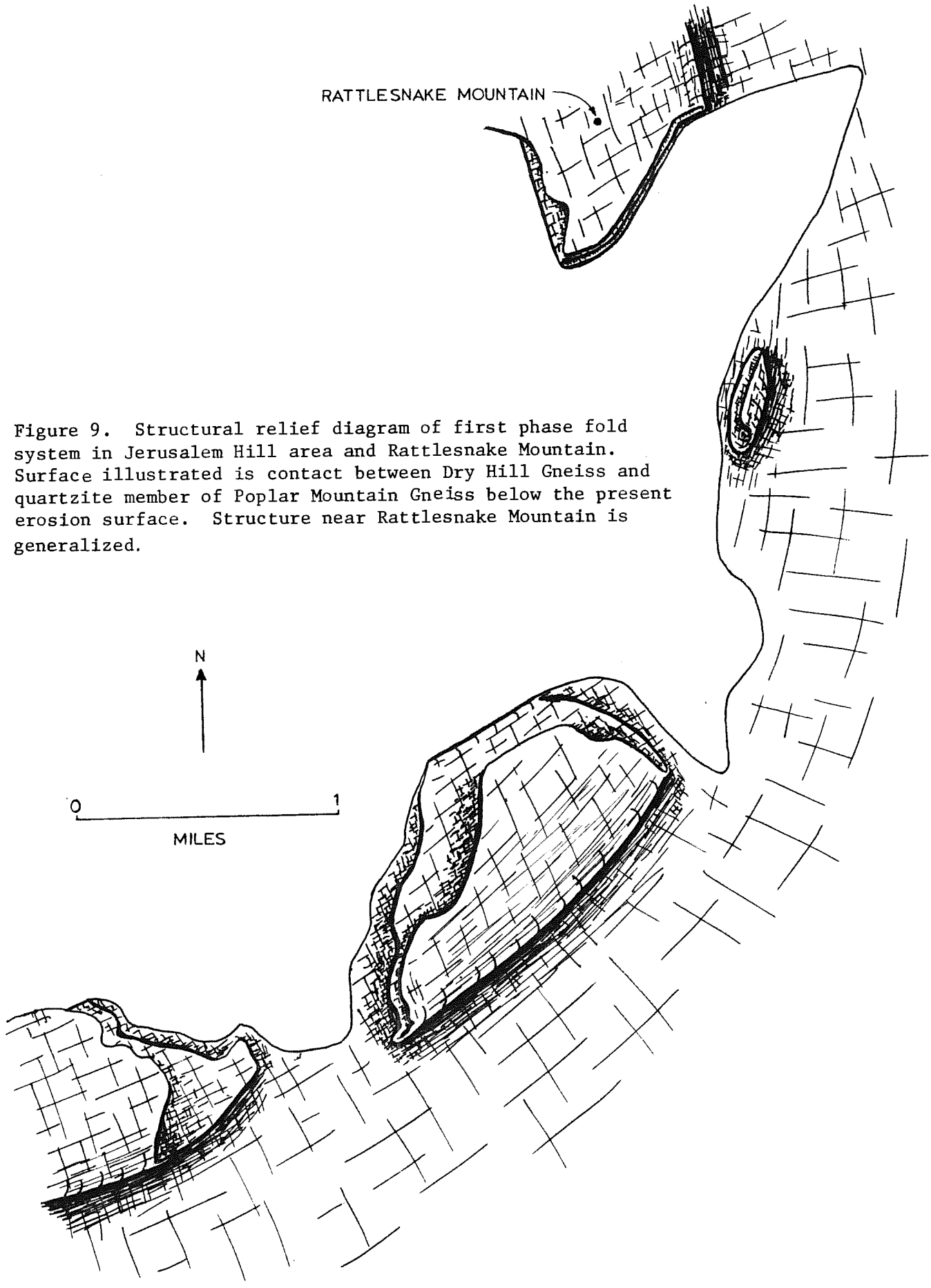

Figure 9. Structural relief diagram of first phase fold system in Jerusalem Hill area and Rattlesnake Mountain. Surface illustrated is contact between Dry Hill Gneiss and quartzite member of Poplar Mountain Gneiss below the present erosion surface. Structure near Rattlesnake Mountain is generalized.

Relation to regional structural features. These folds are thought to belong to one of the two regional generations of recumbent folds discussed earlier in this chapter (1A or 1B of Robinson, 1967a). All the rocks in the map area are on the overturned limb of a major recumbent fold since the stratigraphy is thought to be inverted (Ashenden, 1971, 1973). If this is true, then the gross movement sense of the larger recumbent fold as shown by the asymmetry of the map pattern in the Jerusalem Hill area would be upper layers east towards west with respect to the bottom layers (Figure 10b). This is in conflict with the findings of Robinson (1963) and Ashenden (1971, 1973) to the north, where they interpret the movement to be west towards east based on the map pattern in the vicinity of Crag Mountain, 12 miles northeast of the Jerusalem Hill area (Figure 10a).

This conflict could be resolved in several ways. The fold in the Jerusalem Hill area might be on the limb of a fold intermediate in size to the regional fold giving the wrong asymmetry for the regional fold, but such a fold is not evident. Another way to explain minor folds on opposite limbs having the same rotation sense is by superimposing a second generation fold on the first with its flow planes inclined at a low angle to the early flow planes as shown in Figure 11. If this is the case in the Jerusalem Hill area then the recumbent folds seen in the map pattern are not the earliest structure in the region, but would appear so if the only foliation seen is that of the second generation folds. There is no evidence for two foliations, but perhaps the later foliation obliterated the early one in the hinge regions of the folds such as those at the Jerusalem Hill area.

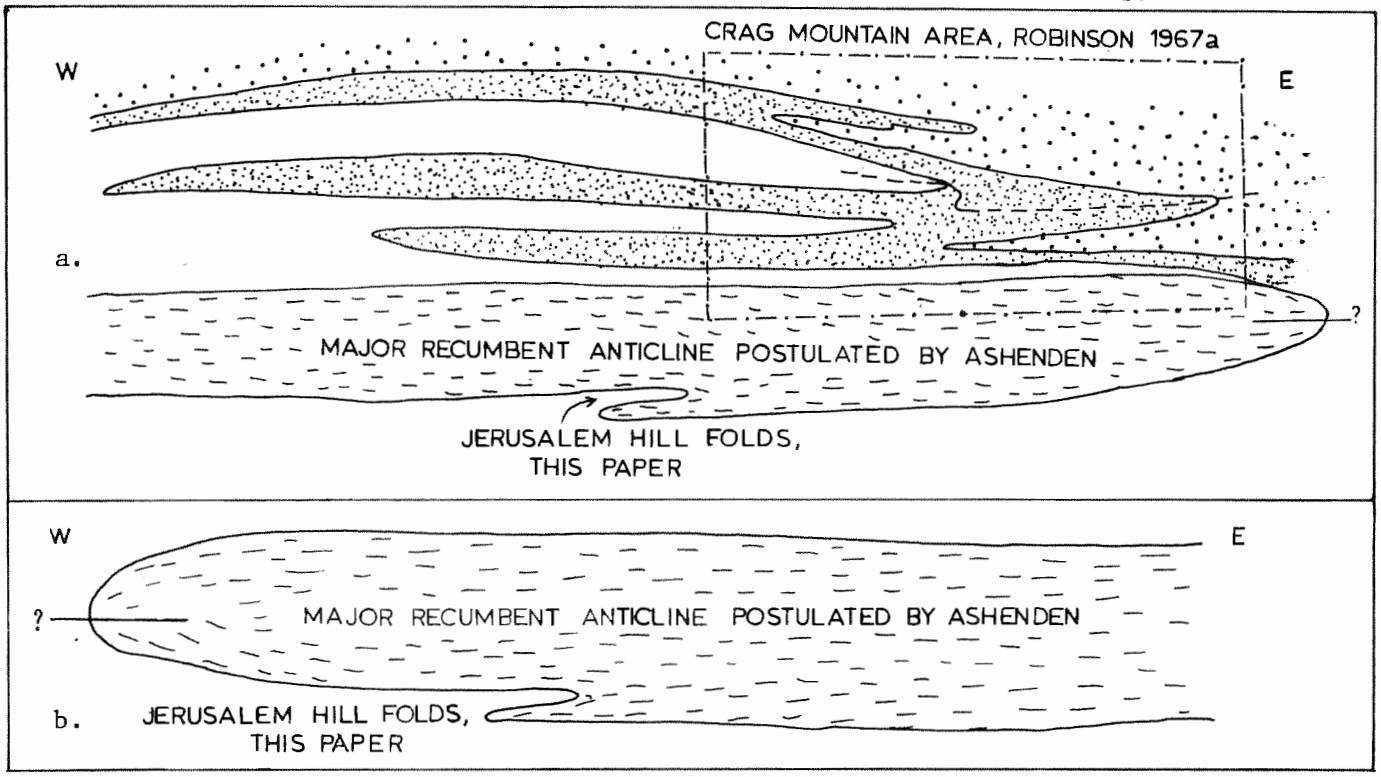

Figure 10. Major folds shown schematically required by the presence of minor folds in a. Crag Mountain area, b. Jerusalem Hill area.

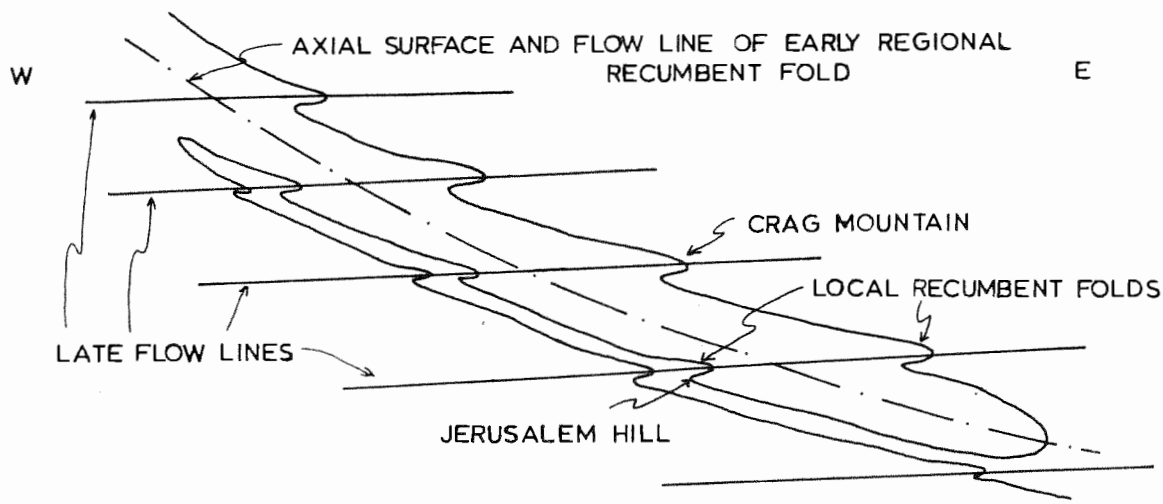

Figure 11. Diagramatic sketch illustrating proposed hypothesis to explain minor folds with the same movement sense on both limbs of early recumbent fold. Angle between early and late flow lines is greatly exaggerated.

Second Phase-Main Phase of Gneiss Dome Formation

Minor folds of this phase were found only in a few isolated localities with the best being in the quartzite member of the Poplar Mountain Gneiss on the SW flank of Bear Mountain. No folds in the gneiss members were found that could positively be related to this phase. The age distinction is based on the fact that these folds fold both foliation and bedding,but are refolded by later phase folds.

Folds. Five folds of this phase were identified and where seen they are generally tight, but not isoclinal and appear to be "similar" in profile. Figure 12 is an equal area plot of the five fold axes, showing no maximum. Some of these axes are steeply plunging as compared with folds of all other phases. This along with the apparent tightness is probably a result of later refolding.

Planar features. The only planar feature noted in association with these folds is a weak incipient axial plane foliation.

Lineations. Mineral lineations were seen that are parallel to the axial directions. Mineral lineations of the folds, where undistrubed by later folding, are parallel to the prominent regional lineation.

Kinematics. If the folds have a similar fold style then they were probably formed by a passive mechanism. This generalization is rather tenuous since few folds of this phase were observed.

Relation to regional structural features. Based on the observed parallelism of some of the second phase fold axes and their incipient mineral lineations with the prominent regional mineral lineation, this phase is believed to be related to the formation of gneiss domes (regional fourth phase as described above, 2B of Robinson, 1967a), but their scarcity makes other interpretations possible.

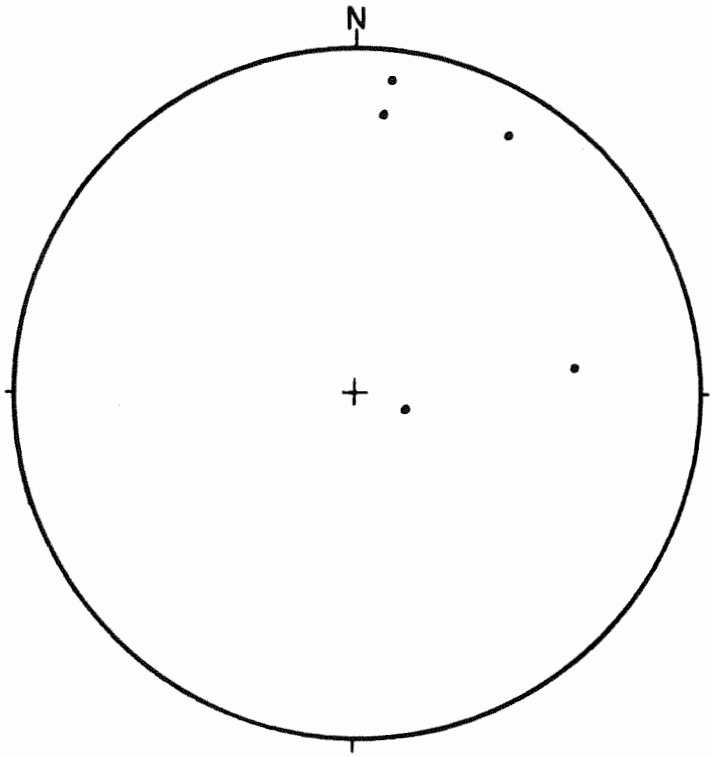

Figure 12. Equal area plot of all second phase fold axes measured in the Jerusalem Hill area.

Third Phase-Late Asymmetric Folds

The majority of the minor structural features seen in the area belong to this phase. Structural features of this phase are found in all rock types, but are especially well developed in the Poplar Mountain Gneiss, quartzite member. Two areas of exposure of quartzite, east of Jerusalem Hill and the southwest flank of Bear Mountain, provide excellent opportunities for detailed examination of the effects of this phase of deformation. The relative age of these structural features can be readily seen. Folds of this phase fold the dominant mineral lineation related to the second phase and the regional foliation which is axial planar to the first phase recumbent folds. They are then deformed by fourth phase shears and fifth phase extensional features.

Folds. The folds of this phase were studied in great detail and were of particular interest for the following reasons: 1. They appear in diverse orientations and styles. 2. Their movement line is almost parallel to the regional mineral lineations. 3. They occur in great abundance in the core of the northern portion of the Pelham dome, but are extremely rare in the younger Paleozoic cover rocks to the east and north. 4. Their relation to the regional geology is not well known. For these reasons great emphasis was placed on deducing the origin and kinematics of these folds and their relation to other structural features.

An attempt is made here to describe as fully as possible the properties of these folds and to quantify properties wherever possible. The relative abundance of folds of this phase makes this type of analysis possible where it would not be so for folds related to other phases. The following properties were used in describing the folds:

1. Style: parallel or similar, symmetric or asymmetric.
2. Nature of hinge line: linear or curved, if curved does it lie in a plane or not?
3. Tightness of fold: interlimb angle.
4. Axial plane features: cleavage, foliation, etc.
5. Linear features other than fold axes: mineral lineation or bedding-foliation, bedding-cleavage intersections.
6. Height to width ratio (H/W): see Figure 13.
7. Depth to width ratio (D/W): see Figure 13.
8. Thickness ratio: ratio of measured thickness of bedding in nose (tn) to thickness of bedding on limb (tl) measured perpendicular to bedding: see Figure 13.

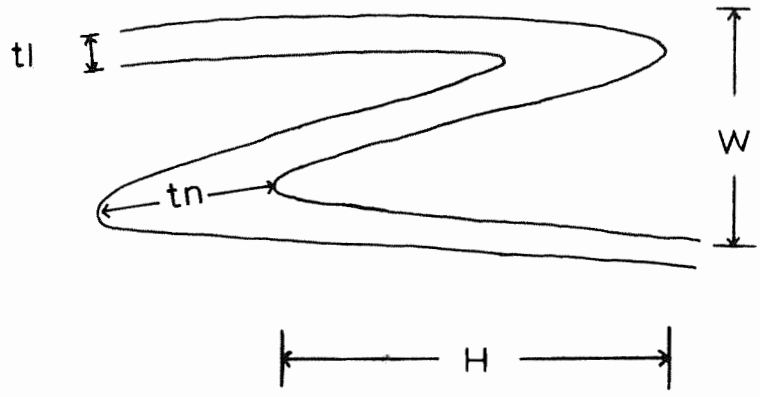

a.

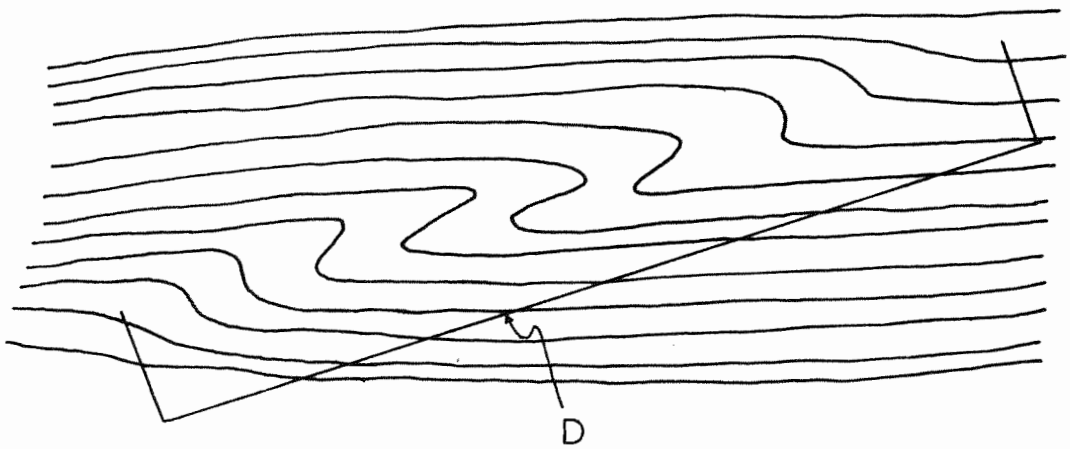

b.

Figure 13. Diagram of fold dimensions that were measured for describing third phase folds. a. tl thickness of limb measured perpendicular to bedding, tn thickness of nose measured perpendicular to bedding, H height of fold, W width of fold. b. D depth of fold. All measurements were taken as close to perpendicular to the fold axis as possible.

9. Movement line: tectonic transport direction determined by various means.
10. Genetic classification: flexural slip, passive slip, etc.
11. Relation to earlier structural features: are various earlier features folded?

On the basis of these properties, the third phase-late asymmetric folds are summarized as follows:

1. Style: Generally parallel with 20-80% flattening, some similar especially in gneissic and schistose beds. All are asymmetric.
2. Nature of hinge line: Generally curved and in a plane.
3. Tightness of fold: Moderate, but highly variable, average interlimb angle is 45^{o} (n=150).
4. Axial plane features: Incipient fracture cleavage or foliation depending on lithology.
5. Linear features: Some weakly developed mineral lineation or intersection lineation of foliation and axial plane cleavage, both are parallel to fold axis.
6. H/W: Mode 1.75 variable (n=68).
7. D/W: Mode 6.5 highly variable (n=31).
8. Thickness ratio: Mode 1.75 (n=60).
9. Movement line: N5W-N5E $10\text{-}19^{o}$, determined from several methods in three separate locations.
10. Genetic classification: Generally flexural slip modified by flattening. Some passive slip folding in the less competent beds.

11. Relation to earlier planar features: Folds both bedding and the regional foliation.
12. Relation to earlier linear features: Folds strong N-S mineral lineation of the second phase by great circle rotation (some originally small circle?).

Planar features. The only planar features associated with these folds are incipient axial plane foliation or cleavage. The foliation commonly occurs in gneissic or schistose rocks while fracture cleavage appears in some of the quartzite beds.

Lineations. Lineations associated with this phase are rarely observed. Where present, they are either a weak mineral lineation or an intersection between bedding and foliation or cleavage and are parallel to the axes of adjacent folds.

There is a possibility that the dominant mineral lineation of the area is a tectonic "a" lineation associated with this phase even though it is folded by the asymmetric folds. It is statistically parallel to the determined movement lines and is an extremely pervasive feature. This possibility will be discussed in detail in a later section.

Quantitative study of fold geometry and style. The style of the folds can be used to deduce the mechanism of folding. One method to study quantitatively the style is to measure the bed thickness in the manner described by Ramsay (1961). Folds were traced from photographs or slabs and measured for bed thickness perpendicular to bedding (t) and parallel to the axial plane (T) at various locations around the fold (Figures 14, 15, 16, 17, and 18). In ideal cases (t) will be

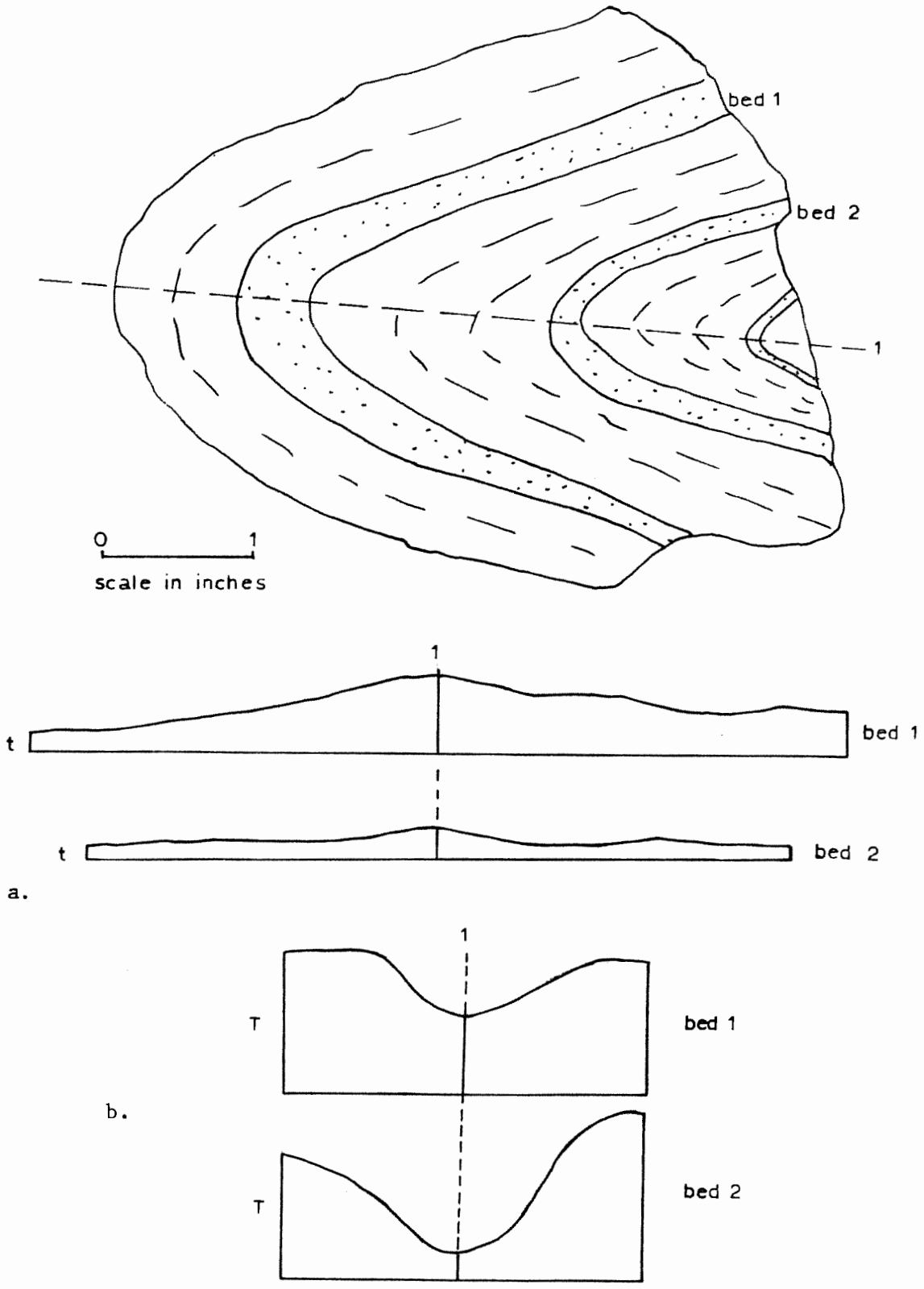

Figure 14. Sketch of third phase fold drawn from polished slab with graphs of thickness of beds 1 and 2. Both beds are quartzite-rich interbedded with gneisses. a. (t). b. (T).

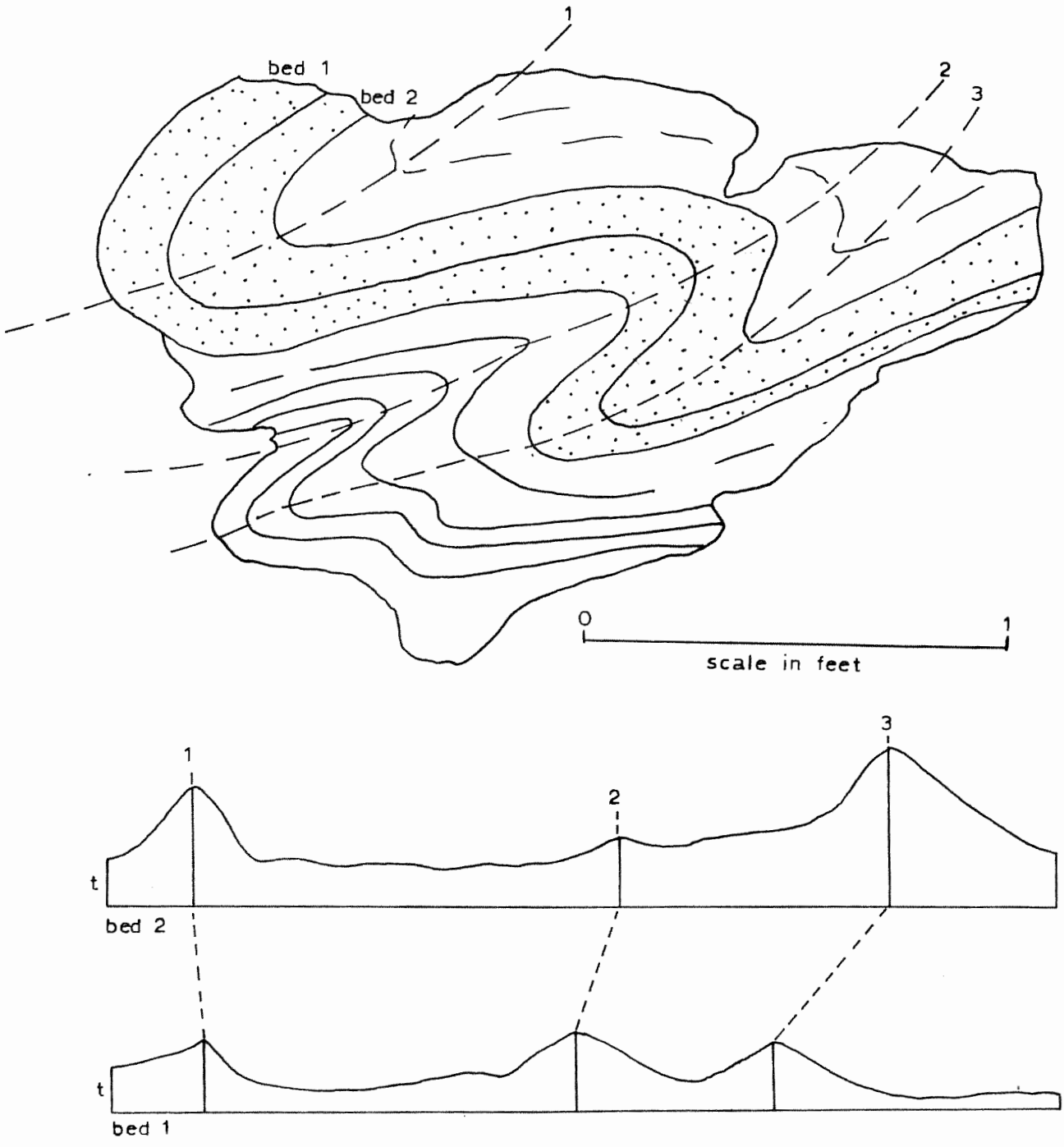

Figure 15a. Sketch of third phase fold drawn from photograph with graphs of thickness (t) of beds 1 and 2. Both beds are quartzite-rich gneiss interbedded with gneisses.

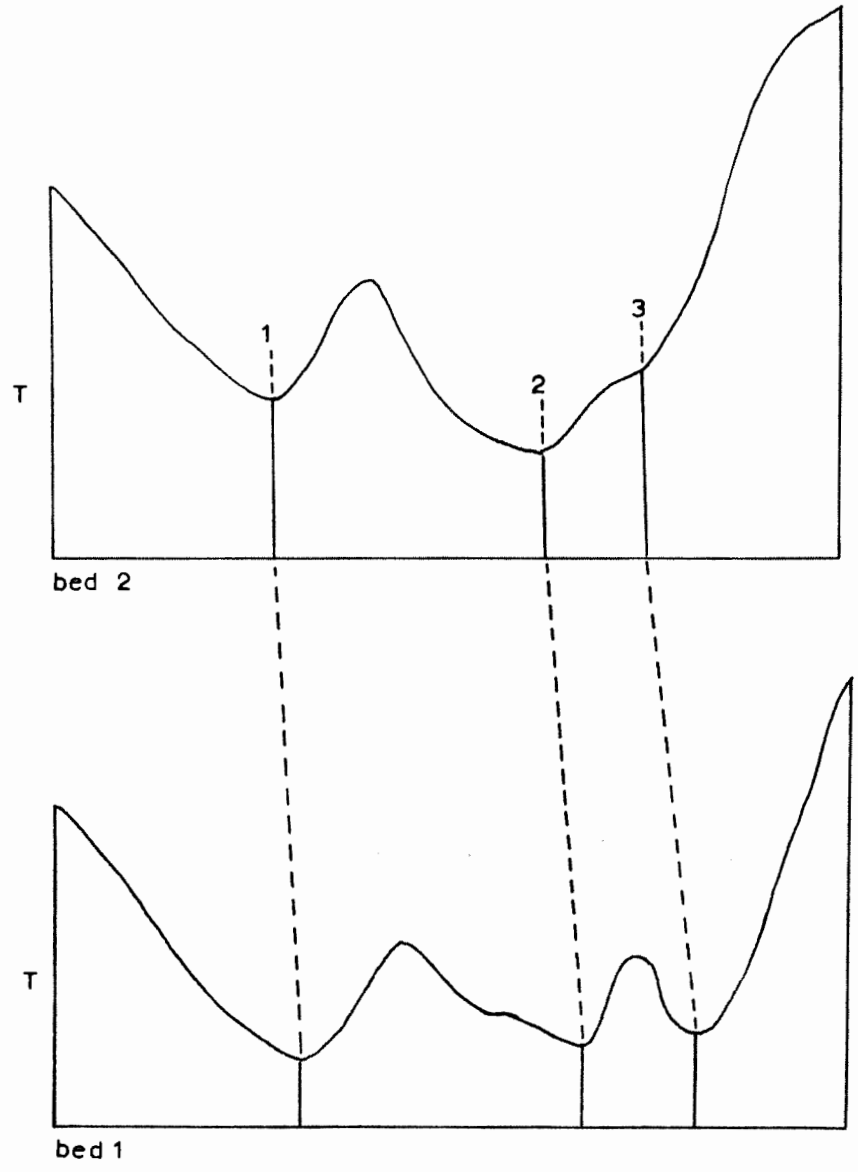

Figure 15b. Graphs of thickness (T) of beds 1 and 2.

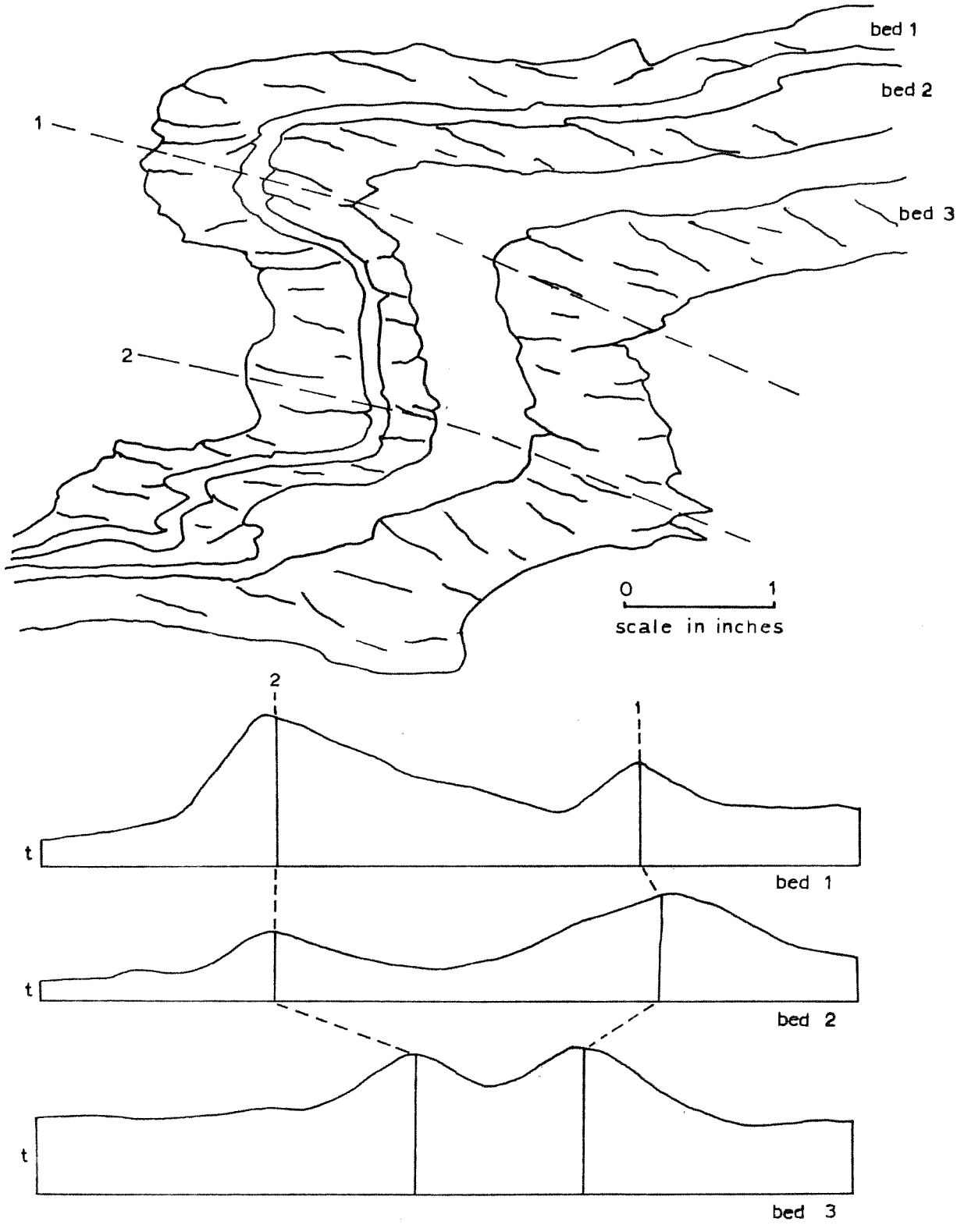

Figure 16a. Sketch of third phase fold drawn from photograph with graphs of thickness (t) of beds 1, 2, and 3 all of which are quartzite interbedded with gneissic layers. Note the development of incipient axial plane fracture cleavage in the quartzite beds.

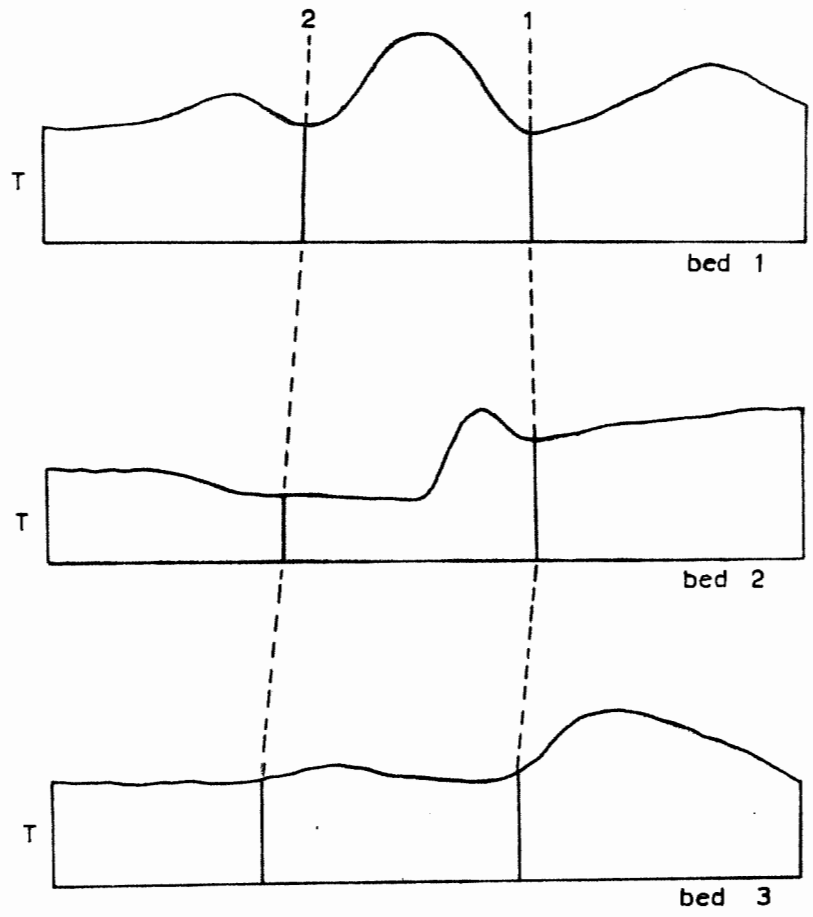

Figure 16b. Graphs of thickness (T) of beds 1, 2, and 3.

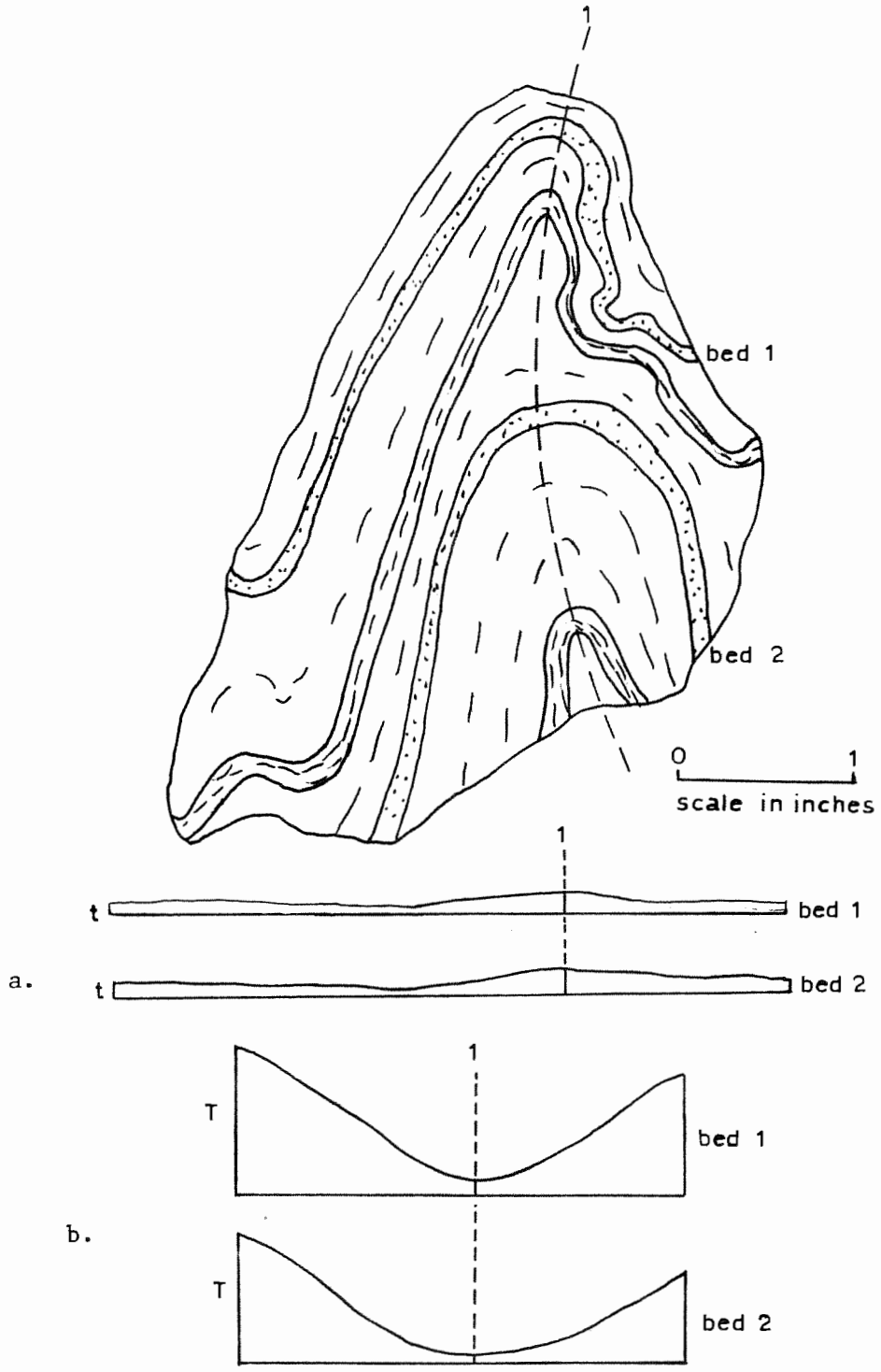

Figure 17. Sketch of third phase fold drawn from polished slab with graphs of thickness of beds 1 and 2. a. (t). b. (T). Both beds are quartzite beds interbedded with amphibolitic and gneissic layers.

constant for pure parallel folds and (T) will be constant for pure similar folds. The beds measured in the first four folds (Figures 14, 15, 16, and 17) were predominantly quartzite from zones of interbedded quartzite and gneiss or amphibolites. The graph of (t) shows small, but significant variations especially in the hinge areas indicating the folds are not pure parallel folds. The graph of (T) shows large variations indicating the folds are not purely similar in style. The variations in (t) in the quartzite beds, as Ramsey (1961) points out, are most likely due to flattening of parallel folds, which is probably the case here since they are far from being similar folds. Another possibility is that they are a combination of parallel and similar fold styles.

If the folds in the quartzite are flattened parallel folds,then the amount of flattening can be calculated by a method described by Ramsay (1961). The fold is measured for thickness (t) at the nose and on the limb (t') where the dip of the bed is α with respect to a perpendicular drawn to the axial surface. The value of t/t' is calculated and along with α is converted to % flattening on a graph described by Ramsay (1961). This value then is the amount in % the fold varied from a pure parallel fold as a result of flattening. Table 5 summarizes sample values calculated for the folds in Figures 14, 15, 16, and 17.

Table 5. Summary of flattening percents of folds in figures 14, 15, 16, and 17.

Figure	axial surface	bed	% flattening
14	1	1	45
	1	2	32
15	1	1	35
	1	2	40
16	1	1	38
	1	2	46
	1	3	55
17	1	1	27
	1	2	35
		mean	39.4

The mean flattening for a number of folds predominantly in quartzites measured directly in the field is also around 40%, but the deviation is large. The deviation from the mean is dependent on lithology, thickness of beds measured, and location of the fold with respect to the larger structural features. Bed thickness and location of the fold will affect the % flattening only slightly while lithology can exert considerable control. Less competent beds will tend to flatten more than will competent ones.

Although most of the folds seen in the quartzite beds were close to parallel in style, folds in the interbedded gneisses, schists and amphibolites displayed more of a similar style. Figure 18 illustrates

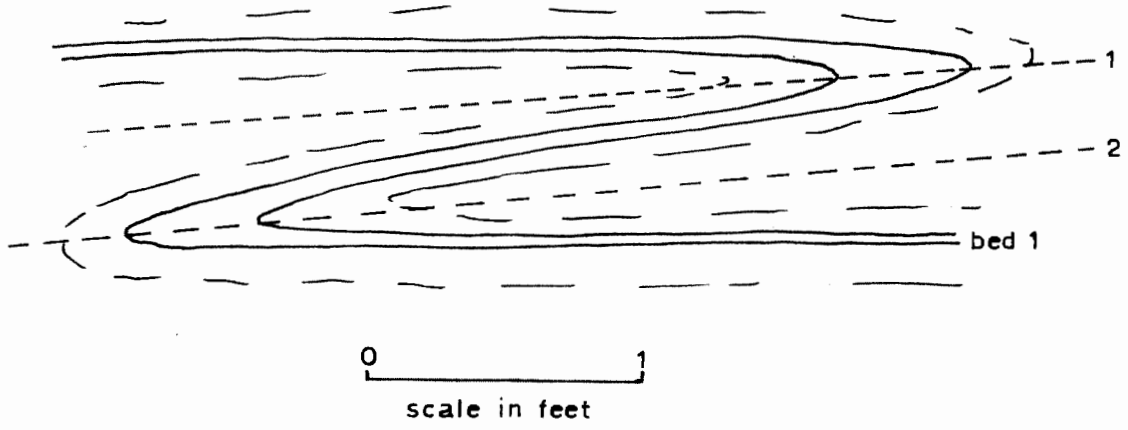

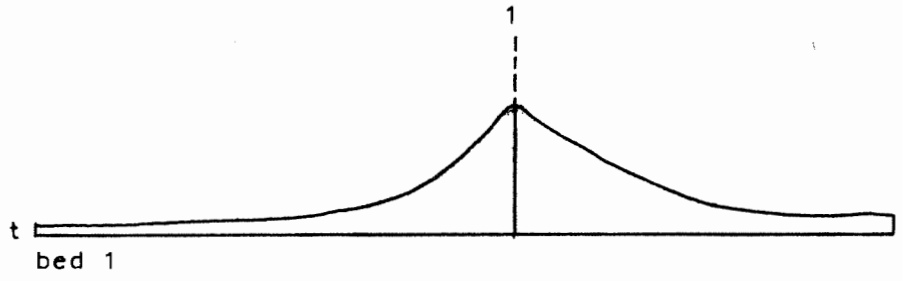

a.

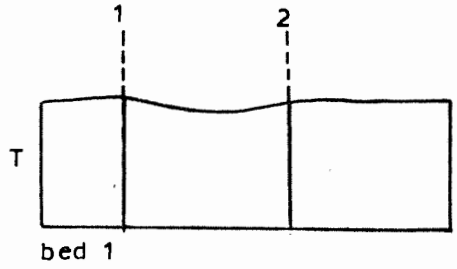

b.

Figure 18. Sketch of third phase fold drawn from photograph with graphs of thickness of bed 1. Fold is in amphibolite. a. Thickness (t) of bed 1 (only hinge 1 shown). b. Thickness (T) of bed 1.

one of these similar folds. The thickness (t) is highly variable while (T) is essentially constant showing that this fold approaches true similar style.

Due to the predominance of quartzite lithologies the dominant mechanism of folding in the quartzite member was by flexural slip with flattening accomplished by flow or slip. Interbedded gneisses, schists and amphibolites folded more by a passive slip or flow mechanism.

From the description of style it is evident that lithology played a significant role in determining the fold mechanism. The most important factor is the bedding anisotropies present during folding as determined by lithology (Donath and Parker, 1964). In zones where there were interbedded quartzites and gneisses or where bedding anisotropies are high, the folding proceeded by flexural slip in the competent layers with a combination of flexural slip and passive slip or flow in the weaker layers. Where there were thick zones of gneissic or other non-quartzite layers, bedding anisotropies were low and folding was accomplished mainly by passive slip or flow. It is doubtful that there was any folding purely by either flexural slip or passive slip or flow, but rather by some intermediate mechanism. It can be said, though, that quartzites tended toward flexural mechanisms while other lithologies tended toward passive mechanisms.

The role of lithology in the development of the folds can be further studied by examination of the data of the various fold dimensions: H/W, D/W, and thickness ratio (tn/tl). The data for these measurements was collected at two main quartzite localities, the SW flank of Bear Mountain and east of Jerusalem Hill. The data from

each locality was plotted separately then divided by lithology. For each ratio, the data was consistent for the two areas.

The H/W ratio for both areas shows a fairly well defined peak with moderate scatter (Figure 19a,b). This scatter expresses the wide variety of fold shapes seen in the area. Dividing the areas up into quartzite and gneissic rocks (Figure 19c,d), some segregation can be seen. The gneiss shows more of a tendency towards a consistent ratio than does the quartzite which was fairly evenly distributed.

The D/W ratio was measured with some difficulty due to the limited number of D measurements available. Figure 20 shows histograms for the two areas that show no well defined maximum. The limited number of data restricts any definite conclusions, but the histograms do illustrate the highly variable nature of the harmony of the folds. The high values represent the similar folds with large depth values while the lower values represent the parallel folds that are highly disharmonic. For this ratio there was no definite separation due to lithology.

The thickness ratio (tn/t1), which can more or less be related to the fold style, showed good results. For both areas there is a well defined peak at 1.5-2.0 (Figure 21a,b). Dividing the data into lithologies, it can be seen that the quartzite shows a more consistent ratio centered about 1.5-2.0 while the gneissic rocks are more evenly distributed and show slightly higher values (Figure 22a,b,c,d). Pure similar folds will have values around 7.0-8.0, while pure parallel folds will have a ratio of 1.0. The fact that the quartzite peaks at 1.5-2.0 shows that they are dominantly parallel folds. The variation

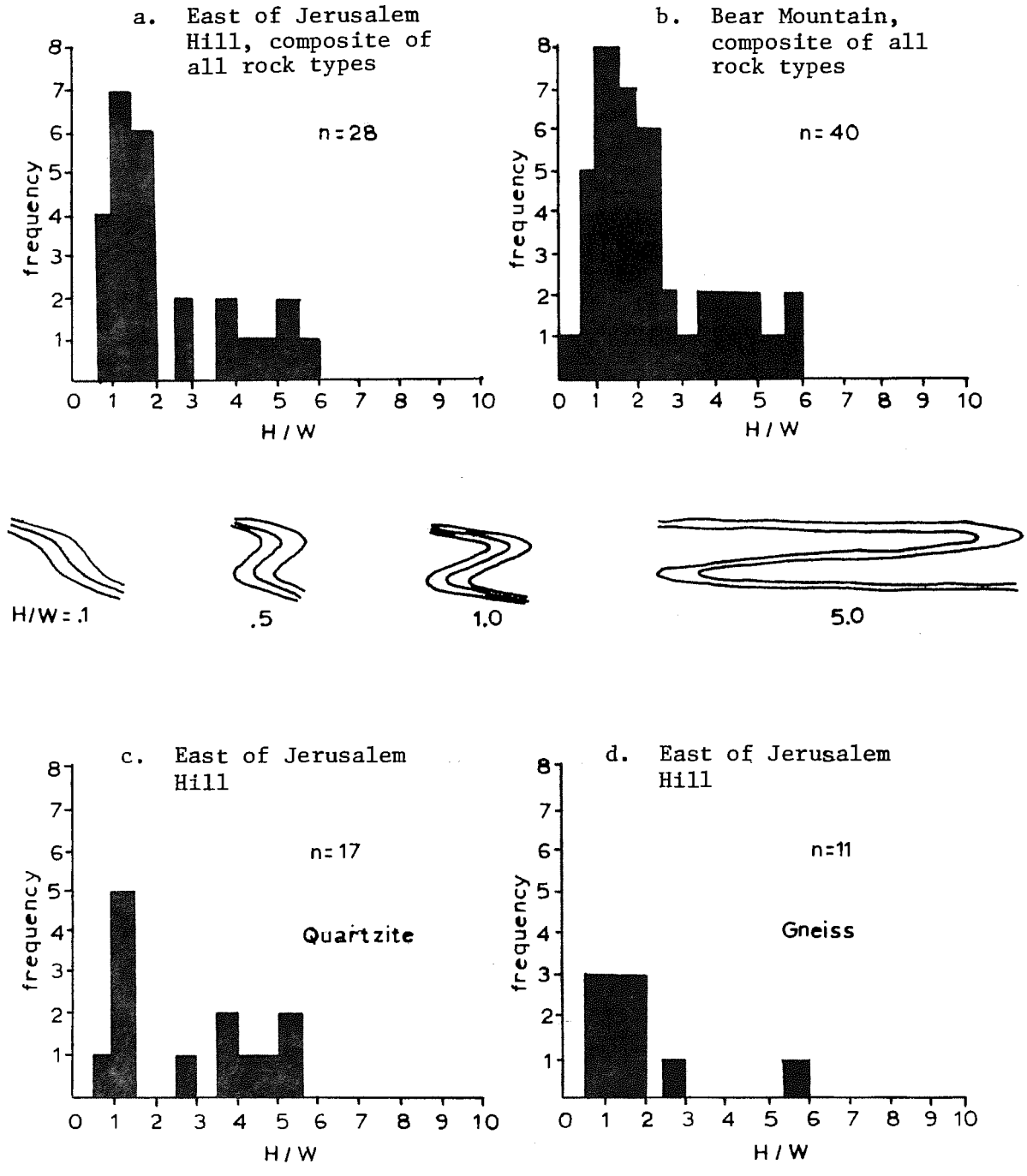

Figure 19. Histograms showing height-width ratios of third phase folds measured in the quartzite member. Folds shown in center illustrate various H/W ratios.

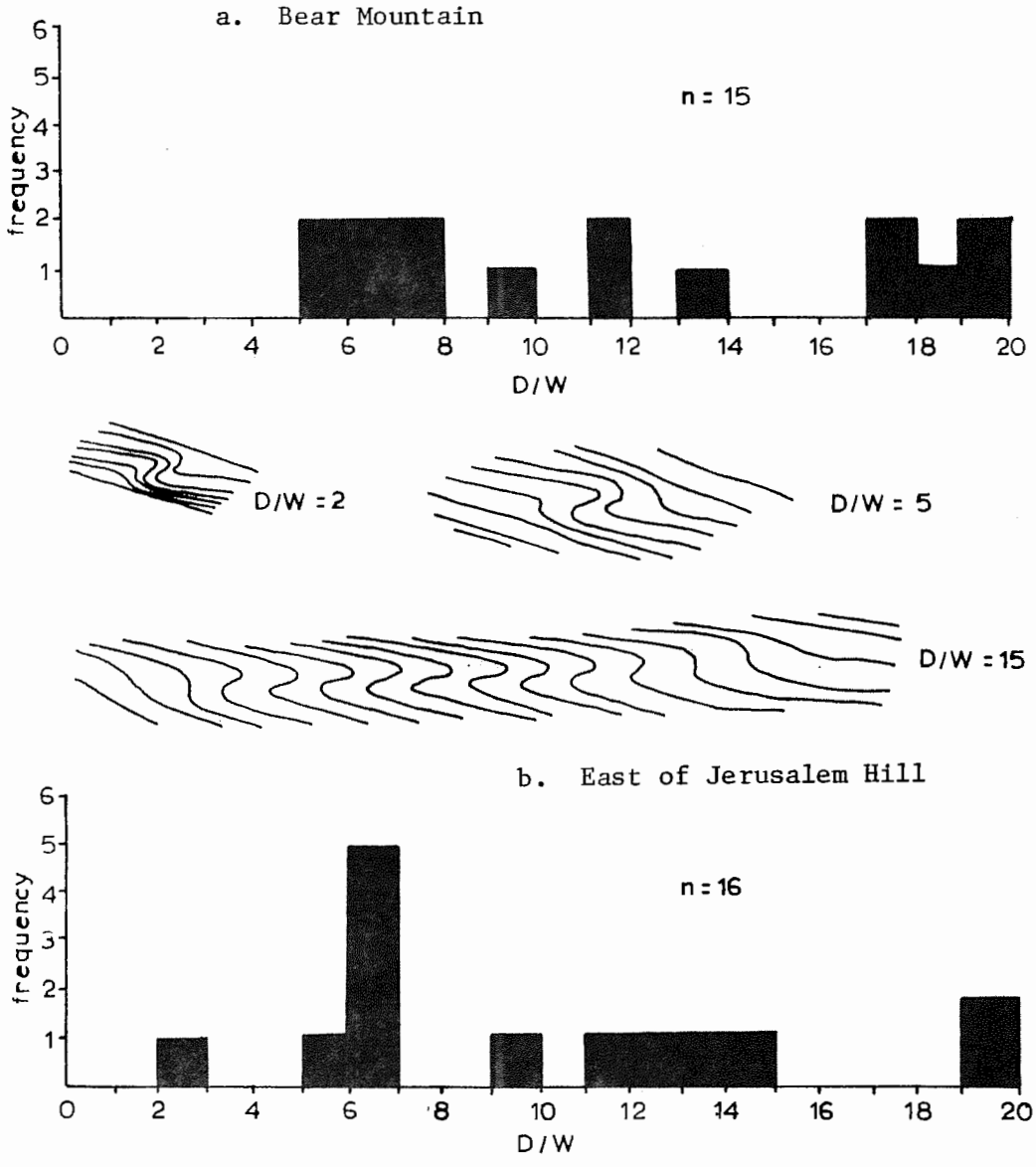

Figure 20. Histograms showing depth-width ratios of third phase folds measured in the quartzite member. Folds shown in center illustrate various D/W ratios.

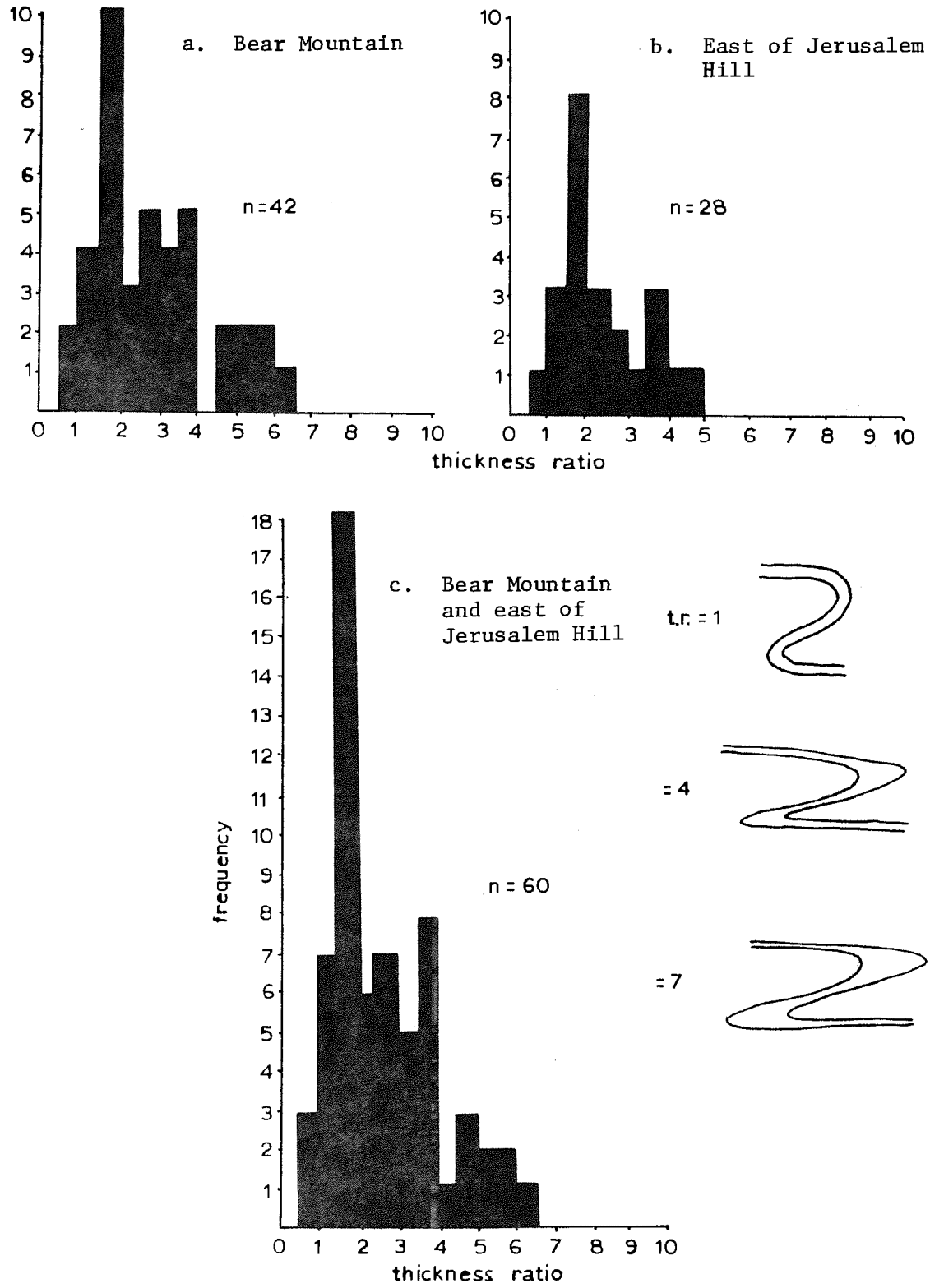

Figure 21. Histograms showing thickness ratios of third phase folds, composite of all rock types in the quartzite member. Folds at right illustrate various thickness ratios.

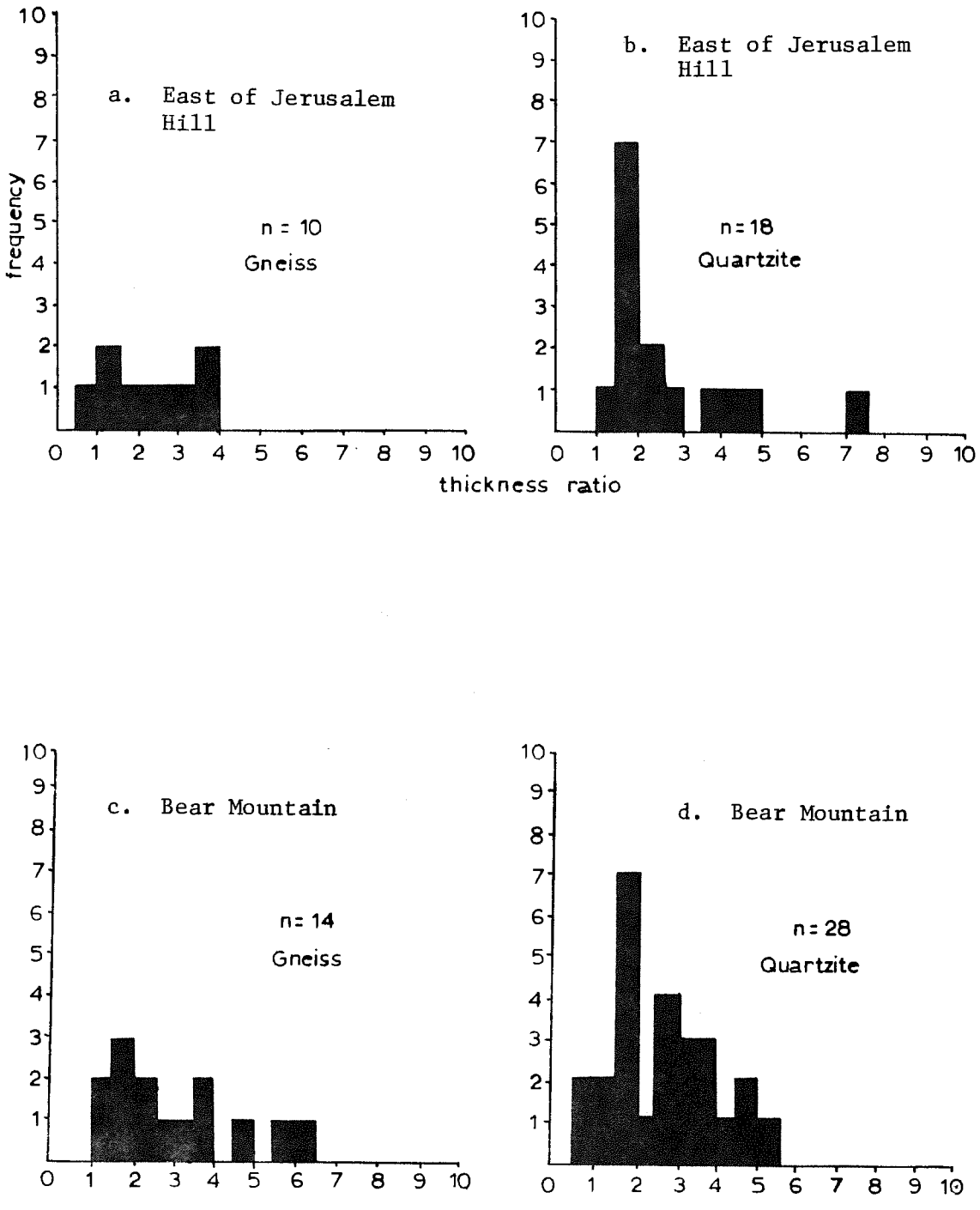

Figure 22. Histograms showing thickness ratios of third phase folds measured in the quartzite member.

from pure parallel folds is a result of the flattening or a combination of flexural and passive folding. It has been shown that the folds were flattened by an average of 40%. This would produce a thickness ratio close to 2.0, consistent with the peak defined by the quartzites. The 1.5-2.0 group could very well be a result of flattening of pure parallel folds by 40% rather than a combination of parallel and similar styles. The higher values shown by the gneissic rocks are consistent with similar folding present in a large degree in the less competent rocks.

Another method of examining the folding mechanism is by studying the folded lineations. Several folded second phase lineations were measured in the area. Almost invariably they define a great circle. Since most of the lineations were measured on gneissic beds there were no small circle rotations observed as would be expected on flexural folds. If there were any folded lineations that originally defined a small circle, subsequent flattening might tend to rotate the lineation towards a great circle. Since most of the mineral lineations were at a large angle to the fold axes, this rotation due to flattening would not need to have been very extensive to produce an apparent great circle distribution for the lineation.

Movement line and movement history. The movement history of the folds was one of the more interesting properties investigated. To examine the movement history, the movement line was calculated. The movement line or slip line for flexural slip folds, as is generally the case here, is the relative movement of one layer past another (Hansen, 1971). For the passive slip folds, the movement line is the

relative movement of adjacent particles (Hansen, 1971). The movement line was calculated by several methods from several areas to check any variations due to geography or method.

The first method is the determination of the separation angle (Hansen, 1971). For this method to be valid, the folds must be either flexural slip or passive slip folds and for the separation angle to contain the movement line, σ_2 must have been parallel to layering during folding (Hansen, 1971). It has been shown that the folds are probably either flexural slip or passive slip and σ_2 has been demonstrated by many workers (McIntyre and Turner, 1953; Scott, Hansen and Twiss, 1965; Carter and Friedman, 1965) to be parallel to layering during folding. The axes lie in a plane and can be divided into two groups of opposite asymmetry separated by some angle, the separation angle (Figure 23a,b,c). This plane in which the fold axes lie is the slip plane. It was determined by drawing the great circle of best fit through the fold axes. In all three areas , Northfield Mountain Underground Powerhouse, SW flank of Bear Mountain, and east of Jerusalem Hill, the separation angle is very small and consistent in orientation. The small variations in the orientation of the slip plane probably are a result of variations in the gross attitude of bedding, which would influence the orientation of the slip plane if flexural slip was important during folding.

The second method used to deduce the movement line is by determining the intersection of the plane containing a rotated lineation with the axial plane of the fold (Ramsay, 1956). The best results were obtained from folds in gneissic beds where passive slip

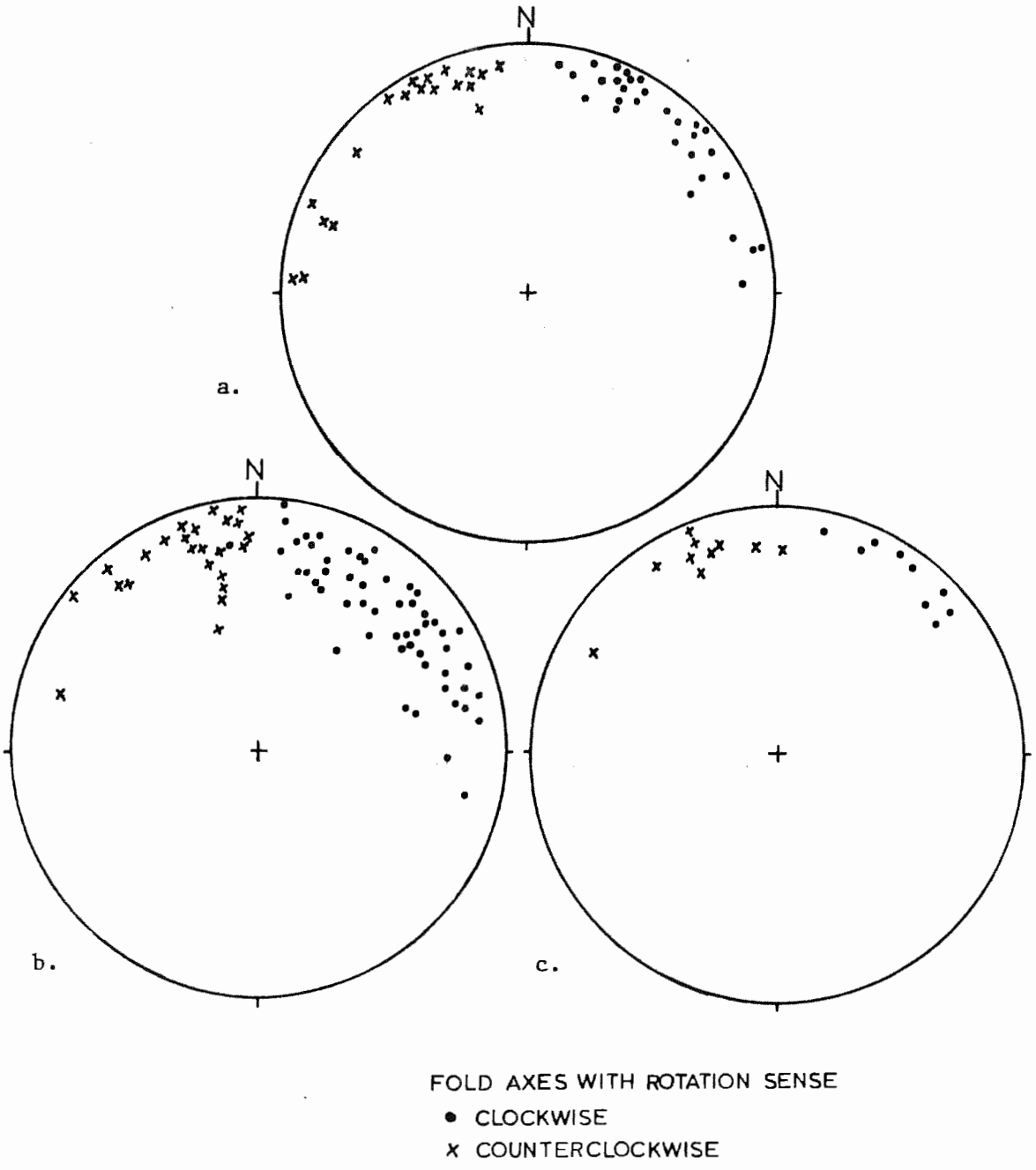

Figure 23. Equal area plots of third phase fold axes showing rotation sense. a. East of Jerusalem Hill. b. Bear Mountain. c. Northfield Mountain Underground Powerhouse measured by Robinson in Ashenden (1973).

folding was a likely mechanism. Figure 24a is an equal area plot of these intersections from three different locations within the Jerusalem Hill area. These results are consistent and agree with the separation angle measurements.

The third method is by plotting the intersections of great circles containing rotated lineations. Each great circle contains the movement line so their intersection defines it. Figure 24b shows beta intersections of five such great circles. Again, these results agree with earlier findings.

The overall consistency of these solutions is impressive and that they were measured from different areas several miles apart shows the pervasiveness of this deformation.

The consistency of the movement line and the pervasive nature of the dominant mineral lineation suggest that the two are related. As mentioned earlier, the two are statistically parallel (Figure 25). If this mineral lineation is an "a" lineation formed during this phase rather than during the second phase as previously interpreted, then it must have formed early in the development of the folds parallel to the tectonic transport direction and then was folded by continuing formation of folds.

The other possibility is that this lineation is an earlier formed "b" lineation belonging to the second phase. The best evidence for this is that most of the fold axes outside the Pelham dome and some inside are parallel to this lineation and may belong to an earlier phase of folding. If this is an earlier "b" lineation associated with folds of the main phase of dome formation three explanations are possible to explain the observed parallelism.

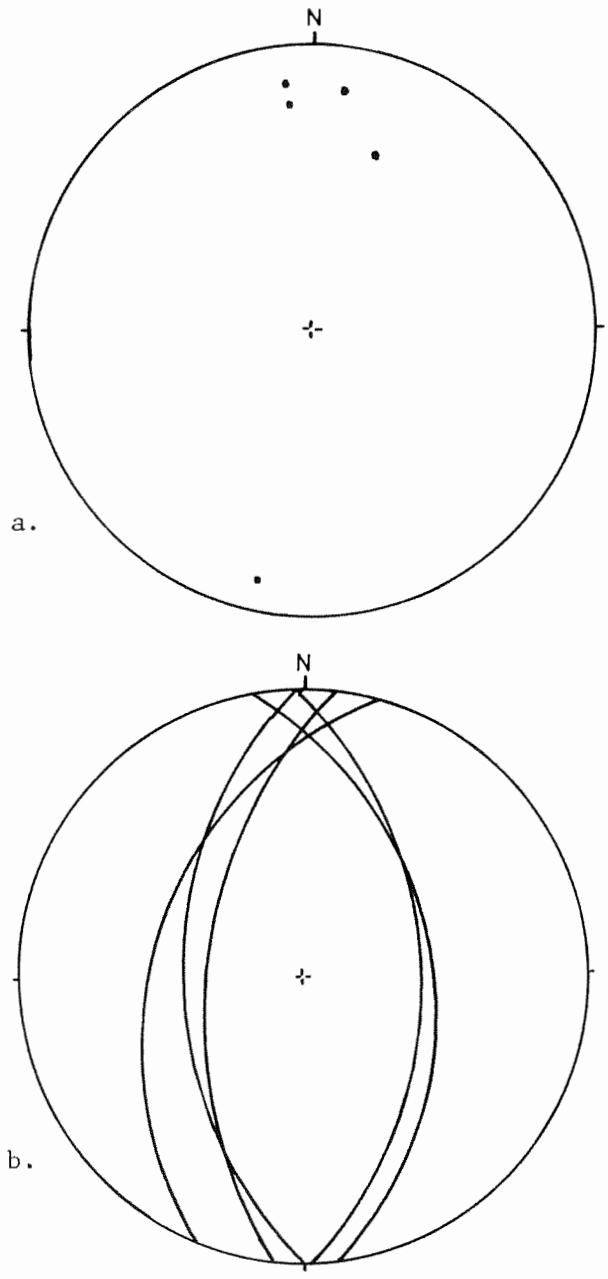

Figure 24. Equal area plot and beta diagram of movement line determinations from the Jerusalem Hill area. a. Intersection of plane containing rotated lineations with axial plane of fold. Five folds with rotated lineations were measured. b. Beta diagram of five planes each defined by a rotated lineation.

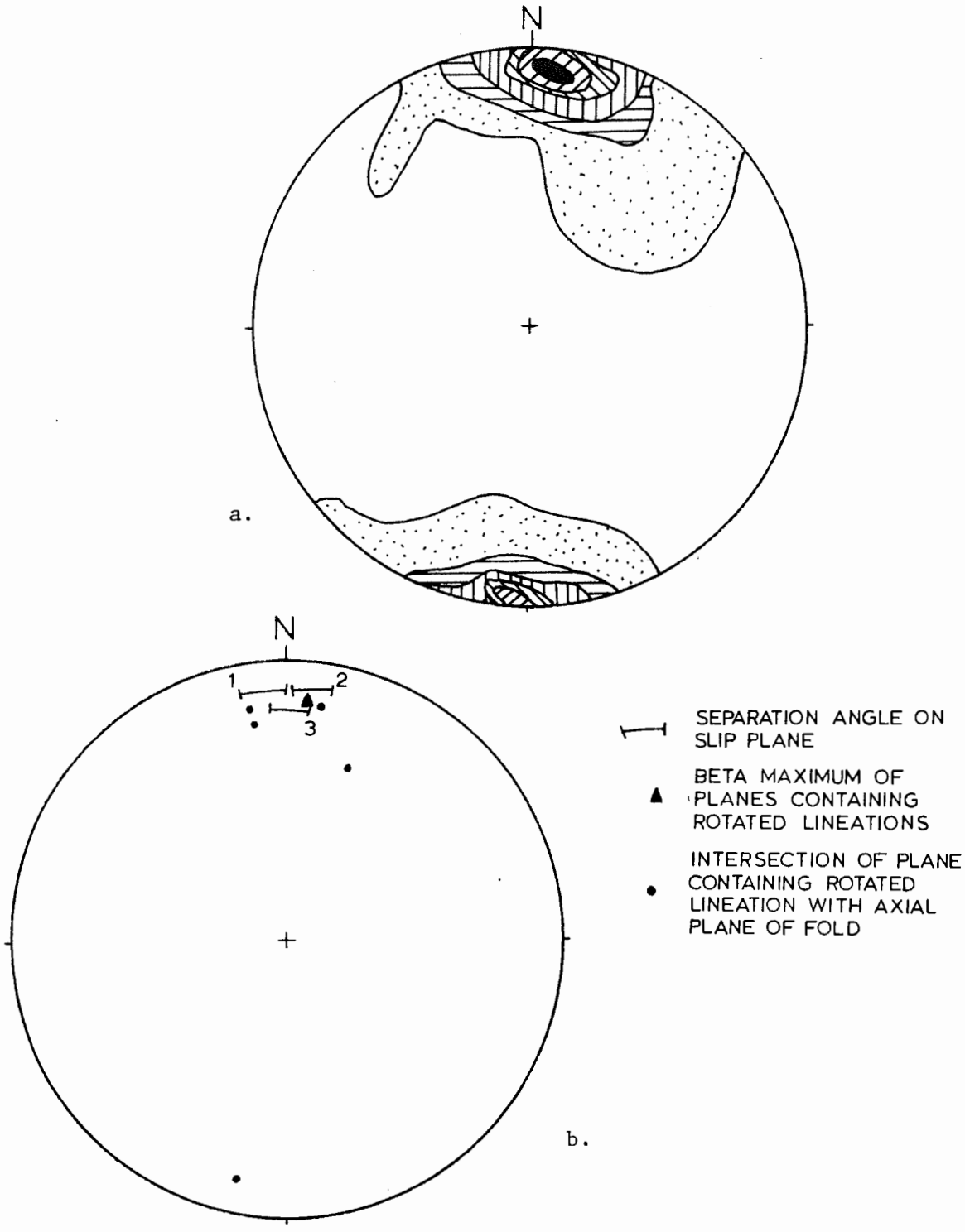

Figure 25. Comparison of regional mineral lineation orientation with movement line orientations of third phase folds. a. Contoured equal area plot of 175 mineral lineations from Jerusalem Hill area. Contours are 1, 4, 8, 12, 16, and 20 percent per 1 percent area. b. Summary of all determined movement lines in area. 1. East of Jerusalem Hill, 2. Northfield Mountain Powerhouse, 3. Bear Mountain.

1. The fold axes formed virtually parallel to the tectonic transport so both "a" and "b" lineations are parallel. This is supported by the presence of extremely elongated features such as stretched pebbles which are parallel to the dominant fold axes outside the dome. Elongated features can form both parallel and perpendicular to the fold axes, but are commonly elongated in the transport direction (Spencer, 1969; Ramsay, 1967).

2. The early formed "b" lineation could have been rotated from a former orientation during the third phase of deformation. It will be shown later that some of the third phase fold axes might have been rotated toward the movement line during this phase. If this phase is very extensive, it could have rotated all early linear features in the area into apparent parallelism with the transport direction. As this rotation proceeded, pebbles and other features would tend to be elongated parallel to the movement line resulting in the observed relations.

3. The third possibility is that the "b" lineation is parallel to the later "a" lineation just by coincidence and there is no genetic relationship between the two.

Large scale zones of folding on Bear Mountain. It was noted on the SW flank of Bear Mountain that the third phase folds were contained in distinct tabular zones which cut the bedding at a low angle (Figure 26a). The orientation of these zones is N70-85W, 10-20NE and the thickness varies from 20-60 feet. The orientation of these zones is approximately the same as the slip planes of the area determined by the separation angle method. These zones can be thought of as tabular

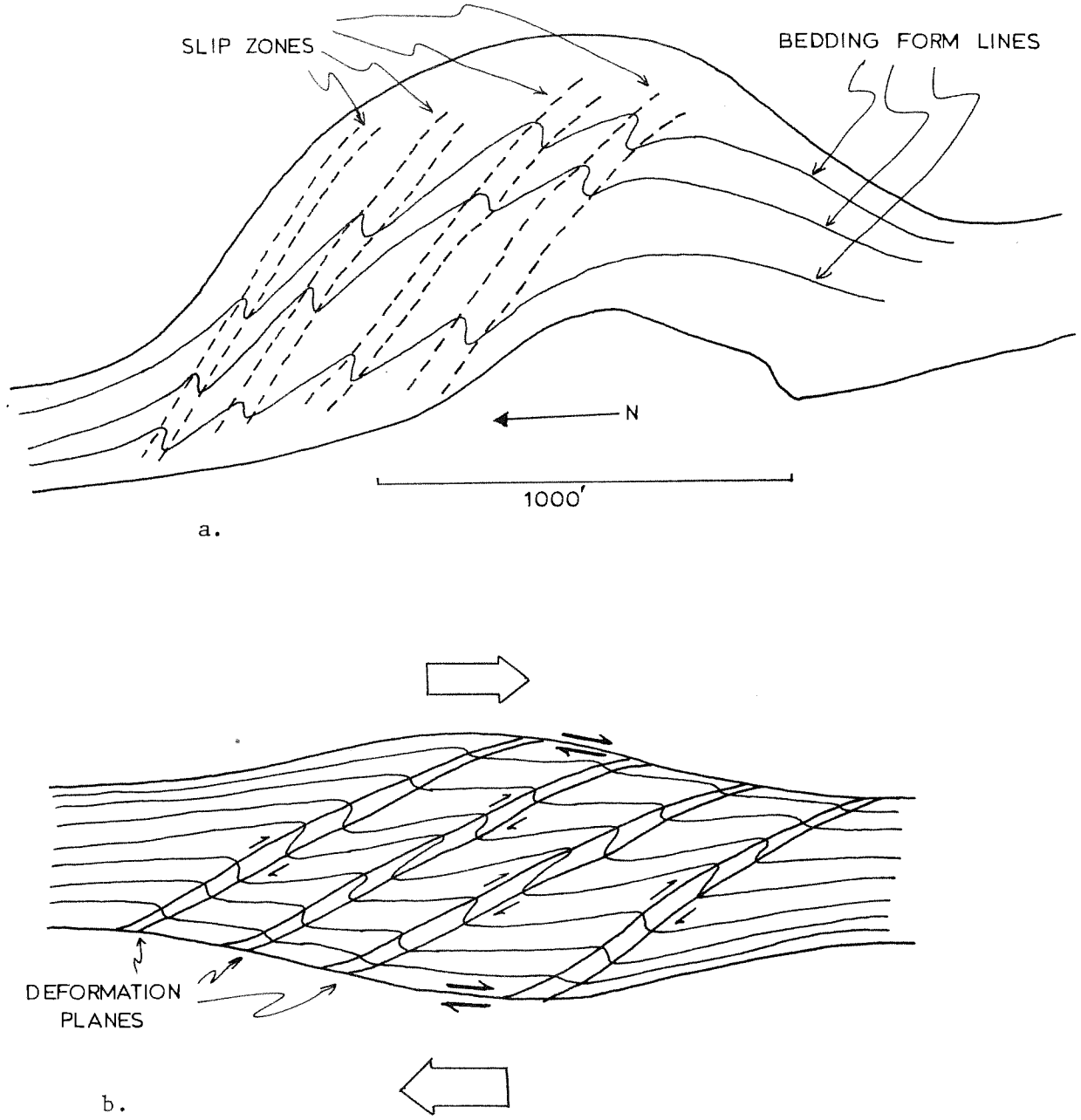

Figure 26. Diagrams of fold zones on the SW flank of Bear Mountain. a. Schematic enlargement of map of quartzite member on Bear Mountain showing orientation of slip zones with respect to sample bedding form lines. b. Hypothetical cross section through quartzite member showing deformation planes cutting through entire quartzite member. Small arrows indicate direction of slip caused by large shear couple shown by large arrows.

slip zones defining the areas of folding. The movement line determinations for Bear Mountain are the movement lines for these large zones. It is believed that during the third phase of deformation, the quartzite member acted as a relatively brittle bed in a ductile mass of gneisses and that movement took place along its boundaries. The movement was a result of a large shear couple acting on the area as seen in the asymmetry of the minor folds. The fold zones are where the movement occurring at the boundaries of the quartzite member moved through the entire quartzite member (Figure 26b). This process is similar to bedding plane thrusts jumping up-section, except that in this case the deformation was by folding rather than faulting. Throughout most of the region the quartzite member is relatively thin and contains few folds of this phase, but where these deformation planes crossed the section the member is thick and highly deformed. Although these tabular fold zones were not mapped elsewhere, it is strongly believed that most of the minor folds of this phase are contained in zones like them.

Axial plane fabrics. The axial plane fabrics of the third phase asymmetric folds were examined in an effort to detect any axial plane rotation during folding and to determine if σ_2 was parallel to layering during folding. Beta diagrams were used to study the fabric of the axial planes. Since the data for these folds contains folds formed by both flexural and passive mechanisms, it was decided to divide the data into these two groups. This was done by determining the dihedral angle between each axial plane and the slip plane of the folds of the Bear Mountain area using the slip plane determined by the separation

angle. Since passive slip folds by definition are folds with the slip plane as the axial plane, all folds with axial planes 15^{o} or less away from the slip plane were classified as passive slip folds (some may be passive flow). Those whose dihedral angle was 20^{o} or greater were classified as flexural slip folds (some may be flexural flow). This method induces some error as some flexural slip folds will have axial surfaces that are close to the slip plane. Where the rock type was recorded for a particular fold, folds in the flexural group are predominantly quartzites while those in the passive group are gneissic or schistose rocks. The beta diagram for the passive folds (Figure 27a) must be analyzed with caution since its pattern is a result of choosing only planes with similar orientations. The maximum in the NE quadrant may be significant, as will be discussed later. The beta diagram for the flexural folds (Figure 27b) shows a strong maximum trending NE. If this beta maximum is a result of axial planes of flexural slip folds with different initial orientations it can be used to see if σ_2 was parallel to layering during folding and also to determine the movement line by a method described by Scott and Hansen (1969). This method involves plotting the intersection of the slip plane with a plane containing the pole to the slip plane and the beta maximum of the axial planes. This intersection is the movement line, and if it lies within the separation angle, σ_2 was parallel to layering during folding. Using the beta maximum for the flexural folds on Bear Mountain, the movement line from this method lies some 30^{o} to the east of the separation angle. This is inconsistent with all other determinations and suggests that σ_2 was not parallel to layering during

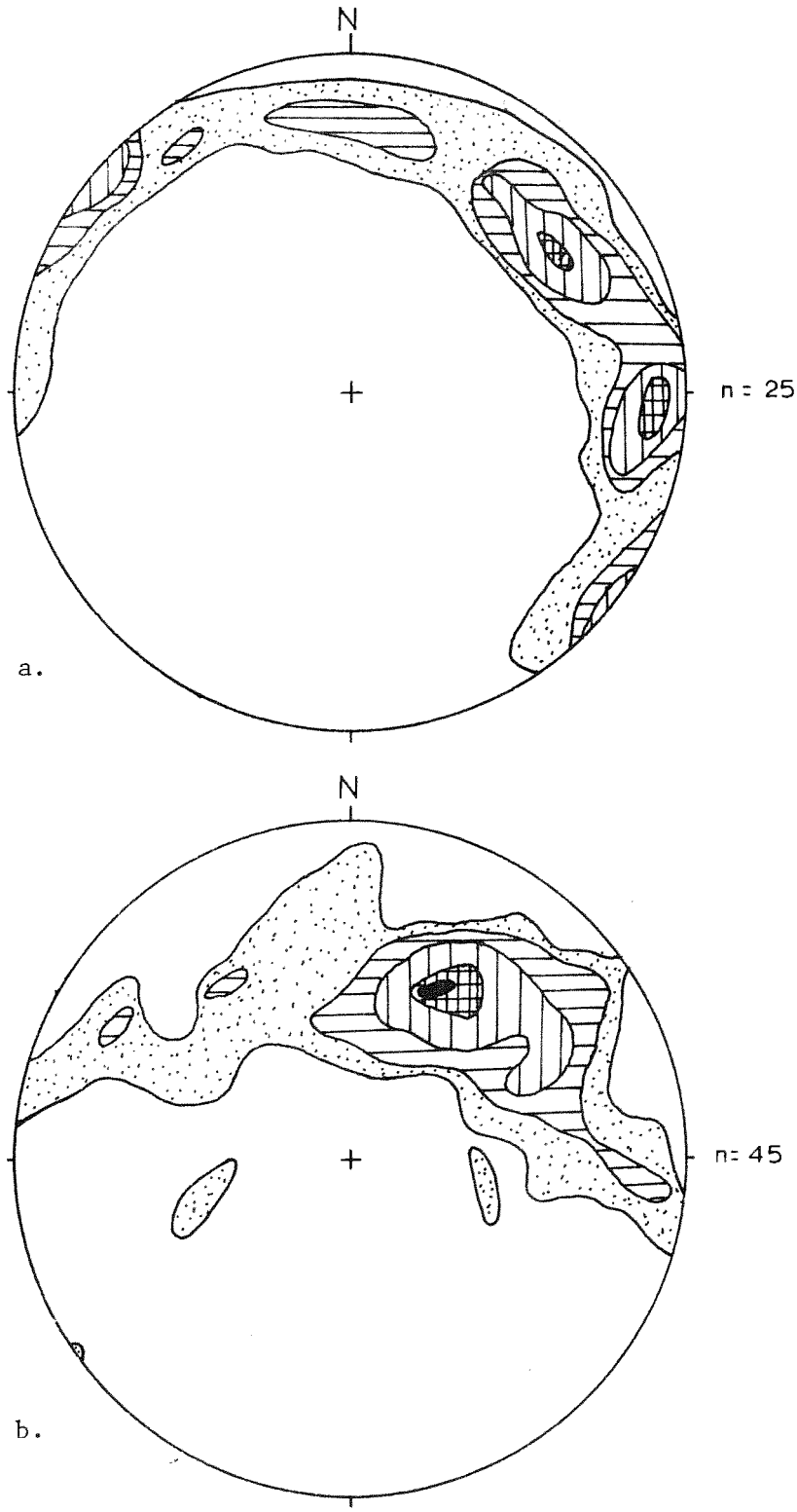

Figure 27. Contoured beta diagrams of axial planes of third phase folds. a. 25 axial planes of suspected passive slip folds. Contours are 1, 3, 7, and 9 percent per 1 percent area. b. 45 axial planes of suspected flexural slip folds. Contours are 1, 3, 5, 7, and 9 percent per 1 percent area.

folding. Because of this inconsistency it is believed that the beta maximum is not a result of initial orientations of axial planes, but rather,curvature of the axial planes caused by different amounts of flattening or slightly different fold mechanisms. It can be demonstrated how curvature of the axial plane can develop by investigating the bedding, axial plane, and slip plane relationships of the passive and flexural end members (Figure 28a,b). In zones where quartzites are interbedded with gneisses the quartzites will fold flexurally while the gneisses will fold passively. It is this combination of the two mechanisms in adjacent beds that causes the axial plane to be curved (Figure 29). This curvature is a commonly observed feature in the field especially in zones of mixed lithologies.

While the folds in Figure 27b are thought to be flexural in nature, they most likely contain different amounts of passive folding. They also will flatten differentially because of small variations in lithology. It is this small but significant variation in style along with different amounts of flattening that results in curvature of the axial planes. It was found that the axis of curvature of the axial plane is coaxial with the fold axis of that particular fold. Since the majority of fold axes at Bear Mountain trend NE (Figure 30a), the axial surfaces of those folds will define a beta maximum in the NE. Because of this origin of the beta maximum, the movement line determination that was inconsistent with the others is not valid and it can then be assumed that σ_2 was parallel to layering since the other movement line determinations did lie within the separation angle.

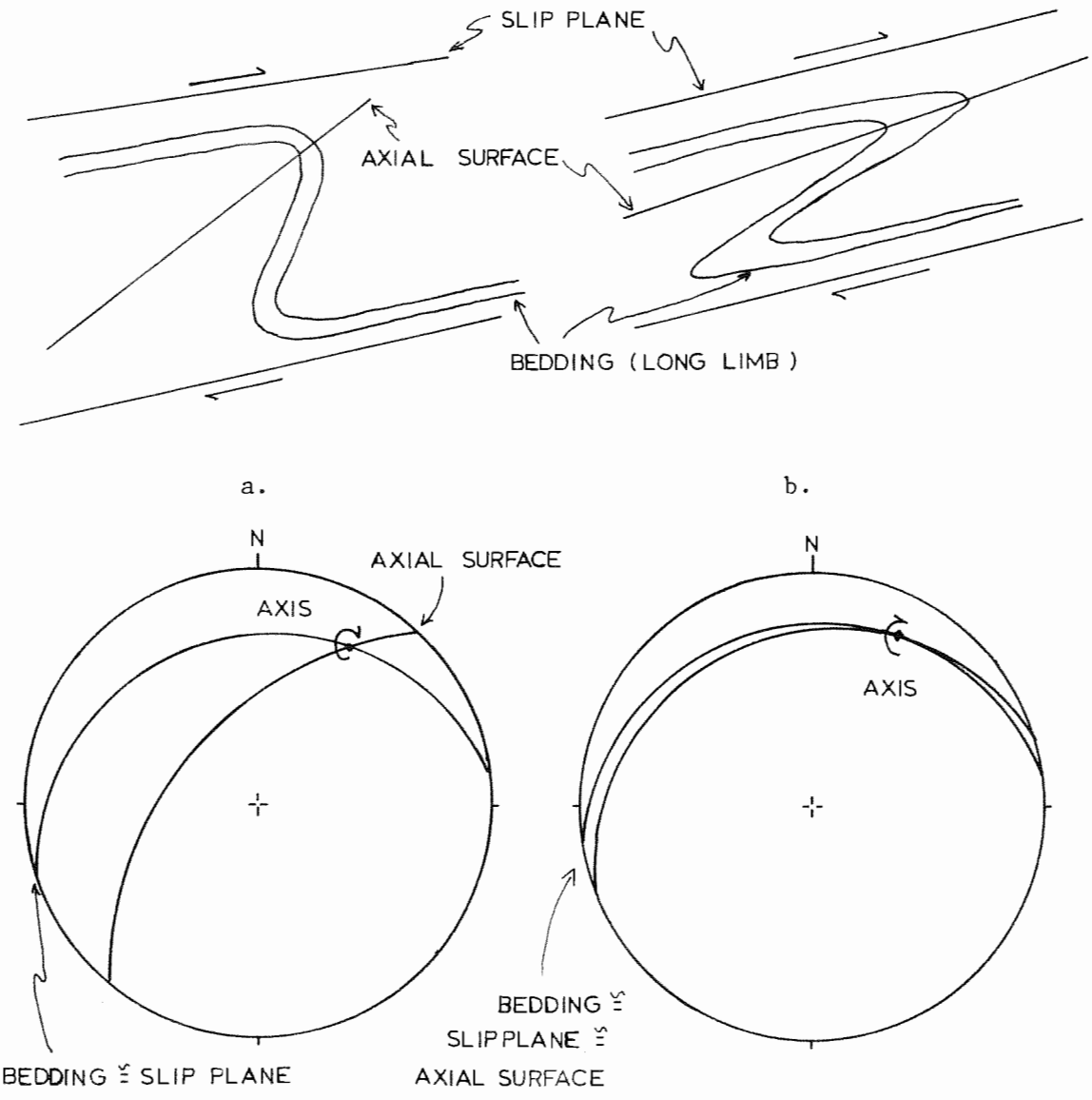

Figure 28. Comparison of bedding, slip plane and axial surface relations for flexural and passive slip folds. Slip plane in this case is parallel to the long limb bedding. a. Flexural slip fold and equal area plot of its relations. b. Passive slip fold and equal area plot of its relations. Small difference between orientation of slip plane and axial plane of passive slip fold is as would occur in natural cases whereas theoretically they would be identical.

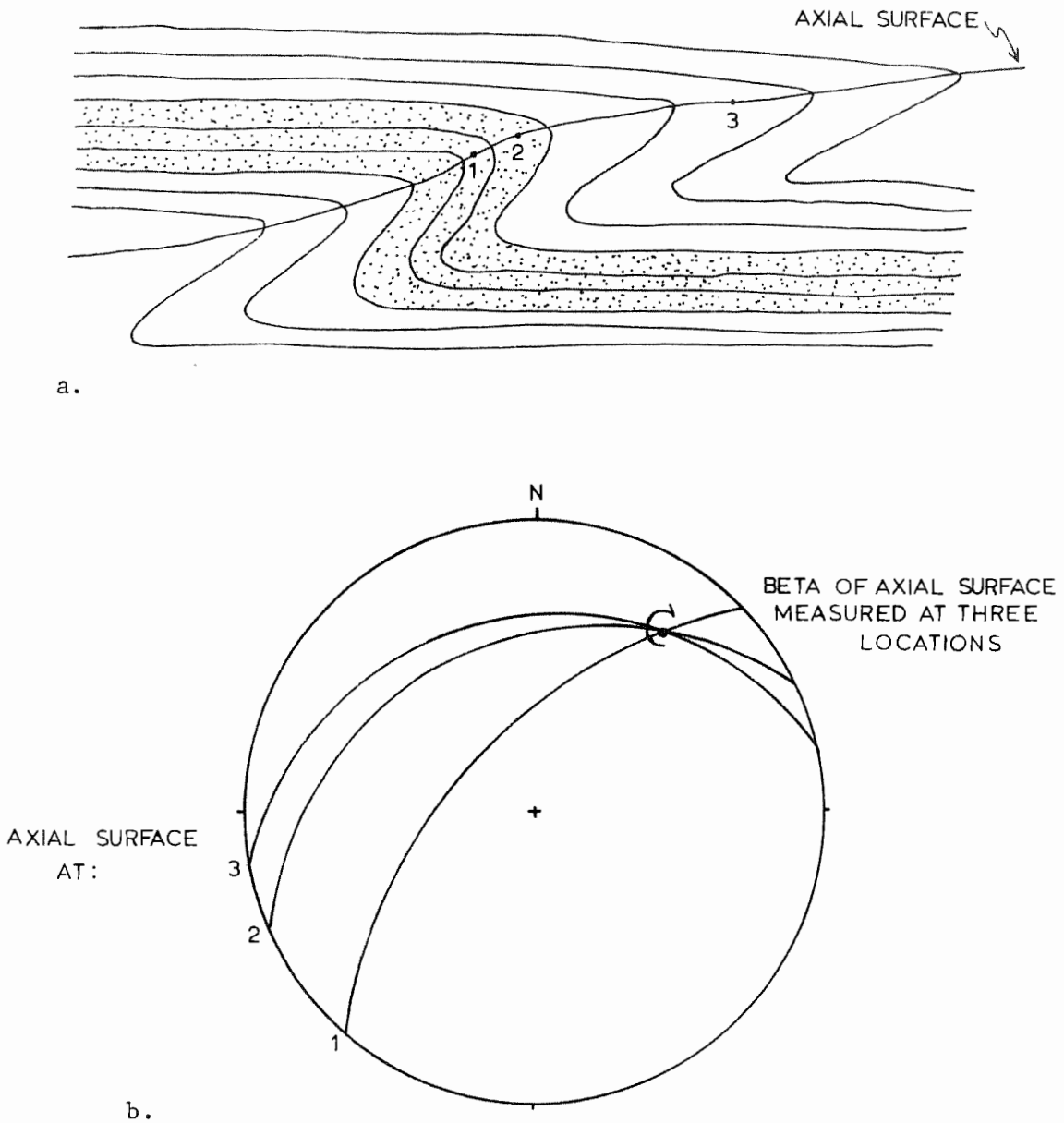

Figure 29. Diagramatic sketch illustrating proposed hypothesis to explain curvature of axial surface and resulting beta maximum of the axial surface. Stipled beds are quartzite-rich, the rest are gneissic or schistose. a. Fold with curved axial surface. b. Equal area plot of the curved axial surface measured at locations 1, 2, and 3.

Figure 30. Equal area plots of third phase fold axes measured on SW flank of Bear Mountain in quartzite member with rotation sense indicated. a. Axes of flexural slip folds. b. Axes of passive slip folds.

These beta diagrams can also be used to detect axial plane rotation. In flexural slip folds axial planes of folds formed early in folding can be rotated toward the slip plane by drag. Scott and Hansen (1966) describe a V pattern seen on beta diagrams of axial planes when rotation occurs. This pattern results from the migration of the zone axis of the axial planes toward the pole to the slip plane. This pattern was not observed, because the curvature of the axial planes would blanket any pattern resulting from rotation of the axial planes.

Since flexural and passive slip folds have different relationships between bedding and slip planes it was of interest to determine the slip plane for both groups of folds. The axes of both groups were plotted separately and the slip plane can be drawn in both cases (Figure 30). For both types of folds the slip plane is very close in orientation and the separation angle is also similar in both cases. This means that separation angle data from any area of both flexural and passive folds will be consistent whether from one or both types of folds. It also appears that the axes of the passive folds are somewhat less spread out away from the separation angle than are the axes of the flexural slip folds. This is probably a result of early formed axes being rotated toward the slip line as commonly occurs in passive folding (Hansen, 1971).

Stress orientations during third phase-asymmetric folding. The folds developed in response to a large shear couple with the top moving south with respect to the bottom. The maximum resolved shear stress or the direction of easiest release is equal to the movement line trending due north and plunging 15^{o} north. σ_1 and σ_3 may now be deduced based on the maximum resolved stress and the orientation of the slip plane (N50W, 20NE). It has been shown in simple cases that σ_1 and σ_3 are oriented in a plane defined by the pole to the slip plane and the slip line, assuming that σ_2 is parallel to layering (Hansen, 1971). The maximum resolved shear stress is equal to the slip line so σ_1 is oriented at about 30^{o} to layering in the plane perpendicular to σ_2. Applying this to the study area, σ_1 must have been oriented with plunge S 7^{o} W at 14^{o} to produce the

observed shear couple. It was then rotated towards parallelism with the slip line. As folding progressed, the fold axes of the passive slip folds and the axial planes of the flexural slip folds were also rotated toward the slip line and slip plane respectively (Hansen, 1971). The orientation of these stress axes can be further refined by looking at the slip zones mapped on Bear Mountain. σ_1 must lie about 30° from this tabular fold zone in the plane of the pole to the zone and the movement line in the direction to produce the proper shear sense. From this, σ_1 = S7°W, 42°; σ_2 = S86°E,12°; σ_3 = N33°W 71°. One should realize that many approximations were made along the way and that generalizations of this type are not to be taken as exact orientations. Nevertheless, they serve as an important guide to the actual conditions.

Since the movement lines in other areas are similar to those from Bear Mountain, the stress orientations must also have been similar.

Relation to regional structural features. The relationship of the third phase asymmetric folds to regional structural features is uncertain. The folds are only found inside the Pelham dome and in rare instances in the adjacent cover rocks to the east. Cover rocks are not exposed on the west flank of the dome at the latitude of the study area but,preliminary work further south suggests third phase asymmetric folds may be prevalent (Scott Laird and Peter Robinson, pers. comm., 1973). Another feature of these folds is that they do not produce any gross map pattern at the scale mapped. It appears that these folds are found on an outcrop scale only (unless at a scale larger than the map area). The only regional structural feature

in the Jerusalem Hill area is the first phase recumbent fold which has an axial orientation that is close to parallel to the movement line of this phase. It is doubtful that the early recumbent fold or any other major folds are associated with this third phase, but its importance in light of its pervasive character must be considered.

One possibility is that this phase is related to the N-S extension of the Pelham dome. This extension could have developed in an E-W compression forcing the dome to elongate N-S. In the northern portion of the dome, the dome gneisses could have moved further N than the overlying mantling strata producing a large shear couple in which the top moved south with respect to the bottom. It was this shear couple that produced the minor folds associated with the third phase. This period of extension and north over south flow would also most likely be the time in which the regional mineral lineation developed suggesting that the mineral lineation and third phase folds might be closely related in time.

Fourth Phase-Late Shears of Reverse Sense

A number of low angle shears are noted throughout the area that cut all structural features up to and including the third phase asymmetric folds (Figure 31a). They are noted in all rock types, but especially in quartzites. The distinguishing feature of these shears is that they have the opposite shear sense from the third phase structures so they cannot be related in a simple way. Besides these shears, some other features such as rotated augen or boudins are seen with this anomalous shear sense (Figure 31b.). In outcrop the length

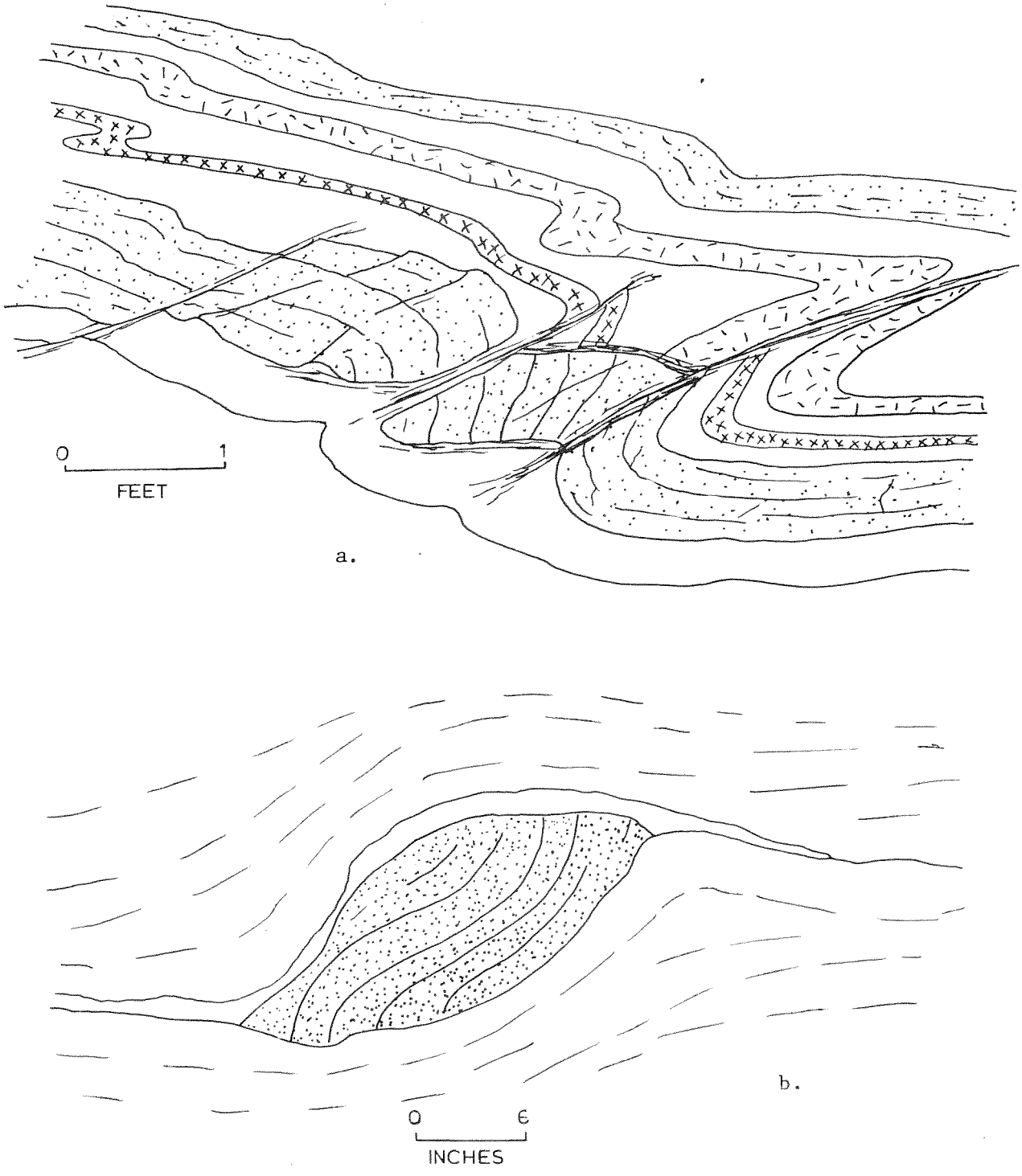

Figure 31. Sketches of fourth phase features. a. Sketch made from photograph of late shears cutting third phase fold in quartzite member. Note that the shear sense of the shears is opposite that of the fold. b. Sketch made from photograph of rotated amphibolite lens in the biotite member of the Dry Hill Gneiss. Both features are on west facing ledges east of Jerusalem Hill and north is to the left in both drawings.

of the shears is never more than several feet and the displacement is less than one foot. The shear planes are oriented approximately N70E, 15NW, but the exact orientation of the movement on these shears is never seen.

Kinematics. The significance of this phase is not understood. The major transport direction in the area during the previous phase was in a N-S direction and the top moved south with respect to the bottom. The fourth phase must then represent a major reorganization of the stresses that previously affected the area. One possibility is that the anomalous shear sense could have developed in a local region of third phase folds where the regional stresses were refracted by the third phase folds such as in a short limb environment. The region around the short limb of a third phase fold would experience an internal rotation opposite that of the rest of the area and if these shears are restricted to these regions and their location with respect to the fold is not seen, they would appear to have a different origin than the third phase folds.

Relation to regional structural features. This phase and shears of this type are not noted on a regional scale so they are thought to be of local significance only.

Fifth Phase-Late Flattening and Extension

Boudinage is a common feature found throughout the area. It is especially well developed near the contacts of the quartzites with the gneisses and in the zones of interbedded gneisses, amphibolites, and quartzites,or when the ductility contrast between layers is high.

Two directions of boudinage were commonly observed in the same outcrop creating a "mattress structure" on the bedding surface. The best examples of this are at contacts of the Dry Hill Gneiss and the Poplar Mountain Gneiss, quartzite member. Associated with these two boudinage directions are two sets of closely spaced high angle joints or fractures that are common throughout the Jerusalem Hill area. It was these associated joints that allowed easy recognition of the age relationships. The joints cut all previously described structural features and along with the presence of boudinaged third phase folds, proved that much of the boudinage is one of the youngest features in the area. These joints trend parallel to the boudin neck lines and are perpendicular to the direction of observed extension. They are common in quartzites, but poorly developed in the gneisses. Figure 32 is an idealized example of the two sets of boudinage and extension joints. An equal area plot of the neck lines shows that the two directions are nearly perpendicular to one another on the bedding surface (Figure 33a). The SE trend is far more common in the field. An equal area plot of the poles to extension joints also shows two directions about 90^{o} apart and parallel in trend to the boudin neck line directions (Figure 33b).

Kinematics. If the two sets of joints are true extension joints, their intersection should approximate the σ_1 direction acting on the bed during formation of the boudinage. Another commonly observed feature is the rotation of the dominant N-S mineral lineation about the boudin. If the plane of rotation of the lineation is plotted with the "axial plane" of the boudin (plane perpendicular to the extension

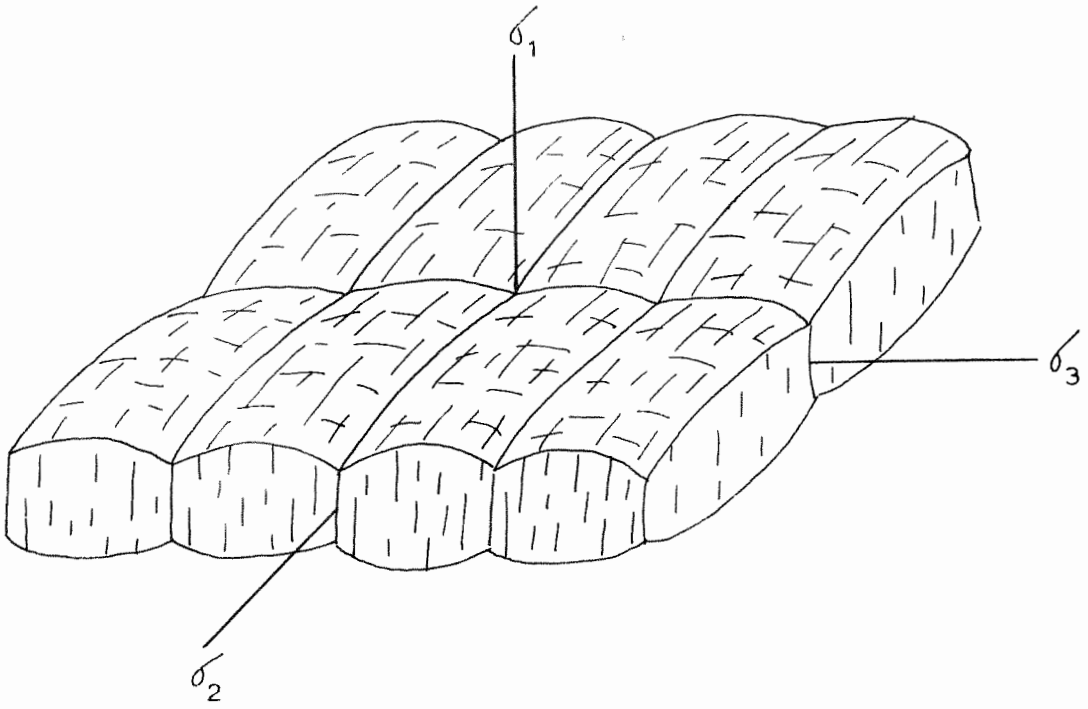

Figure 32. Idealized sketch of a bed boudinaged in two directions 90° from each other resulting in a "mattress structure". Also shown are extension joints associated with each boudinage direction.

direction), the intersection should yield a theoretical movement line of the material that flowed into the thinned areas. Since material probably flowed in all directions from the areas adjacent to the boudin, the movement line is not actually the path that material took when it flowed into the thinned areas. This movement line is actually the trajectory of the contact surface of the two rock types. Several of these directions were calculated and generally are steeply plunging to the SE. An equal area plot comparing a calculated intersection of extension joints from one outcrop with the movement lines of the boudin surface shows that they are close to parallel (Figure 33c).

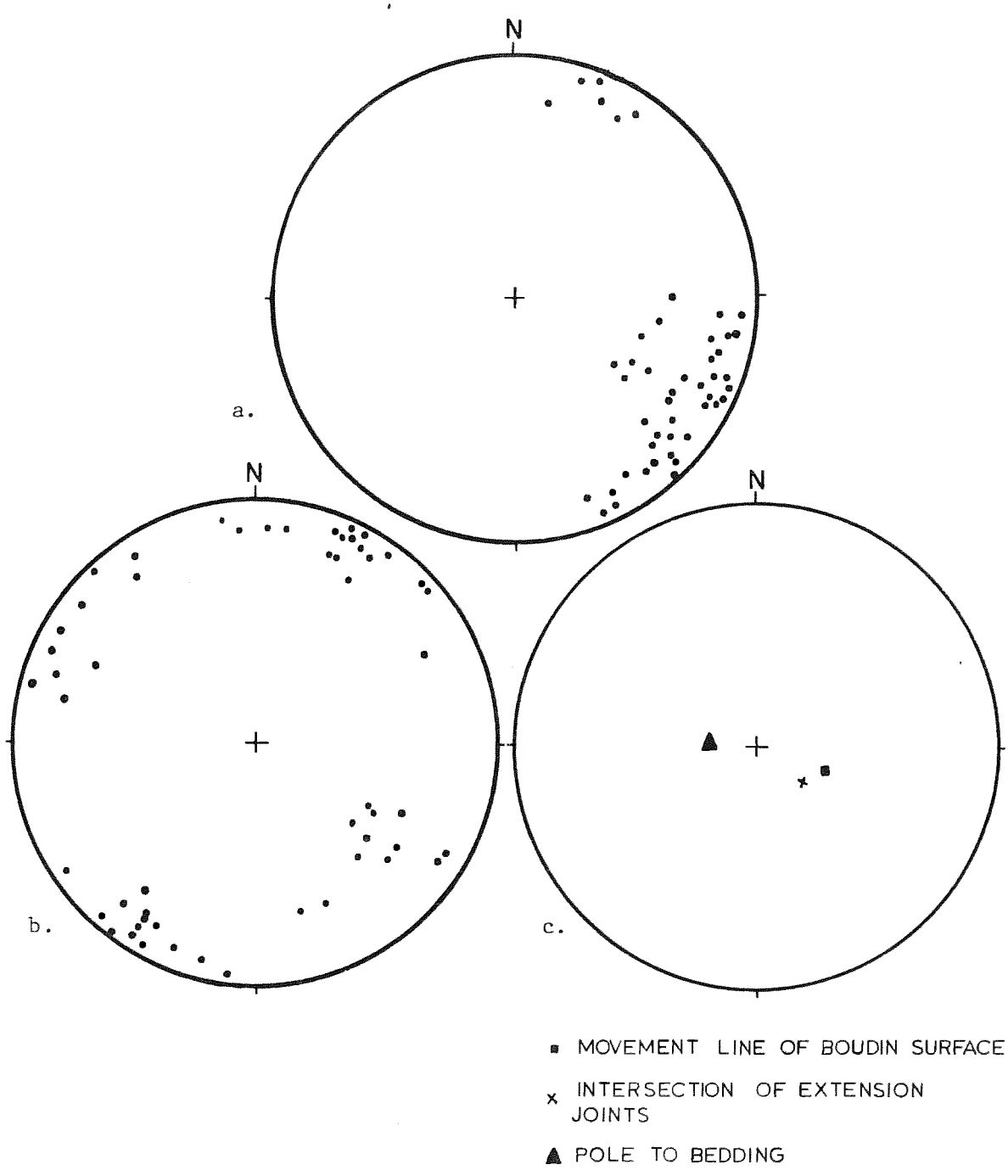

Figure 33. Equal area plots of features associated with fifth phase boudinage. a. Plot of all measured boudinage neck lines. b. Plot of all measured poles to extension joints. c. Plot of calculated movement line of boudin surface and extension joint intersection for one outcrop with bedding shown

It can then be said that the direction of movement of the surrounding boudin surface is parallel to σ_1. Regionally, since the SE set of neck lines is dominant, σ_3 is oriented perpendicular to the SE neck lines, and σ_2 would be perpendicular to the NE set.

Complications of these relationships were noted in some areas where σ_1 was inclined at some angle to the bedding, producing a shear couple on the bedding surface. This resulted in the formation of rotated boudins by the process described by Ramberg (1955). The amount of rotation is a function of the attitude of the bedding rather than a change of stress orientation. This rotation would alter the relationship between the movement direction of the boudin surface and the intersection of the extension joints so that they are no longer parallel. This could not be proven since no measurements were taken from rotated boudin surfaces. It is interesting to note that boudinage was not seen on bedding surfaces with a dip greater than about 35-40^{o} even though the extension joints are present in their normal orientation.

It is possible that the boudinage might be related to the formation of the third phase asymmetric folds. The dominant SE direction of boudinage is about perpendicular to the movement line of the third phase. Since boudins can form perpendicular to the tectonic "a" direction these boudins may be related to the third phase asymmetric folds. If boudinage and late asymmetric folds are related, the boudins are definitely younger. The ductilities of the rocks involved would have changed somewhat with the quartzites yielding by

fracture rather than by folding. The flattening of the third phase folds may have also occurred during this phase since they may be closely related in space and time.

Relation to regional structural features. Although boudinage is a common feature in the region, no age correlation can be made with any particular generation of boudinage outside the dome. In the Northfield syncline northeast of the Pelham dome, boudinage neck lines trend generally E-W approximately normal to mineral lineations and fold axes of the main phase of gneiss dome formation.

Sixth Phase-Triassic Gravity Faulting

The youngest deformation that affected the area is a period of jointing and faulting probably associated with the formation of the large normal fault along the Triassic border to the west. Numerous joints and a low angle gravity fault exposed in the gorge of Lyons Brook, north of Arch Road, are probably part of this phase. The displacements on these features appear to be very small. These features are usually accompanied by some hydrothermal alteration.

SUMMARY OF CONCLUSIONS

Phases of Deformation

As shown by the minor structural features, the area has undergone six phases of deformation. The first five of these are closely related in space and time, and occurred during the Acadian orogeny while the sixth occurred in the Triassic. Some of these phases can be directly related to regional structural features. A summary of these phases and their possible correlation to regional structural features is as follows:

1. First phase-early recumbent folds. Formation of isoclinal folds of diverse orientations with a strong axial plane foliation, forming the foliation of the area. Folds formed mainly by passive slip or flow resulting in similar fold shapes. The study area contains a large fold of this age which is probably a minor fold on the inverted limb of a large recumbent fold belonging to the second regional phase (1B of Robinson, 1967a).

2. Second phase-main phase of gneiss dome formation. Formation of generally tight folds with diverse orientations. Folds formed by passive slip with a weak incipient axial plane foliation and a mineral lineation parallel to the fold axis. This phase may be associated with the formation of gneiss domes and the strong mineral lineation (2B of Robinson, 1967a).

3. Third phase-asymmetric folds. Formation of asymmetric folds with curved hinge lines and diverse orientations, all of which have a shear sense with top moved south over bottom. This is the most prevalent

phase in the Jerusalem Hill area. Folds are generally flattened parallel folds with some similar styles. They formed predominantly by flexural slip with later flattening by flow or slip. Movement lines from different areas are similar in orientation and trend N0-5°E, 10-15°N. There appear to be no regional structural features correlative to these folds outside the Pelham dome to the north and east and their regional significance is unknown.

4. Fourth phase-late shears of reversed sense. Formation of low angle shear planes with a S over N shear sense opposite that of the third phase. These shears are of local importance only and were not correlated on a regional scale.

5. Fifth phase-late flattening and extension. Formation of boudinage in two directions at right angles creating a "mattress structure" where both are present. Associated with these boudins are two sets of extension joints also at right angles. This boudinage may correlate to one of the stages of boudinage in the surrounding area.

6. Sixth phase-Triassic gravity faulting. Formation of late joints and faults associated with the development of the Triassic border fault (4 of Robinson, 1967a).

Stress Orientations

The stress axes have been determined where possible. For phase one, no accurate determinations were made, but estimates can be made. If these folds are a part of a regional recumbent fold or nappe system, they could have moved mainly under the influence of gravity.

σ_1 would be almost vertical, σ_3 parallel to the movement line (probably in a general E-W direction), σ_2 would be 90^{o} from this direction in the plane of layering. The stress orientations for the second phase are unknown. For the third phase at Bear Mountain and probably elsewhere, the initial orientations were calculated at σ_1 = S7^{o}W, 14^{o}; σ_2 = S86^{o}E, 12^{o}; σ_3 = N33^{o}W, 71^{o}. No stress directions were calculated for the fourth phase due to its questionable significance. The fifth phase has its stress axes oriented σ_1 = S50^{o}E, 70^{o}; σ_2 = N50^{o}W, 20^{o}; σ_3 = N40^{o}E, 0^{o}. The stress axes for the sixth phase were also not calculated.

REFERENCES CITED

Alden, W. C., 1924, The physical features of central Massachusetts: U. S. Geol. Survey Bull. 760-B, p. 13-105.

Ashenden, D. B., 1971, Stratigraphy and structure of the northern portion of the Pelham dome, north-central Massachusetts: Geol. Soc. Amer. Abstr., vol 3, no. 1, p. 15.

_____, 1973, Stratigraphy and structure of the northern portion of the Pelham dome, north-central Massachusetts: M. S. thesis, Univ. of Mass., p.

Balk, R., 1956, Bedrock geology of the Millers Falls quadrangle, Massachusetts: U. S. Geol. Survey Quad. Map GQ-93.

Billings, M. P., 1937, Regional metamorphism of the Littleton-Moosilauke area, New Hampshire: Geol. Soc. Amer. Bull., v 48, p. 463-566.

Carter, N. L., Friedman, M., 1965, Dynamic analysis of deformed quartz and calcite from the Dry Creek Ridge anticline, Montana: Amer. Jour. Sci., v. 263, p. 747-785.

Davis, W. M., 1895, The physical geography of southern New England: Nat. Geogr. Soc., Nat. Geogr. Mon. 1, no. 9, p. 269-304.

Donath, F. A., Parker, R. B., 1964, Folds and folding: Geol. Soc. Amer. Bull., v. 75, p. 45-62.

Emerson, B. K., 1898, Geology of Old Hampshire county, Massachusetts: U. S. Geol. Survey Mon. 29, 790 p.

_____, 1917 , Geology of Massachusetts and Rhode Island: U. S. Geol. Survey Bull. 597, 289 p.

Hansen E., 1971, Strain facies: New York, Springer Verlag, 207 p.

Lyons, J. B., Faul, H., 1968, Isotope geochronology of the Northern Appalachians: Studies of Appalachian geology: Northern and Maritime, New York, Interscience Pub., p. 305-318.

McIntyre, D. B., Turner, F. J., 1953, Petrofabric analysis of marbles from Mid-Strathspey and Strathavon: Geol. Mag. 90, p. 225-240.

Naylor, R., 1970, Radiometric dating of pennine-type nappes in the Northern Appalachians: Eclogae Geol. Helv., v. 63/1, p. 230.

_____, Boone, G., Boudette, E., Ashenden, D., Robinson, P., 1973, Pre-Ordovician rocks in the Bronson Hill and Boundry Mountain anticlinoria, New England, U. S. A.: Abstr., Amer. Geophys Union Trans., v. 54 no. 4, p. 495.

Ramberg, H., 1955, Natural and experimental boudinage and pinch-and-swell structures: Jour. Geol., v. 63, p. 512-526.

Ramsay, J. G., 1962, The geometry and mechanics of formation of "similar" type folds: Jour. Geol., v. 70, p. 309-327.

_____, 1967, Folding and fracturing of rocks: New York, McGraw Hill Co., 568 p.

Robinson, P., 1963, Gneiss domes of the Orange area, Massachusetts and New Hampshire: Ph. D. thesis, Harvard Univ., 253 p.

_____, 1967a, Gneiss domes and recumbent folds of the Orange area, west central Massachusetts: Guidebook New England Intercollegeate Geol. Confr., Amherst, Mass., p. 17-47.

_____, 1967b, Geology of the Quabbin Reservoir Area, Central Massachusetts: Guidebook New England Intercollegeate Geol. Confr., Amherst, Mass., p. 115-127.

_____, 1972, Stratigraphy and structure of nappes and gneiss domes of the Bronson Hill anticlinorium and the Merrimack synclinorium, west-central Massachusetts: Unpubl. NSF Grant Proposal.

Scott, W. H., Hansen, E., Twiss, R. J., 1965, Stress analysis of quartz deformation lamellae in minor folds: Amer. Jour. Sci., v. 263, p. 729-746.

_____, Hansen, E., 1969, Movement directions and the axial fabrics of flexural folds: Carnegie Inst. Wash. Year Book 67, p. 254-258.

Spencer, E. W., 1969, Introduction to the structure of the earth: New York, McGraw Hill Co., 597 p.

Thompson, J. B. Jr., 1956, Skitchewaug Nappe, a major recumbent fold in the area near Claremont, New Hampshire: Abstr., Geol. Soc. Amer. Bull., v. 67, p. 1826-1827.

_____, Robinson, P., Clifford, T. N., Trask, N. J. Jr., 1968, Nappes and gneiss domes in west-central New England: Studies of Appalachian geology: Northern and Maritime, New York, Interscience Pub., p. 203-218.

PLATE 1. GEOLOGIC MAP OF THE NORTHERN PORTION OF THE PELHAM DOME

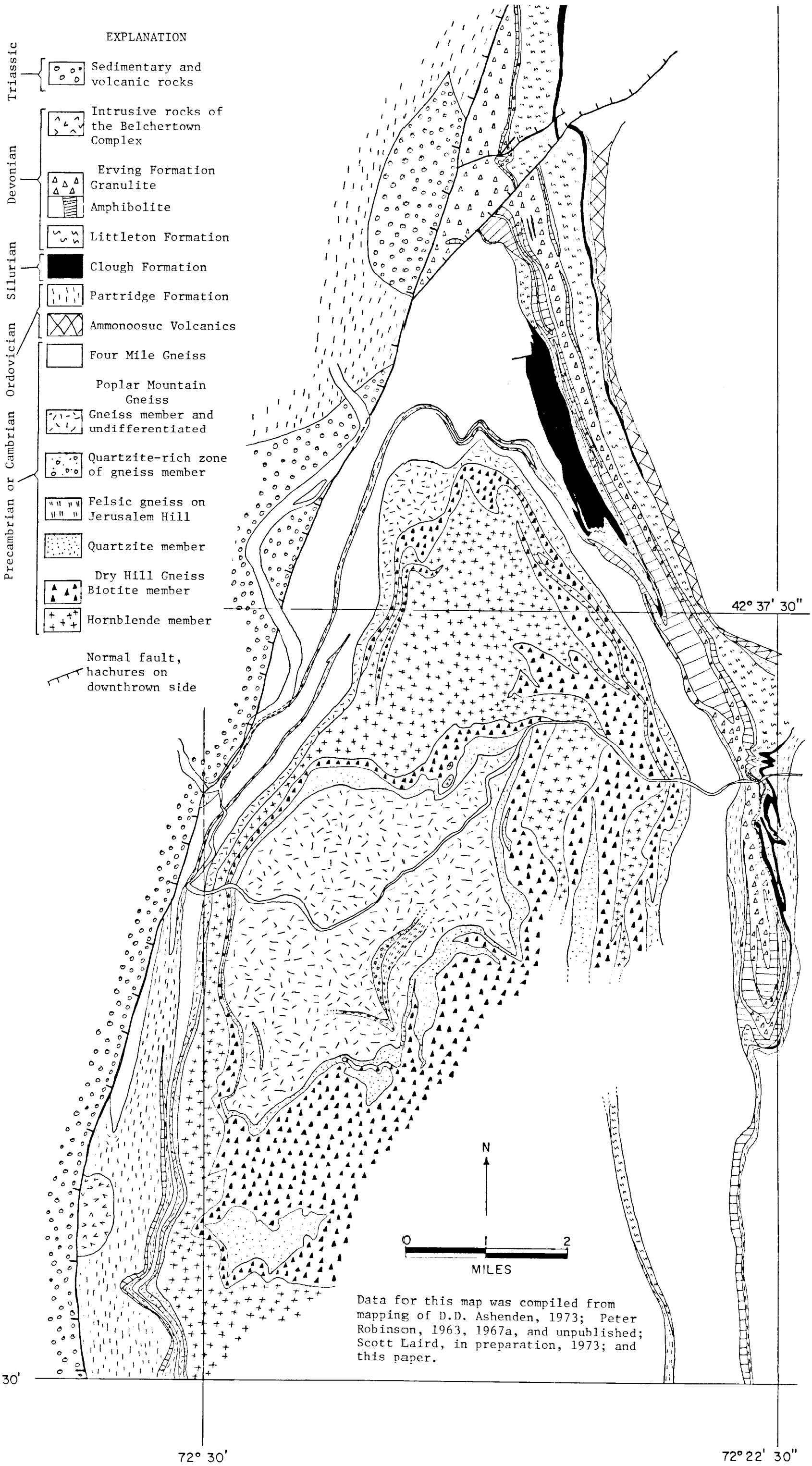

Data for this map was compiled from mapping of D.D. Ashenden, 1973; Peter Robinson, 1963, 1967a, and unpublished; Scott Laird, in preparation, 1973; and this paper.

PLATE 2. GEOLOGIC MAP OF THE NORTH-CENTRAL PORTION OF THE PELHAM DOME

EXPLANATION

Rock Units

Cambrian or Precambrian

pm, pmqz, pmjh, pmbs, pma, pmq

Poplar Mountain Gneiss-gneiss member: pm, coarse to medium-grained, gray quartz-biotite-microcline-plagioclase gneiss with conspicuous megacrysts of feldspar up to 4" across and minor interbeds of quartzite, calc-silicate gneiss, and leucocratic gneiss; pmqz, quartzite-rich zone of gneiss member: numerous 1-3" quartzite beds; pmjh, felsic gneiss on Jerusalem Hill: medium-grained, tan, rotten weathering quartz-microcline-biotite-plagioclase gneiss.

Poplar Mountain Gneiss-quartzite member: pmq, tan to buff well bedded, pure to feldspathic quartzite with minor calc-silicate gneiss beds; pmbs, biotite schist: dark gray biotite-quartz-plagioclase schist and fine-grained gray gneiss; pma, amphibolite: dark gray to black fine-grained amphibolite with minor epidote, calc-silicate gneiss and hornblendite layers and boudins.

db, dbq, dh

Dry Hill Gneiss-biotite member: db, well bedded to massive, medium-grained pink to tan quartz-microcline-oligoclase-biotite gneiss with minor leucocratic gneiss and quartzite layers; dbq, quartzite: impure quartzite and leucocratic gneiss.

Dry Hill Gneiss-hornblende member: dh, similar to biotite member, but with conspicuous knots of hornblende ($2V=0^{\circ}$) up to 1" across.

Symbols

- Contact, location accurate
- Contact, location approximate
- Contact, location inferred
- 47 Strike and dip of bedding
- 52 Strike and dip of foliation
- 48 Trend and plunge of mineral lineation

14° MAGNETIC NORTH, TRUE NORTH

APPROXIMATE MEAN DECLINATION, 1961

1 MILE

1000 0 1000 2000 3000 4000 5000 6000 7000 FEET

1 .5 0 1 KILOMETER

PLATE 3. GEOLOGIC STRUCTURE SECTIONS

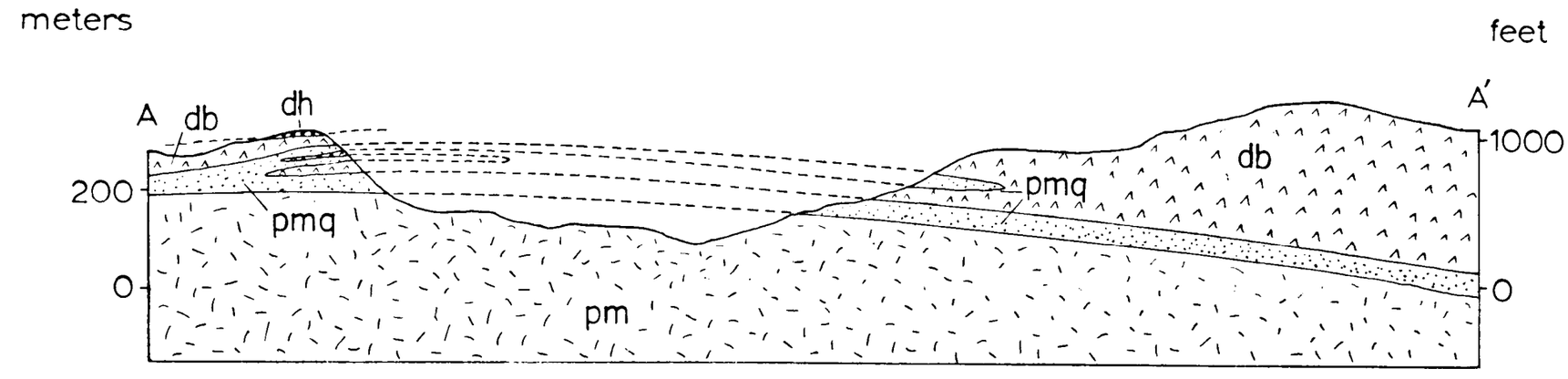

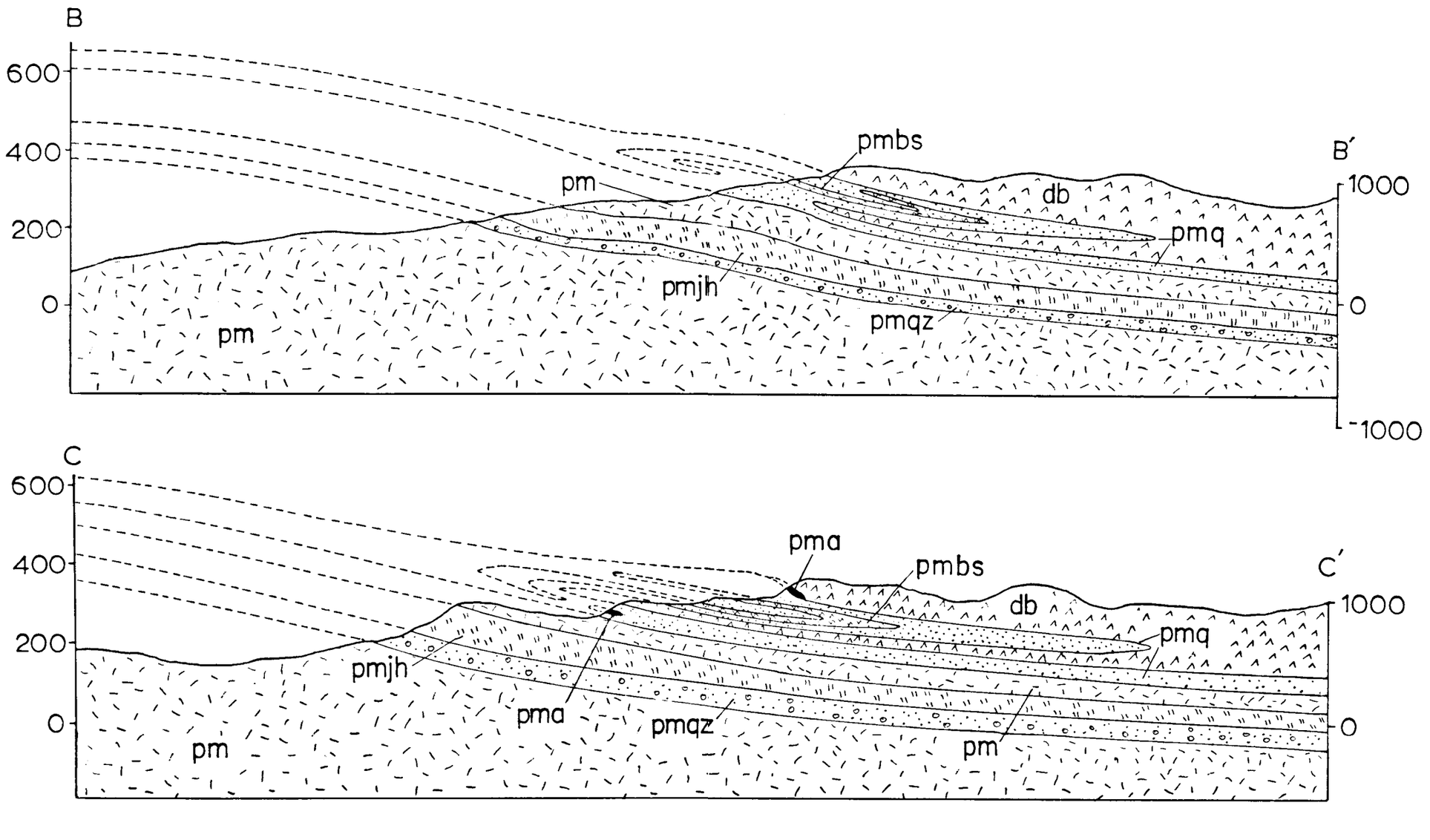

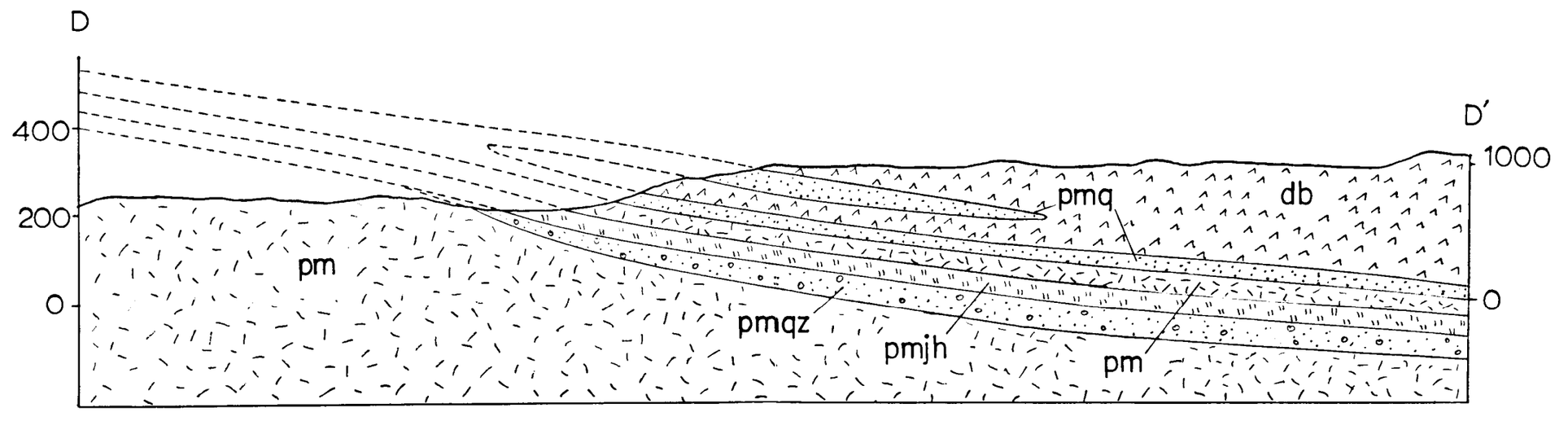

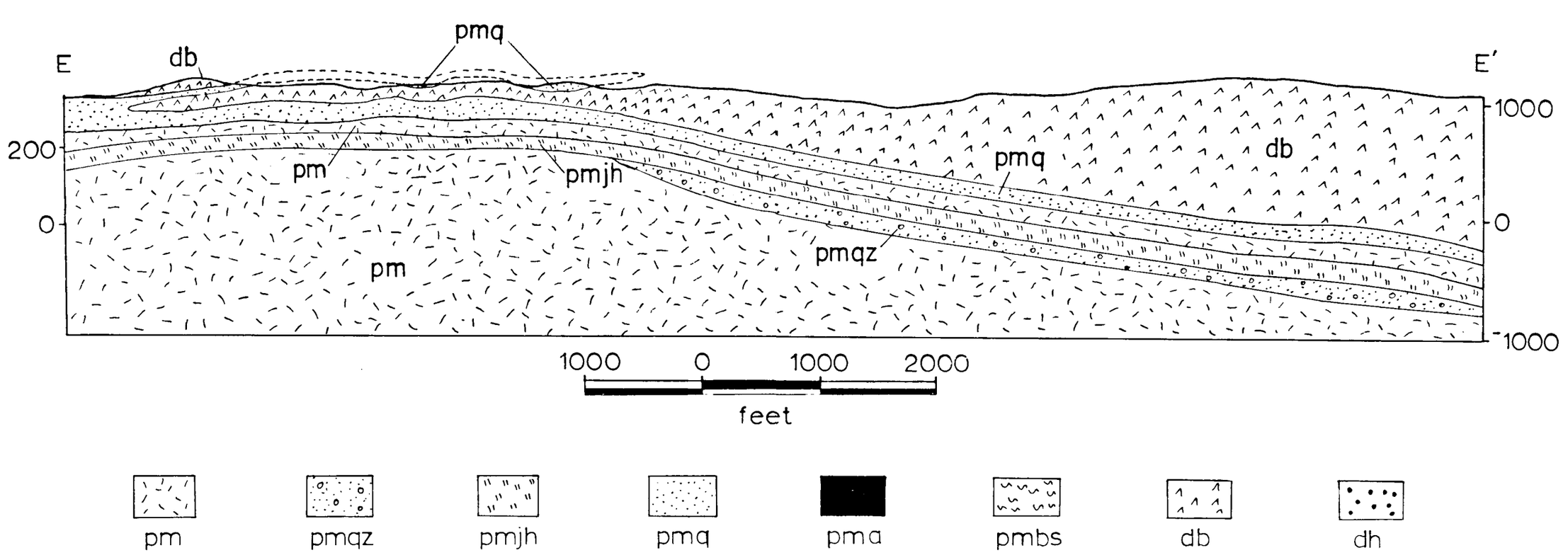

PLATE 4. MAP OF PLANAR STRUCTURAL FEATURES

EXPLANATION

39 STRIKE AND DIP OF FOLIATION

49 STRIKE AND DIP OF BEDDING

0 .5

MILES

N

pmq

pm

db

pmq

pma

pmqz

pmjh

pm

pmq

pma

db

pma

pmbs

db

dbq

pmq

pmjh

pm

db

pmq

db

db

PLATE 5. MAP OF LINEAR STRUCTURAL FEATURES

EXPLANATION

TREND AND PLUNGE OF MINERAL LINEATION

TREND AND PLUNGE OF FOLD AXIS SHOWING ROTATION SENSE

0 .5

MILES

N

pmq

pm

db

pmq

pma

pmjh

pmqz

pm

pmq

pma

db

pmbs

pma

dbq

pmq

pmjh

pm

db

pmq

db

db

PLATE 6. OUTCROP LOCATION MAP

EXPLANATION

OUTCROP

AREA OF 75% OR GREATER OUTCROP

0 .5

MILES

N

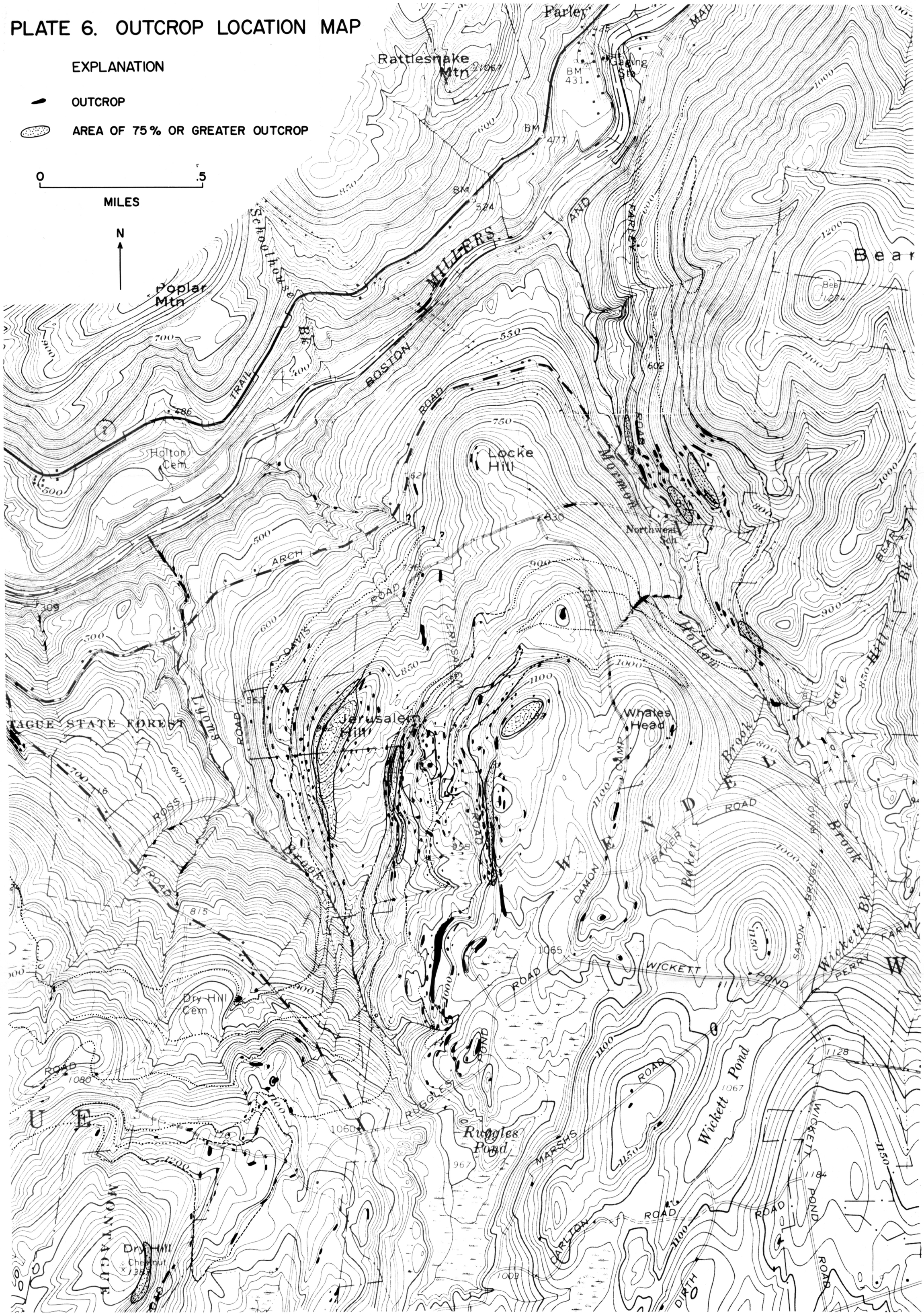

1 ½ 0 1 MILE

1000 0 1000 2000 3000 4000 5000 6000 7000 FEET

1 .5 0 1 KILOMETER

CONTOUR INTERVAL 10 FEET

DATUM IS MEAN SEA LEVEL